MONTHLY NOTICES

OF THE

ROYAL ASTRONOMICAL SOCIETY

Vol. 107 No. 4

MEETING OF 1947 OCTOBER 10

Professor W. M. H. Greaves, President, in the Chair

The President referred to the death on 1947 September 6 of Dr Paul Guthnick, an Associate of the Society, and paid a short tribute to him (the Fellows standing).

The election by the Council of the following Fellows was duly confirmed :—

Patrick Maynard Stuart Blackett, 5 Oak Drive, Manchester;

Robert R. Coles, Hayden Planetarium, American Museum of Natural History, New York, U.S.A.;

James Cecil Farrer, 10 Bancroft Avenue, Cheadle Hulme, Stockport;

Shirley I. Gale, Hayden Planetarium, American Museum of Natural History, New York, U.S.A.; and

Nicholas Bryan John Stapleton, 71A Denmark Villas, Hove, Sussex.

The following candidates were proposed for election as Fellows of the Society, the names of the proposers from personal knowledge being appended :—

John Werner Abrams, Ph.D., Wesleyan University, Middletown, Connecticut, U.S.A. (proposed by C. L. Stearns);

Catharine E. Barry, Hayden Planetarium, The American Museum of Natura History, New York, U.S.A. (proposed by C. Fisher);

Frank George Griffith Carr, National Maritime Museum, Greenwich, London, S.E.10 (proposed by Sir H. Spencer Jones);

The Rev. Herbert Gilgryst, Clifton Vicarage, York (proposed by I. F. H Carr-Gregg);

Herbert Victor Griffiths, B.B.C. Measurement and Receiving Station, Tatsfield (proposed by Sir H. Spencer Jones);

Karel Hujer, D.Sc., University of Chattanooga, Chattanooga, Tennessee U.S.A. (proposed by F. J. M. Stratton);

Anthony William Jewiss, 146 Lennard Road, Beckenham, Kent (proposed by R. G. Foster);

Donald H. Menzel, Harvard College Observatory, Cambridge, Massachusetts, U.S.A. (proposed by H. H. Plaskett);

Sydney William Royle Mottram, 30 Hartington Road, Chorlton-cum-Hardy, Manchester 21 (proposed by H. R. Didcock);

Robert Naismith, M.I.E.E., 41 Downs Road, Slough, Bucks (proposed by H. W. Newton);

B. V. Raman, D.Sc., Ph.D., Seshadripuram, P.O. Malleswaram, Bangalore, India (proposed by V. M. Sundara Rajan);

The Rev. John Gammon Read, The Parsonage, Wortwell, Harleston, Norfolk (proposed by W. H. Coombs);

Alfred Athelstan Smart, 2 Ferntower Road, Highbury, London, N.5 (proposed by H. Simmons); and

Samuel Tolansky, D.Sc., Ph.D., D.I.C., 16 Sheen Common Drive, Richmond, Surrey (proposed by W. H. McCrea).

Two hundred and six presents were announced as having been received since the last meeting, including :—

M. Davidson, *Elements of Mathematical Astronomy* (presented by the author);

P. Doig, *An Outline of Stellar Astronomy* (presented by the author);

Pascual Jordan, *Die Herkunft der Sterne* (presented by Professor O. Heckmann);

Newton Tercentenary Celebrations (presented by the Royal Society);

J. W. N. Sullivan, *Isaac Newton*, 1642–1727 (presented by Dr G. Merton);

Will Whiston, *The Transits of Mercury and Venus over the Sun*, 1723 (presented by Mr G. H. Wyatt); and

Explosions on the Sun, a film prepared at the High Altitude Observatory of Harvard University (presented by Professor D. H. Menzel).

MEETING OF 1947 NOVEMBER 14

Professor W. M. H. Greaves, President, in the Chair

The President announced that the Council had approved the presentation of the following Loyal Address to His Majesty the King on the occasion of the wedding of H.R.H. Princess Elizabeth :—

"MAY IT PLEASE YOUR MAJESTY

"We, the President, Council and Fellows of the Royal Astronomical Society humbly offer to Your Majesty this expression of our heartfelt congratulations on the occasion of the marriage of Her Royal Highness Princess Elizabeth, Heiress Presumptive to the Throne, to Lieutenant Philip Mountbatten, R.N. We venture to convey to Your Majesty the hope that long life and great happiness be vouchsafed to Her Royal Highness in her marriage, and that her joy may bring comfort to Your Majesty, Her Majesty the Queen, and all the members of the Royal Family. On behalf of Astronomers throughout Your Majesty's Commonwealth and Empire we respectfully express the ardent hope that the life of service to which Her Royal Highness has dedicated herself may be a time of tranquillity and true progress for all Your Majesty's peoples.

"We, the Fellows of the Society, also humbly beg Your Majesty to accept this Address as an expression of our loyalty to the Throne and to the Person of Your Majesty our Patron, and we pray that, with the blessing of God, Your Majesty and our Gracious Queen may long be spared to rule over the Kingdom of Great Britain and Ireland and the British Dominions beyond the Seas."

The election by the Council of the following Fellows was duly confirmed :—

Michael Percy Dandridge, 13 Pickhurst Rise, West Wickham, Kent;

Herbert Fletcher, 7 Salt Hill Way, Slough, Buckinghamshire; and

Albert George Shrimpton, 16 Kingsway, Wembley, Middlesex.

The following candidates were proposed for election as Fellows of the Society, the names of the proposers from personal knowledge being appended :—

Charles Richard Peter Allix, British Horological Institute, Ltd., 35 Northampton Square, London, E.C.1 (proposed by Sir H. Spencer Jones);

Francis Bolam Cowen, British Horological Institute Ltd., 35 Northampton Square, London, E.C.1 (proposed by Sir H. Spencer Jones);

John Theodore Foxell, M.A., 128 Abbey Foregate, Shrewsbury, Shropshire (proposed by L. J. Comrie);

Thomas F. Gaskell, Ph.D., c/o Anglo-Iranian Oil Co., Britannic House, Finsbury Circus, London, E.C.2 (proposed by E. C. Bullard);

Kenneth Pritchard Harrison, King's College, Cambridge (proposed by A. D. Thackeray);

Louis G. Henyey, Professor of Astrophysics, Berkeley Astronomical Dept., University of California, U.S.A. (proposed by S. Chandrasekhar);

Rudolph Luss, 87 Shlomo Hamelech Street, Tel Aviv, Palestine (proposed by J. G. Porter);

Alfred Lauck Parson, M.A., Hillcroft (Allonby), Mowbray Road, Maryport, Cumberland (proposed by R. A. Lyttleton);

Michael William Richey, 68 Cadogan Square, London, S.W.1 (proposed by G. C. L. Saul);

John Noel Taylor, Lt.-Cdr. R.N.V.R., 56 Arragon Gardens, Streatham, London, S.W.16 (proposed by O. M. Watts); and

Francis Harry Thornton, Grove Mount, Davenham, Nr. Northwich, Cheshire (proposed by F. J. Hargreaves).

Seventy-four presents were announced as having been received since the last meeting, including :—

Manuscript letters from the Rev. T. W. Webb, Fellow of the Society, 1852-1885, to Arthur C. Ranyard, Fellow of the Society, 1863-1894 (presented by Mrs O. L. Meyrick-Jones).

NOTE ON THE CONDENSATION OF INTERSTELLAR MATERIAL INTO STARS

F. Hoyle

(Received 1947 May 9)

Summary

An attempt is made to obtain a criterion for determining the degree of condensation of interstellar material into stars. The application of this criterion suggests that both the nuclei of disk-shaped nebulae and the elliptical nebulae must be almost wholly condensed, whereas the main body of a disk-shaped nebula such as M31 is largely uncondensed.

A simple calculation indicates that the ages of the extragalactic nebulae are of order 5×10^9 years.

---

1. *Introduction.*—It is assumed that the extragalactic nebulae initially consist of diffuse gaseous material, and that condensations subsequently form within the material. Some condensations achieve a very high degree of concentration and appear as stars, but other comparatively diffuse condensations may also be formed. Indeed we may expect the densities in different condensations to vary between the mean interstellar density and densities of stellar order.

The observational data for disk-shaped nebulae, such as M31 and M33, suggests that only a small fraction of the total mass is in the form of stars. On the other hand Oort finds * that the elliptical nebula NGC 3115 must be almost wholly composed of stars. This difference raises the important question:—

What considerations determine the fraction by mass of a nebula that is condensed into stars?

The present paper attempts to give a preliminary discussion of this problem.

2. *The Luminosity Function.*—In the neighbourhood of the Sun the number of stars per unit mass range decreases rapidly with increasing mass. This dependence is remarkable, because large condensations must tend to form more readily than small ones, since a larger internal gravitational field is better able to overcome the factors that tend to prevent condensation (for example, gas pressure gradients).

The luminosity function cannot be explained simply by the exhaustion of the hydrogen supply in massive stars, since the characteristic form of the luminosity function is maintained down to stars of small mass, whose lifetimes in the main sequence state are very long compared with normal estimates for the age of the universe. A more hopeful line of attack on the problem seems to be given by a consideration of the rapid initial rotation that must occur in condensations of stellar dimensions. An attempt has already been made to discuss this question †, but I think that an assumption was made that cannot now be accepted. Accordingly it is preferable to proceed *ab initio.*

* J. H. Oort, *M.N.*, **106**, 159, 1946.

† *M.N.*, **105**, 305, 1945.

It has been shown * that the rate of rotation of a stellar condensation is least when the star is formed from a cylindrical portion of the nebula, the axis of the cylinder being perpendicular to the plane of the nebula. The earlier work gives †

$$M \simeq \pi a^2 \rho t, \tag{1}$$

$$u \simeq \frac{M}{2\pi \rho t R} \left| \frac{dV}{dr} + \frac{V}{r} \right|, \tag{2}$$

where a is the radius of the cylinder, ρt is the mass per unit area of the nebula, V is the rotational velocity of interstellar material at distance r from the centre of the nebula, M, R, u are the mass, radius, and equatorial rotational velocity of the star.

Now the velocity of escape at the surface of the star is of order

$$6{\cdot}17 \times 10^7 (MR_\odot / M_\odot R)^{\frac{1}{2}} \text{ cm. per sec.}$$

Thus

$$\frac{u}{\text{Velocity of Escape}} \simeq 1{\cdot}47 \times 10^{14} xy, \tag{3}$$

where

$$x = (MR_\odot / M_\odot R)^{\frac{1}{2}}, \quad y = (\tfrac{1}{2}\rho t) \,.\, |\, dV/dr + V/r \,|\,.$$

To a sufficient approximation the criterion for the stellar condensation to be rotationally stable is that (3) must be less than unity.

Values of x for main sequence stars are given as a function of $M/M_\odot$ in the following table:—

$M/M_\odot$	0·2	0·25	0·45	1	2·39	12·42	17·38	33·88
x	0·68	0·70	0·75	1	1·16	1·52	1·72	1·58

These values were obtained from data given by Kuiper in his discussion of the empirical mass-luminosity relation.‡ In the main body § of a nebula such as M31 or M33, we have $\rho t \simeq 1/5$ g. per cm.^{2}, and dV/dr, V/r are both close to $2 \cdot 10^{-15}$ sec.$^{-1}$. Thus (3) becomes equal to unity for $x \simeq 0{\cdot}68$. That is, for

* *Loc. cit.* The discussion was based on a calculation of the time of condensation of small stars of high hydrogen content. The gravitational potential energy of a star of mass M and radius R is of order GM^2/R. The time of condensation is of order GM^2/RL, where L is the luminosity. The calculation then involved the determination of L, which was found by using the usual theory of photoelectric opacity. This assumes that heavy elements are present in appreciable concentration (on this basis a star of high hydrogen content would contain about 90 per cent hydrogen and 10 per cent heavy elements). Now a recent discussion (F. Hoyle, *M.N.*, **106**, 255, 1946) has shown that the amount of heavy elements must be far less than was formerly supposed. This change produces a reduction in opacity, and a corresponding increase in L, both by a factor of about 100. The time of condensation of small stars is then reduced from the previous value of about 10^{11} years to about 10^9 years. This reduction throws doubt on the previous arguments concerning the luminosity function.

† *Loc. cit.*, equations (10), (11) and also the footnote on page 312. The analysis leading to the factor $|dV/dr + V/r|$ is given in detail in F. Hoyle, *M.N.*, **106**, 406, 1946.

‡ G. P. Kuiper, *Ap. J.*, **88**, 472, 1938.

§ The word "nucleus" is used in the present discussion for the central regions of a nebula where either or both of the mass per unit area ρt and the differential rotation dV/dr are varying rapidly with r. The "main body" is an extensive region lying outside the nucleus that contains the main mass of the nebula, and in which both ρt and dV/dr are approximately independent of r. In M31 the nucleus extends to about 500 parsecs and the main body to about 6000 parsecs from the centre. Outside the main body the "outer fringes" occur where ρt decreases fairly rapidly with increasing r. The differential rotation dV/dr is positive in the main body, but decreases to zero and becomes negative in the outer fringes.

$M/M_\odot \simeq 0{\cdot}2$. It follows therefore that condensing stars with masses exceeding about $0{\cdot}2\,M_\odot$ must become rotationally unstable before reaching the main sequence state. Such stars must then evolve by ejecting material until their masses are reduced below the critical value. Furthermore, all information at present available suggests that the ejected material is thrown off to infinity. We therefore reach the conclusion that stars forming in the main body of a nebula such as M 31 or M 33 have masses $\leqslant 0{\cdot}2\,M_\odot$ at the time of condensation to the main series state. The masses can subsequently increase above $0{\cdot}2\,M_\odot$ through accretion of further quantities of interstellar material.

3. *The Condensation of Interstellar Material into Stars.*—The values given above refer to the particular value of y chosen for the main bodies of M31 and M33. It is of interest also to consider the values of y that are applicable to (i) the nuclei of disk-shaped nebulae, (ii) the outer fringes of disk-shaped nebulae, and (iii) the elliptical nebulae. The following table is important in this connection:—

$10^{14}y$	1	0·91	0·68	0·59	0·45	0·40
x	0·68	0·75	1	1·16	1·52	1·72
$M/M_\odot$	0·2	0·45	1	2·39	12·42	17·38

The corresponding values of x, y are chosen so that (3) is equal to unity, and the values of $M/M_\odot$ give the maximum stellar masses that can be formed by direct condensation. The latter values are very sensitive to y. Thus the interstellar material may be characterized as "difficult" to condense into stars if $y > 10^{-14}$, and "readily" condensed into stars if $y < 5{\cdot}10^{-15}$. These results lead to interesting consequences.

(i) *The nuclei of disk-shaped nebulae.*

We expect ρt to be larger in the nucleus than in the main body of a nebula. This suggests a smaller value of y in the nucleus. This suggestion is supported by the values of $V(r)$ obtained by Babcock * for M31. It was found that dV/dr and V/r are of opposite sign for values of r between about 250 and 500 parsecs. This sign difference reduces the factor $|dV/dr + V/r|$ and also leads to a reduction of y. Thus probably throughout, and certainly in parts of the nuclei, the material must be largely condensed into stars.

(ii) *The outer fringes of disk-shaped nebulae.*

Here ρt is appreciably less than the value 1/5 g. per cm.^{2} used in Section 2. Thus at first sight it might appear that y is large and that the material should be almost wholly uncondensed. But it must be remembered that dV/dr and V/r are of opposite sign in the outer parts of a nebula. Accordingly in certain regions the factor $|dV/dr + V/r|$ must become small. There may be appreciable condensation in such regions.

(iii) *The elliptical nebulae.*

It is probable that the condensation in elliptical nebulae is similar to the condensation in the nuclei of disk-shaped nebulae.

4. *The Age of the Extragalactic Nebulae.*—The highly condensed state of the nuclei of disk-shaped nebulae and elliptical nebulae has an interesting application. When interstellar material is absent, the luminosities of the brightest stars must depend on the age of the nebulae. Accretion cannot provide a steady supply of bright stars, as it can in the main bodies and outer fringes of

* H. W. Babcock, *Lick Obs. Bull.*, **19**, 41, 1939 (No. 498).

disk-shaped nebulae. The bright stars simply burn up their supplies of hydrogen without any replenishment taking place, and the age of the nebulae at any epoch is given by the lifetimes of the brightest stars then present.

This provides a method of estimating the age of the nebulae since the luminosities of the brightest stars now present in the nuclei have been found by observation to be about 10^{36} ergs per sec. and their masses (as given by the mass-luminosity relation) are about $5M_{\odot}$. The conversion of hydrogen to helium supplies an energy of about $7{\cdot}2 \times 10^{18}$ ergs per gram. The lifetimes of these stars are accordingly of order $7{\cdot}2 \times 10^{16}$ secs. $= 2{\cdot}4 \times 10^{9}$ years. This somewhat underestimates the age, since it assumes a luminosity of 10^{36} ergs per sec. throughout the whole lifetime, whereas the luminosity must have been smaller in the past. But allowance for this would not increase the age appreciably above 10^{10} years.

St. John's College,
Cambridge :
1947 *May* 9.

MAGNETIC AND ELECTRIC PHENOMENA IN THE SUN'S ATMOSPHERE ASSOCIATED WITH SUNSPOTS

R. G. Giovanelli

(Received 1946 December 9; received in final form 1947 December 29)

Summary

The magnetic field in the Sun's atmosphere near a sunspot, and the electric field resulting from changes in the magnetic field, are computed for an isolated sunspot growing in a non-conducting, and also in a uniformly conducting, medium. For a conductivity of 10^{-8} e.m.u., which applies in the absence of a magnetic field, it is shown that the velocity of propagation of the magnetic field is very slow; the conductivity must be less than 10^{-13} e.m.u. if the field is to penetrate to distances of the order of 3×10^9 cm. in the time of growth of the sunspot. It is shown, however, that a rapid propagation can be brought about in the atmosphere by the decrease in conductivity perpendicular to the magnetic field. The discussion is extended to include fields resulting from the growth of bipolar groups.

If the magnetic field due to other sources is negligible the current density is low, as the electric field is everywhere perpendicular to the magnetic field, in which direction the conductivity is low. When an external magnetic field is taken into consideration very different results are obtained, and currents can circulate. For a general magnetic field inclined to the Sun's surface, the currents are of two types: (*a*) a current sheet in which all the current passes through the neighbourhood of a neutral point in the magnetic field, (*b*) a volume current, all of which passes through a sunspot. This latter type is possible because the conductivity across the magnetic field increases with depth inside a sunspot. Both types of current are discussed in some detail. The present theory forms the basis of a theory of flares which will be presented subsequently.

Introduction

The magnitudes of the magnetic and electric fields in the chromosphere and corona near growing sunspots, and the associated currents, are discussed in this paper.

It is usually assumed that the magnetic field above a sunspot is similar to that from either a vertical magnetic dipole or a magnetic pole, as convenient, without examination of the rate of propagation of the field into the atmosphere. Normally the atmosphere is a good electrical conductor and, as the velocity of propagation is then very small, the above assumption needs investigation. While magnetic fields can be transported by a bulk movement of conducting material, and large movements of matter do occur in the Sun's atmosphere, our discussion is restricted to the case of a static atmosphere. A mechanism whereby electromagnetic fields can penetrate to considerable distances in a reasonably short time is given in some detail.

Consideration of the magnetic fields in the atmosphere shows that there are certain conducting paths along which current can flow if the magnetic flux linkages through them vary. Attempts are made to estimate the magnitudes of the resulting currents.

The treatment is exploratory, rather than exhaustive. In subsequent papers, theories of phenomena observed in the Sun's atmosphere, including chromospheric flares and one type of prominence, will be developed on the basis of the conclusions derived here.

Propagation of Electromagnetic Fields in the Sun's Atmosphere

Magnitudes of the Fields Assuming a Non-conducting Atmosphere.—Associated with sunspots are magnetic fields of the order of 2000 gauss (**1**), the observed direction of the field being vertical at the centre of the sunspot and horizontal at the outer edge of the penumbra. In general, the flux from the sunspot passes to some other part of the Sun's surface and does not return directly to the same sunspot, although there are rare exceptions to this. If the magnetic flux through the surface of the sunspot varies, as during its growth, an electric field must be induced in the neighbourhood. The magnetic and electric fields depend in an important manner on the conductivity of the atmosphere, but as a guide to subsequent discussion the fields will first be evaluated assuming the atmosphere to be non-conducting.

For simplicity we shall here consider two models of an isolated sunspot: (i) a current in a circle of fixed radius b equal to that of the sunspot and having an axial magnetic field H_0 equal to that observed at the centre; (ii) a semi-infinite cylindrical current sheet of the same radius and with the same axial magnetic field at its end. In both cases, the sunspot axis will be assumed vertical.

In case (i), the magnetic field H in the plane of the current is perpendicular to the Sun's surface and is given to sufficient accuracy by

$$H = b^3 H_0 / 2a^3$$

at a distance a from the centre of the sunspot, where a is large compared with b. The induced electric field E is everywhere perpendicular to the magnetic field, the lines of electric force being circles coaxial with the sunspot and parallel to the Sun's surface. In the plane of the current,

$$E = (b^3/2a^2)(dH_0/dt).$$

In case (ii), the lines of magnetic force near the sunspot are approximately radial from its centre. H is given to sufficient approximation by

$$H = H_0 b^2 / 2a^2,$$

while

$$E = (b^2/2a)(dH_0/dt),$$

the lines of electric force again being circles coaxial with the sunspot.

To illustrate the average values of E and final values of H around a growing sunspot, it will be assumed that H_0 grows at a constant rate to 2000 gauss in 50 hours, b being constant and equal to one-hundredth of the Sun's radius (i.e. approximately 7×10^8 cm.). Values of E and H in a plane containing the sunspot, as computed from the above formulae, are given in Table I. The magnitudes are similar for the two models.

Magnitudes of the Fields Assuming an Atmosphere of Uniform Conductivity.—The rate of propagation of an electromagnetic field through a medium depends on its conductivity. The Sun's atmosphere is normally a conductor, and its properties have been discussed by Cowling (**2**), who has shown that in the presence of a magnetic field, the conductivity becomes anisotropic; the conductivity

TABLE I

Electric and Magnetic Fields Surrounding a Sunspot in a Non-conducting Medium

Model	Distance from Centre of Sunspot (cm.)	Magnetic Field (gauss)	Electric Field (e.m.u.)
Circular current	$3{\cdot}5 \times 10^9$	8	$1{\cdot}55 \times 10^5$
	$1{\cdot}75 \times 10^9$	64	$6{\cdot}2 \times 10^5$
Cylindrical current sheet	$3{\cdot}5 \times 10^9$	40	$7{\cdot}7 \times 10^5$
	$1{\cdot}75 \times 10^9$	160	$15{\cdot}6 \times 10^5$

For a spot of diameter one-hundredth that of the Sun, the above distances correspond to 5 and 2·5 times the spot radius from the centre of the spot. The magnetic fields are for an axial magnetic field of 2000 gauss, and the electric fields are the average induced fields when the magnetic field grows uniformly to 2000 gauss in 50 hours. The results apply only in the plane of the Sun's surface.

at right-angles to the magnetic field decreases as the latter increases in strength. Thus a discussion of the effects of the real atmosphere becomes complex, and we shall consider first the case of an ideal atmosphere of constant conductivity.

The circular current sunspot model is used and we shall consider only its magnetic moment which may be represented during the growing stage by $\frac{1}{2}b^3H_0 \sin \omega t$. The fields will be regarded as those due to a magnetic dipole situated at the centre of the sunspot and having a moment equal to the imaginary part of $\frac{1}{2}b^3H_0e^{-i\omega t}$. Thus we require the fields due to a dipole whose moment is zero before time $t=0$, and has the above value subsequently, but as the sunspot moment can only be represented in the above way for the first quarter period, the results will be valid only during this time.

The electromagnetic field surrounding a continuously oscillating magnetic dipole in a homogeneous isotropic conducting medium is well known (3). In a plane containing the dipole, and perpendicular to its axis,

$$E = \mathscr{I} k^2(\mu/\epsilon)(1/a + i/ka^2)Ce^{-i\omega t^*},$$

$$H = \mathscr{I}(1/a^3 - ik/a^2 - k^2/a)Ce^{-i\omega t^*},$$

where $\omega/2\pi$ and C are the frequency and the amplitude of the magnitude moment of the dipole, σ and μ are the conductivity and permeability of the surrounding medium, $\epsilon = \epsilon_0 + i\sigma/\omega$ is its complex dielectric constant, $k^2 = \epsilon_0\mu\omega^2 + i\omega\mu\sigma$, $\omega t^* = \omega t - ka$, and a is the distance from the dipole; the symbol $\mathscr{I}$ indicates that the imaginary part of the whole of the expression is to be taken. In the above equations, all terms are in unrationalized (e. g. c.g.s. electromagnetic) units. In practice ω is extremely small, a value of $5{\cdot}6 \times 10^{-6}$ sec.$^{-1}$ corresponding to a sunspot growth time, from first appearance to maximum size, of 78 hours. (This value yields the same maximum value of E for $\sigma = 0$ as the simple treatment of the preceding section.) Thus unless σ is negligibly small (less than 5×10^{-27} e.m.u.), $\epsilon = i\sigma/\omega$ and $k^2 = i\omega\mu\sigma$.

We shall first discuss the magnetic field H, concerning which there is some observational evidence. The original function for the magnetic moment of the sunspot may be replaced by

$$\mathscr{I} \frac{C}{2\pi i} \int_L \frac{e^{st}}{s + i\omega} ds,$$

where $is/2\pi$ may be treated as a component frequency in the original function, and the path of integration L is a line parallel to, and to the right of, the imaginary axis, and extending from $\gamma - i\infty$ to $\gamma + i\infty$(4). Then

$$H = \mathcal{I}(C/2\pi a^3 i)\int_L \{1 - ika - k^2a^2\}\{\exp(st + ika)\}/(s + i\omega) \, . \, ds$$

$$= \mathcal{I}(C/2\pi a^3 i)\int_L \{1 + \alpha s^{\frac{1}{2}} + \alpha^2 s\}\{\exp(st - \alpha s^{\frac{1}{2}})\}/(s + i\omega) \, . \, ds,$$

where $\alpha = a(\mu\sigma)^{\frac{1}{2}}$. Now

$$\int_L \exp(st - \alpha s^{\frac{1}{2}})/(s + i\omega) \, . \, ds =$$

$$\pi i e^{-i\omega t}[\exp\{(1 - i)\alpha(\omega/2)^{\frac{1}{2}}\} \operatorname{erfc}\{\alpha/2t^{\frac{1}{2}} + (1 - i)(\omega t/2)^{\frac{1}{2}}\}$$

$$+ \exp\{-(1 - i)\alpha(\omega/2)^{\frac{1}{2}}\} \operatorname{erfc}\{\alpha/2t^{\frac{1}{2}} - (1 - i)(\omega t/2)^{\frac{1}{2}}\}],$$

which we may write as $\pi i f(\alpha, t)$, where

$$\operatorname{erfc} z = 2\pi^{-\frac{1}{2}}\int_z^\infty \exp(-x^2)dx.$$

Also

$$\int_L \alpha s^{\frac{1}{2}}\{\exp(st - \alpha s^{\frac{1}{2}})\}/(s + i\omega) \, . \, ds = -\alpha\pi i \frac{df(\alpha, t)}{da}$$

$$= -\alpha\pi i(1 - i)(\omega/2)^{\frac{1}{2}} e^{-i\omega t}[\exp\{(1 - i)\alpha(\omega/2)^{\frac{1}{2}}\} \operatorname{erfc}\{\alpha/2t^{\frac{1}{2}} + (1 - i)(\omega t/2)^{\frac{1}{2}}\}$$

$$- \exp\{-(1 - i)\alpha(\omega/2)^{\frac{1}{2}}\} \operatorname{erfc}\{\alpha/2t^{\frac{1}{2}} - (1 - i)(\omega t/2)\}] + 2i\pi^{\frac{1}{2}}\alpha t^{-\frac{1}{2}} \exp\{-\alpha^2/4t\},$$

which we may write as

$$\pi i[-\alpha(1 - i)(\omega/2)^{\frac{1}{2}} g(\alpha, t) + 2\alpha(\pi t)^{-\frac{1}{2}} \exp\{-\alpha^2/4t\}].$$

Again,

$$\int_L \alpha^2 s \exp(st - \alpha s^{\frac{1}{2}})/(s + i\omega) \, . \, ds = \pi i \alpha^2 \frac{df(\alpha, t)}{da}$$

$$= \pi i[-i\alpha^2\omega f(\alpha, t) + \alpha^3\pi^{-\frac{1}{2}} t^{-\frac{3}{2}} \exp\{-\alpha^2/4t\}].$$

Hence

$$H = \mathcal{I}(C/a^3)[\tfrac{1}{2} f(\alpha, t)(1 - i\alpha^2\omega) - (\alpha/2)(1 - i)(\omega/2)^{\frac{1}{2}} g(\alpha, t)$$

$$+ (\alpha/2)(2 + \alpha^2/t)(\pi t)^{-\frac{1}{2}} \exp(-\alpha^2/4t)].$$

It may be noted that the first factor is simply the amplitude of the magnetic field in a non-conducting atmosphere.

Values of $\operatorname{erfc} z$ for a complex z having a positive real part may be obtained from a table given by Born (5), while values for z having a negative real part are readily obtained from the relation

$$\operatorname{erfc} z + \operatorname{erfc}(-z) = 2.$$

Values of H for $\omega = 5{\cdot}6 \times 10^{-6}$ sec.$^{-1}$ and $t = 10^5$ sec., and for various values of K, where $\alpha = K(2\omega)^{\frac{1}{2}}t$, are given in Table II. a is then K times as great as the distance travelled at the so-called "phase velocity" in time t. H is expressed as a fraction of the magnetic field expected at time t in a non-conducting atmosphere. It will be noticed that the magnetic field does not differ greatly from the latter, provided $K < 3$, but is negligible when $K > 3$. Thus the magnetic field grows as if propagated at about three times the "phase velocity" $(2\omega/\mu\sigma)^{\frac{1}{2}}$, of a wave of angular frequency ω.

TABLE II

Electric and Magnetic Fields Surrounding a Magnetic Dipole in a Uniformly Conducting Medium

$K\left(=\frac{a}{t}\left\{\frac{\mu\sigma}{2\omega}\right\}^{\frac{1}{2}}\right)$	1	2	3	4	5
$H/H_{\sigma=0}$	1·18	0·82	0·30	0·057	0·0057
$E/E_{\sigma=0}$	0·98	0·60	0·20	0·035	0·0034

The values given above are the ratios of the actual magnetic and electric fields in a plane perpendicularly bisecting the axis of a magnetic dipole situated in a homogeneous isotropic conducting medium, to the corresponding fields when the medium is a non-conductor. The dipole has zero moment before time $t=0$, and moment $C=C_0 \sin \omega t$ subsequently. K gives the ratio of the distance of the point considered from the dipole to the distance travelled by a disturbance at the " phase velocity " $(2\omega/\mu\sigma)^{\frac{1}{2}}$. The particular values for which the above table applies are $\omega=5{\cdot}6\times10^{-6}$ sec. and $t=10^5$ sec.

If the magnetic field is to penetrate to distances of the order $3{\cdot}5\times10^9$ cm. in the time of growth of the sunspot, $2{\cdot}8\times10^5$ sec., then σ must not exceed about 10^{-13} e.m.u. It is generally accepted that the magnetic field from a sunspot penetrates to distances greater than this, and if this be so, the effective conductivity of the atmosphere has an upper limit of 10^{-13} e.m.u. On the other hand, it is known that in the absence of a magnetic field, the electrical conductivity is much greater than this, being of the order of 10^{-8} e.m.u. This immediately raises the question whether the magnetic field can penetrate into the atmosphere in a reasonable time, a matter to be discussed in following sections.

As with the magnetic field, the electric field due to the growing sunspot is given by

$$E=\mathscr{I}(C\mu^{\frac{1}{2}}/2\pi a^2 i)\int_L\{ak^2+ik\}\{\exp(st+ika)\}/\epsilon^{\frac{1}{2}}(s+i\omega)\,.\,ds,$$

which reduces to

$$E=\mathscr{I}(C\mu\omega/a^2)[(i/2)f(\alpha,\,t)-(1+i)(\alpha/2)(\omega/2)^{\frac{1}{2}}g(\alpha,\,t)$$
$$+\{(2i-\alpha^2/2\omega t^2)/2(\pi t)^{\frac{1}{2}}\}\exp(-\alpha^2/4t)],$$

where the first factor is simply the amplitude of the induced field in a non-conducting atmosphere.

Values of E for $\omega=5{\cdot}6\times10^{-6}$ sec.$^{-1}$ and $t=10^5$ sec., and for various values of K, are also given in Table II, E being expressed as a fraction of the induced electric field expected in a non-conducting atmosphere.

The Electrical Conductivity of the Sun's Atmosphere.—Cowling (**2**) has shown that as regards electrical conductivity the solar chromosphere and corona behave as highly ionized gases, and has expressed the electron conductivity, when the electric and magnetic fields are mutually perpendicular, in the form

$$\sigma^{\mathrm{I}}+i\sigma^{\mathrm{II}}=(rZT^{-\frac{3}{2}}-i\,8{\cdot}6\times10^3 HT/p)^{-1}\text{ e.m.u.},$$

where σ^{I} and σ^{II} are the direct conductivity (i. e. in the direction of the electric field) and transverse conductivity (i. e. in a direction mutually perpendicular to the electric and magnetic fields) respectively, Z is the mean degree of ionization (equal to unity for hydrogen), T the electron temperature (deg. K.), and p the electron pressure. r is a quantity which varies but little over a wide range of

electron concentrations and temperature, and for the chromosphere its value is approximately $1{\cdot}1 \times 10^{14}$.

The values given by the above formulae are approximations only; a better approximation is obtained when σ^{II}/σ^{I} is small by putting, for hydrogen, $Z = 0{\cdot}51$. Cowling's formula does not include the positive ion conductivity, which is of considerable importance here, and a mean free path treatment including electron and positive ion conductivities is given below.

To find the current, we follow the normal practice of resolving the electric field along and perpendicular to the magnetic field. The respective conductivities are denoted by σ_0 and σ^{I}, while the transverse conductivity, in a direction perpendicular to the plane containing the electric and magnetic fields, is denoted by σ^{II}. The conductivity σ_0 is effectively the electron conductivity, and is given by

$$\sigma_0 = ne^2\tau/m,$$

where n is the number of electrons per c.c., e and m are the electron charge and mass, and τ, the mean free time between collisions of electrons with protons, is given by

$$\tau = u^3/\pi\beta^2 NZ^2,$$

where u is the mean electron velocity, N the number of positive ions per c.c., and β a constant, equal to $1{\cdot}57 \times 10^9$ cm.^{3}/sec.^{2} (**6**). Thus putting $n = N$ and $Z = 1$,

$$\sigma_0 = e^2u^3/\pi\beta^2 m,$$

which has the value $4{\cdot}88 \times 10^{-9}$ e.m.u. if u corresponds to 5750 deg. K., as compared with Cowling's more accurate value of $7{\cdot}8 \times 10^{-9}$ e.m.u. when $Z = 0{\cdot}51$.

The direct conductivity σ^{I} is given by

$$\sigma^{I} = \frac{ne\omega\tau}{H(1+\omega^2\tau^2)} + \frac{Ne\Omega\tau}{H(1+\Omega^2\tau^2)},$$

where the first and second terms are the contributions from electrons and positive ions respectively, $\omega = eH/m$ and $\Omega = e_pH/M$, e_p and M being the proton charge and mass (**7**). For small values of H, the proton contribution is negligible, but for large values of H it predominates. If $n = N$, it is found on substituting for ω, Ω and τ that σ^{I} is a function of H/n; values of σ^{I} are given in Table III for $T = 5750$ deg. K.

The transverse conductivity σ^{II} is given by

$$\sigma^{II} = \frac{ne\omega^2\tau^2}{H(1+\omega^2\tau^2)} - \frac{Ne\Omega^2\tau^2}{H(1+\Omega^2\tau^2)}.$$

When H is small, so that $\Omega^2\tau^2 \ll 1$, the proton contribution is negligible, but when $\Omega^2\tau^2 \gg 1$, the terms become numerically equal, and σ^{II} vanishes. We shall assume that σ^{II} plays little part in the general behaviour of the electromagnetic field in the atmosphere, although it may be of importance in other respects. It will be neglected for the remainder of this paper.

The electron concentration, required for the evaluation of σ, has been given by Cillié and Menzel (**8**) as

$$n = 3{\cdot}9 \times 10^{11} \exp(0{\cdot}77 \times 10^{-8}x) \text{ per c.c.},$$

where x is the height above the base of the chromosphere. The corresponding electron pressure, at a temperature 5750 deg. K., is

$$p = 0{\cdot}30 \exp(0{\cdot}77 \times 10^{-8}x) \text{ dynes/cm.}^2.$$

TABLE III

The Electrical Conductivity of the Chromosphere

H/n gauss cm.^{3}	Electron Conductivity e.m.u.	Proton Conductivity e.m.u.	σ^I e.m.u.
0	$4{\cdot}9\times10^{-9}$	$2{\cdot}7\times10^{-12}$	$4{\cdot}9\times10^{-9}$
10^{-12}	$4{\cdot}5\times10^{-9}$	$2{\cdot}7\times10^{-12}$	$4{\cdot}5\times10^{-9}$
$3{\cdot}2\times10^{-11}$	$2{\cdot}5\times10^{-9}$	$2{\cdot}7\times10^{-12}$	$2{\cdot}5\times10^{-9}$
10^{-11}	$4{\cdot}7\times10^{-10}$	$2{\cdot}7\times10^{-12}$	$4{\cdot}7\times10^{-10}$
$3{\cdot}2\times10^{-10}$	$5{\cdot}2\times10^{-11}$	$2{\cdot}7\times10^{-12}$	$5{\cdot}5\times10^{-11}$
10^{-10}	$5{\cdot}2\times10^{-12}$	$2{\cdot}7\times10^{-12}$	$7{\cdot}9\times10^{-12}$
$3{\cdot}2\times10^{-9}$	$5{\cdot}2\times10^{-13}$	$2{\cdot}7\times10^{-12}$	$3{\cdot}2\times10^{-12}$
10^{-9}	$5{\cdot}2\times10^{-14}$	$2{\cdot}6\times10^{-12}$	$2{\cdot}7\times10^{-12}$
$3{\cdot}2\times10^{-8}$	$5{\cdot}2\times10^{-15}$	$2{\cdot}1\times10^{-12}$	$2{\cdot}1\times10^{-12}$
10^{-8}	$5{\cdot}2\times10^{-16}$	$7{\cdot}1\times10^{-13}$	$7{\cdot}1\times10^{-13}$
$3{\cdot}2\times10^{-7}$	$5{\cdot}2\times10^{-17}$	$9{\cdot}3\times10^{-14}$	$9{\cdot}3\times10^{-14}$
10^{-7}	$5{\cdot}2\times10^{-18}$	$9{\cdot}7\times10^{-15}$	$9{\cdot}7\times10^{-15}$

The conductivities given in the above table are based on the assumption that the chromosphere behaves as a highly ionized gas at a temperature of 5750 deg. K.

Electromagnetic Fields in an Ionized Atmosphere.—We shall now consider the propagation of an electromagnetic field into a static ionized medium, the discussion being restricted to the simple case where the induced electric field is perpendicular to the magnetic field; as, for example, the case where the magnetic field is due to no other cause than the growing sunspot.

If throughout the region under consideration there be a magnetic field of sufficient intensity, the conductivity of the Sun's atmosphere in the direction of the induced electric field, i.e. perpendicular to the magnetic field, will be so low that changes in the field, such as postulated above, will be propagated rapidly. On the other hand, the rate of propagation is very small when the magnetic field is small, and at first sight it might appear that the magnetic field could not increase sufficiently, in the time available, to allow rapid propagation. It is necessary, therefore, to find the rate of propagation of a magnetic field into a medium whose conductivity depends on the magnitude of the field. A simple and rigorous treatment seems impracticable, but we may be able to infer the general nature of the solution from a consideration of a simpler problem, namely, the one dimensional propagation of a magnetic field, whose boundary conditions are initially $H=H_z$, $a<0$ and $H=0$, $a>0$, into a medium of constant conductivity. In cases with which we are concerned, H_z will be of the order of hundreds of gauss close to a sunspot and of the order of tens of gauss farther away. The solution may be obtained by a method similar to that used earlier in this paper, or from analogy with a formally similar and well-known problem in heat conduction. The solution is $H=H_z\,\mathrm{erfc}\,(\alpha/2t^{\frac{1}{2}})$, where, as before, $\alpha=a(\mu\sigma)^{\frac{1}{2}}$. Let $\alpha/2t^{\frac{1}{2}}=h$ when H has some given value. Then $(d\alpha/dt)_{H\ \mathrm{constant}}=h^2/2\alpha$ is a measure of the velocity of propagation of any particular value of H and is infinite for $a=0$. If a be large, the velocity of propagation into a medium in which $\sigma=10^{-8}$ e.m.u. is so small that the magnetic field of a sunspot could not penetrate an appreciable distance during its time of growth. However, we see from this problem that when the gradient of H is large the rate of propagation is large.

When we take into account the reduction in conductivity perpendicular to the magnetic field (which is the only direction of importance) caused by fields greater than about one gauss, the value of $h^2/2\alpha$ yields large velocities of propagation wherever σ is very small. At the same time the gradient of the magnetic field for H less than one gauss is maintained at such a value that the velocity of propagation equals that for the higher fields, so that the governing factor in determining the velocity is the value of σ for a large magnetic field.

For illustration purposes, the rate of penetration, which is of the order of $3(2\omega\ \mu\sigma)^{\frac{1}{2}}$, may be given for a typical case, $\omega = 5{\cdot}6 \times 10^{-6}$ per sec., $\mu = 1$, $H = 100$ gauss (which corresponds to $\sigma = 7{\cdot}1 \times 10^{-13}$ where $n = 10^{10}$ per c.c.). The velocity is then $1{\cdot}2 \times 10^4$ cm. sec. For higher values of H (i.e. closer to the sunspot) or for smaller values of n (i.e. higher in the chromosphere) the velocity will be greater.

It is worth noting that if the effects of mass movements be excluded, magnetic fields cannot be propagated to any appreciable distance beneath the Sun's surface during the time of growth of the sunspot; for the electron pressure is so high there that the conductivity is scarcely affected by magnetic fields of the magnitude expected in the case of a non-conducting surrounding medium. Since the conductivity is at least as great as 10^{-8} e.m.u., the "phase velocity" is no more than 33 cm. sec., and in a day the field penetrates, at three times this velocity, a distance of only about 86 km.

In that region of the atmosphere where H exceeds a few gauss, the electric field is essentially equal to that for similar conditions in a non-conducting atmosphere, and this is simply the induced electric field. The current density at any point is small because the conductivity in the direction of the electric field is small. Outside this region, E is very small, so that again the current density is small. It follows that under such conditions no significant amount of energy can be acquired from these fields by electrons.

The Influence of the Sun's Surface on the Fields.—So far we have discussed the fields as set up by a magnetic dipole situated in a uniform medium. Sunspots, however, appear near the boundary of two media which are individually reasonably uniform in electrical properties but differ markedly from one another; viz. the Sun's atmosphere, in which the conductivity is a function of the magnetic field strength, and the body of the Sun where, except perhaps within sunspots, the conductivity is generally unaffected by the magnetic field. The flux returning to the Sun from the atmosphere cannot rapidly penetrate the surface, as magnetic fields are propagated only very slowly through the body of the Sun. Thus the flux cannot be represented everywhere by that from a vertical magnetic dipole. Surface currents are set up which, at least during the growth of the sunspot, just neutralize at the surface any vertical component of the magnetic field due to the sunspot; at the same time these currents affect the magnetic and electric field in the atmosphere.

Usually sunspots occur in bipolar groups, and the effect of the conducting surface is to prevent the flux from one sunspot returning to the Sun elsewhere than at one or more other sunspots of opposite polarity. The magnetic field away from the immediate neighbourhood of the sunspots is almost the same as that due to two isolated poles on the Sun's surface. To the same approximation, the electric field may also be regarded as due to equal simultaneous changes in the strengths of the two poles. Further we may assume that, away from the

immediate neighbourhood of the sunspots, the electric field is due to a magnetic dipole whose axis lies in the plane of the surface, and whose magnetic moment U is equal to that of the spot group. In this case, assuming a non-conducting atmosphere,

$$E = U\mu\omega \cos \omega t \,.\, (\sin \theta)/a^2,$$

where θ is the angle between the axis of the dipole and the radius vector from the centre of the dipole. U is given simply by $lb^2H_0/2$, l being the separation between the centres of the two sunspots. Putting $\mu = 1$,

$$E = lb^2H_0\omega \cos \omega t \,.\, (\sin \theta)/a^2.$$

In conformity with data previously used, put $H_0 = 2000$ gauss, $\omega = 5{\cdot}6 \times 10^{-6}$ sec.$^{-1}$, $b = 7 \times 10^8$ cm., $l = 1{\cdot}5 \times 10^9$ cm., $a =$ (i) $1{\cdot}75 \times 10^9$ cm., (ii) $3{\cdot}5 \times 10^9$ cm. Then for $t = 0$, $E = 1{\cdot}3 \times 10^6 \sin \theta$ and $3{\cdot}4 \times 10^5 \sin \theta$ e.m.u. respectively. In this case, the lines of electric force are circles coaxial with the axis of the spot group, and thus rise vertically from the surface of the Sun.

Since the induced electric and magnetic fields are still mutually perpendicular, no appreciable currents can result from the above electric field, and also the fields are propagated through the Sun's atmosphere at the same rates as discussed in the previous sections.

Currents in the Sun's Atmosphere

The Influence of the Sun's General Magnetic Field.—Thus far we have considered orthogonal electric and magnetic fields. If there be superimposed on the field of a growing sunspot a steady magnetic field of some other origin, then the induced electric field remains unchanged but the magnetic field is altered, and the two need no longer be mutually perpendicular. The induced electric field may indeed have a strong component in the direction of the magnetic field, in which direction the conductivity is high. Such a state of affairs may be brought about by the Sun's general magnetic field (which is about 50 gauss at the poles and 25 gauss at the equator (**9**)) or may be due to other sunspots in the same or a nearby spot group.

Under these conditions, the rate of propagation of the sunspot's magnetic field into the Sun's atmosphere needs re-examination. This complex problem cannot be treated simply, and we first investigate the types of current paths which may occur on the assumption that changes in the magnetic field are propagated rapidly. We then estimate the resistances of various current paths and finally examine the rate of propagation of changes in the magnetic field.

The general magnetic field is permanent and therefore we assume that it passes through the Sun's surface unchanged in magnitude or direction. It is presumably roughly north-south and inclined to the surface. As it is of the same magnitude as the sunspot's magnetic field at distances of the order of 3×10^9 cm. from the sunspots, the two fields exactly neutralize one another at a point at some such distance, and the point where this occurs will be called a neutral point.

Some of the lines of force from the sunspot can now lead down into the body of the Sun, as is illustrated in Fig. 1, which represents a vertical plane containing a neutral point and a sunspot. The general field below the Sun's surface remains constant and this limits the number of lines of force which can pass from the sunspot down into unit area of the surface of the Sun. If we consider

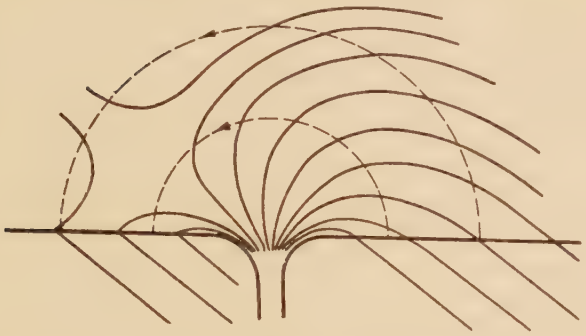

FIG. 1.—*Section through neutral point and sunspot, showing lines of magnetic force.*

A section, by a vertical plane, of the magnetic field resulting from the Sun's general magnetic field and that due to a bipolar spot group. The section, which is perpendicular to the axis of the spot group, includes a neutral point and its associated sunspot. Note that the magnetic field remains unchanged below the Sun's surface. The direction of the induced electric field is indicated by broken lines.

a spot group containing two sunspots of equal and opposite polarity, the arrangement of the lines of force will depend on the orientation of the external constant field to the axis of the group. This will probably be approximately 90° in the case of the Sun's general field and, in a plane containing the neutral point and spot group axis, the lines of force will be as shown in Fig. 2. Discussion of the currents will be limited to the case of relatively weak sunspots where the lines

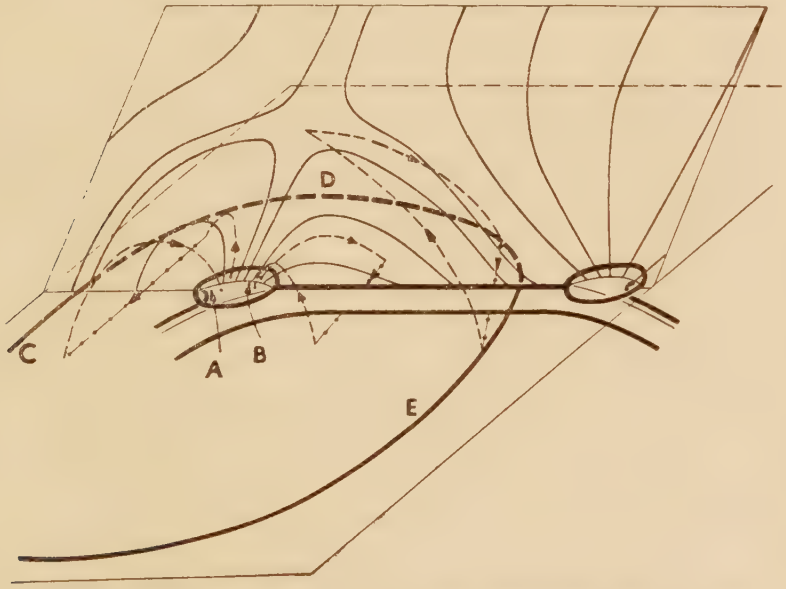

FIG. 2.—*Magnetic field and current distribution in a growing bipolar spot group.*

The lines of magnetic force are shown in a plane containing the Sun's general magnetic field, and intersecting the two sunspots (the "dividing" plane). Portion of the sub-surface toroidal magnetic field is also shown. The sunspots are relatively weak, so that their flux is captured by the general field. Typical "neutral point" and "spot" currents, as well as their relative directions, are also given. The line AB is the locus of points on the surface of the sunspot from which lines of magnetic force return to the Sun along the axis of the spot group. The curve CDE is the locus of points where lines of magnetic force from near the neutral point meet the Sun's surface, and is thus the line along which the neutral point current sheet meets the surface.

of force from the spots are all captured by the Sun's general field. This certainly does not happen with all spot groups, nor is it certain that it happens with any. Nevertheless, some of the lines of force from every spot group are captured by the general field, and the following discussion applies equally to these groups.

Currents Through a Neutral Point.—Since in the atmosphere currents must follow the direction of the magnetic field, unless the latter be weak, complete conducting circuits can occur only in limited ways. One such circuit may commence at the Sun's surface, and coincide with lines of magnetic force except close to the neutral point, near which it passes; beyond, it again coincides with the magnetic field down to the Sun's surface. Below the surface the conductivity is unaffected by the general magnetic field, and the circuit may be completed by subsurface paths on either side of the sunspot. Owing to the great cross-section available, the subsurface resistances are effectively zero.

Rather than evaluate the total e.m.f. around such a circuit from field theory, we shall find it more convenient for the remainder of this paper to estimate it from the rate of change of magnetic flux through the circuit. The question then arises, can the magnetic flux through any such circuit change?

Hale and Nicholson's remarks on the growth of a spot group have been summarized by Chapman as follows (**1**). "A typical spot group begins as two small spots, or groups of spots of opposite polarity, nearly in the same latitude, and 3° or 4° apart in longitude. The two principal spots grow rapidly and separate in longitude to a distance of 10° or more; the rear spot attains its maximum area in 3 or 4 days; the leader attains a larger maximum area in 7, 8 or 9 days. Many smaller spots develop within the group, mostly near the two main ones. The dipole moment of the group is greatest when the spots are largest and furthest apart".

Owing to the high conductivity of the Sun's surface surrounding a spot it may be expected that during its growth, there would be set up in the immediate neighbourhood currents resulting in the return of magnetic flux immediately outside the spot. Such a field in the opposite direction to that in the centre of the sunspot has not been reported and is presumably non-existent. We shall assume, therefore, that in the absence of a general magnetic field, the flux from a sunspot would pass entirely to one or more other sunspots.

The current distribution in the atmosphere depends in an important manner on the means whereby the sunspot is created, so that it is desirable to consider this. We shall, in fact, evaluate the currents on an assumed mechanism for the creation of sunspots, although the results are reasonably general; for any other mechanism, currents of the same type and magnitude will result, although their location and direction may be different. The mechanism adopted, however, must be in conformity with the observed growth of sunspots.

The exact nature of the origin of a sunspot is still not clear. There is good reason to believe that the magnetic field of the sunspot has been in existence beneath the Sun's surface for many years before the appearance of the spot. Alfvén (**10**) and Walén (**11**), for example, have proposed a theory in which the original magnetic field is approximately toroidal, the current creating the magnetic field flowing in a circle around every right section of the toroid. When such a toroid reaches the surface of the Sun, the magnetic field is thought to break through to form two spots. Alfvén attributes the breaking through the surface to the decrease in density there, but from our previous discussion, a decrease

in conductivity, such as occurs perpendicular to a magnetic field in the atmosphere, seems essential. In either case, the magnetic field during the formation of the spots is probably somewhat as shown in Fig. 3, where some of the lines of force have already broken through to form two sunspots. As further lines of force break through the surface, they add to the flux from the sunspots. We shall now use this as our sunspot model, although the following arguments can readily be modified to suit any other model of a growing sunspot.

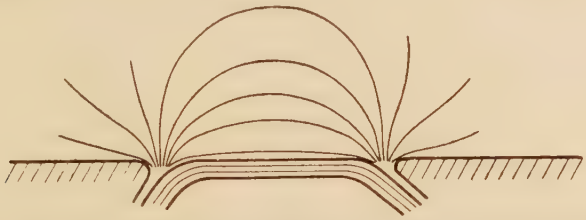

FIG. 3.—*Vertical cross-section through bipolar spot group during growth.*

The magnetic field near a sunspot group during its growth is presumably somewhat as shown above. Part of the original toroidal magnetic field is still below the surface. As lines of force break through, they give rise to an increase in the flux from the sunspots.

Although all atmospheric conducting paths of the type described above pass close to the neutral point, they are not confined to one fixed direction, for near the neutral point the magnetic field is symmetrical about the line joining the neutral point and sunspot; in general, circuits come in to the neutral points from all directions perpendicular to this line.

We shall now discuss the case in which the general magnetic field is perpendicular to the axis of the spot group (i. e. the line joining the two sunspots), and inclined to the Sun's surface at an angle ψ (see Fig. 2). Since the conductivity at right-angles to the magnetic field is high only when the field is weak, there will be only a small region near the neutral point where the current density perpendicular to the magnetic field is high. The current is elsewhere directed along lines of magnetic force, and assumes the form of a thin sheet. This is illustrated in part in Fig. 4.

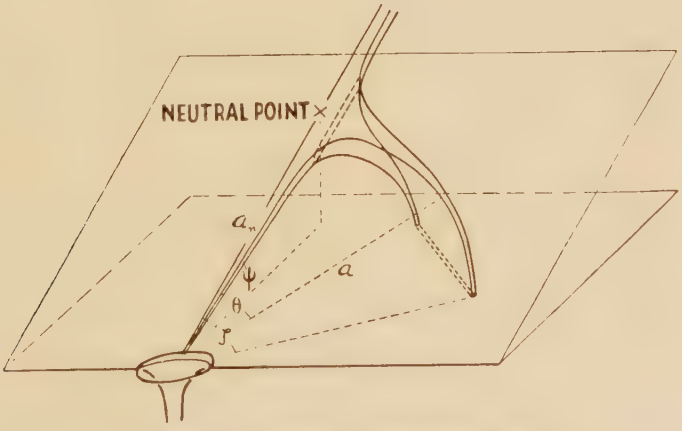

FIG. 4.—*" Neutral " point current sheet.*

Portion of a neutral point current sheet is shown above, the inclined plane lying in the direction of the Sun's general magnetic field and meeting the Sun's surface in a line containing the axis of the spot group.

With a bipolar group produced by a subsurface magnetic field parallel to the surface and which breaks through the surface as in our adopted model, the induced electric field in a non-conducting atmosphere would take the form of semicircles, concentric with the axis of the spot group, i.e. the line joining the two sunspots, and would be directed in the same sense around all these semicircles.

In considering the real atmosphere, we find it convenient to define the plane containing the Sun's general magnetic field and the axis of the bipolar group as the "dividing plane". Then since the lines of magnetic force act as conductors, the components of the induced field along the lines of magnetic force reverse direction as we pass from lines of magnetic force on one side of the dividing plane to the other. This may be seen from Fig. 1, where the magnetic field is shown in a section passing through a sunspot and perpendicular to the axis of the bipolar group. Consequently currents flow *towards* the neutral point on one side of the dividing plane, and *away* from the neutral point on the other.

Alternately, it may be seen from Fig. 2 that any circuit to the right of the neutral plane (the vertical plane containing the neutral point and its associated sunspot) which is linked with the toroid below the surface and has paths from the surface to near the neutral point, one on each side of the dividing plane, will have a flux linkage through it which, because of loss from the toroid, decreases as the sunspots grow. The above current cannot be short-circuited immediately above the toroid since, if the magnetic flux is to escape, the conductivity there must be low. Any similar circuit to the left of the neutral plane may be completed along or beneath the Sun's surface, and through this the flux linkages increase. In both circuits the currents on the same side of the dividing plane are directed both towards or both away from the neutral point.

The e.m.f. around such a circuit to the right of the neutral plane, both paths of which lie close to and on either side of the dividing plane, will be given by $\pi b^2 H_0 \cos \omega t$, the rate of change of flux through the sunspot. We shall assume here that the penetration of the magnetic field through the current sheet takes place sufficiently rapidly for the above formula to hold. The penetration is, in fact, very rapid once the magnetic field penetrates the surrounding atmosphere, and this more important factor is discussed later in this paper.

To obtain the resistance around such a path, we shall treat for convenience the case in which the magnetic field is similar to that from an isolated magnetic pole in a uniform general field G. Then

$$H = G\{(a_n^2/a^2 - \cos\theta)^2 + \sin^2\theta\}^{\frac{1}{2}},$$

where θ is the angle between the lines joining the sunspot to the neutral point and the point concerned, while a_n is the distance of the neutral point from the sunspot (see Fig. 4).

Over the greater part of this circuit, $a \doteqdot a_n$, and

$$H \doteqdot 2G \sin\theta/2.$$

Along the length of any current filament, the cross-sectional area A varies inversely as the magnetic field strength, provided this field guides the current. Thus $A = P/\sin(\theta/2)$, P being a parameter defining any current tube. Near the neutral point the magnetic field cannot guide the current, and we suppose this happens for $\theta < \theta_1$. In general θ_1 is small and, in evaluating the resistance,

may be assumed zero. Then the resistance R along any current tube, to the position $\theta=\zeta$, is easily found to be

$$R=2a_n(1-\cos\zeta/2)/\sigma_0 P.$$

To estimate the current density near the neutral point, we deduce from Cowling's conductivity formula that at right-angles to the magnetic field the conductivity is roughly constant for $Hp<2$, but is quite small for $Hp\gg 2$. We suppose the current to be directed along lines of magnetic force when Hp is greater than 2; for smaller values of Hp, the conductivity is assumed independent of the magnetic field. This assumption neglects the leakage of current across the magnetic field when $Hp>2$, and leads to a lower limit for the current density near the neutral point.

We may now calculate the cross-section of the region near the neutral point which carries currents across lines of magnetic force. The lines of force which limit the conducting path in the current sheet are those along which the minimum value of the magnetic field is $2p$, where p is the electron pressure at the neutral point. The locus of points at which the magnetic field is minimum along a line of magnetic force passing near the neutral point is the cone

$$2\Delta a=a_n\theta,$$

where $\Delta a=a_n-a$. On this cone

$$H=3^{\frac{1}{2}}G\theta$$

(the numerical factor does not quite agree with that used in the approximation for obtaining R, but this is of little importance).

The cross-sectional area A of the entire conducting sheet to the right of the neutral plane and above the dividing plane is approximately $2(\Delta a)^2$ near the neutral point. Thus for the whole of this sheet,

$$P=AH/2G=2a_n^2\,p^3/3G^3$$

and

$$R_1=3G^3(1-\cos\zeta_1/2)/\sigma_0 a_n p^3,$$

ζ_1 being a mean value of ζ for points where the current sheet on one side of the dividing plane enters the Sun. Similarly R_2, the resistance of the path on the other side of the dividing plane, is given by a similar formula in which ζ_1 is replaced by the corresponding mean value of ζ, viz. ζ_2. The total resistance $R=R_1+R_2$.

The total current I to the right of the neutral plane is given roughly by putting $\zeta_1=\zeta_2=\pi/2$; then

$$I=\pi b^2 H_0\cos\omega t\,.\,\sigma_0 a_n p^3/6G^3(1-\cos\pi/4)$$

which, using data previously given, and putting $a_n=3{\cdot}5\times10^9$ cm. and $t=0$, becomes $2{\cdot}2\times10^{13}p^3$ e.m.u.

To the left of the neutral plane (see Fig. 2) the induced current is rather smaller in magnitude. The current density, in fact, decreases gradually from a maximum near the dividing plane on the right of the neutral plane, to zero near the dividing plane on the left of the neutral plane.

The current density near the neutral point is approximately $i\,2(\Delta a)^2=1{\cdot}7\times10^{-3}p$ e.m.u., and the corresponding electric field is $1{\cdot}7\times10^5 p$ e.m.u. The cross-section of the conductor decreases away from the neutral point, and hence the current densities and electric fields inside the conductor increase correspondingly.

Currents Passing into Sunspots.—A current system of a different type can occur in the atmosphere near a sunspot group if the currents can pass through a sunspot itself. If this be so, currents could rise from the surface of a sunspot and flow along lines of magnetic force until they descend to the Sun's surface. Other currents could rise from the Sun's surface at other places and flow to the sunspot along lines of magnetic force (Fig. 2). Whether or not such currents can flow depends on the conductivity of the sunspot material perpendicular to the spot's internal magnetic field.

It is usually thought that sunspots contract below the surface, and that the magnetic field there is considerably increased. Chapman has estimated (**1**) that the field may reach 5×10^8 gauss, although the validity of his argument has recently been questioned (**12**). Walén's (**11**) treatment indicates a much smaller maximum value of about 10,000 gauss at $2{\cdot}5 \times 10^9$ cm. below the surface.

Although these magnetic fields are high, the temperature and electron pressure increase rapidly beneath the Sun's surface. It is difficult to estimate the departure of the temperature and electron pressure inside a sunspot from normal conditions at the same depth below the Sun's surface, and in the absence of better information we shall assume them identical. The conductivity at a depth of 10^9 cm. is then found to be approximately

$$\sigma^{\mathrm{I}} + i\sigma^{\mathrm{II}} = (4{\cdot}2 \times 10^6 - i26{\cdot}5H)^{-1} \text{ e.m.u.},$$

by putting $Z=3$ in Cowling's conductivity formula, and using Eddington's formula (**13**) for the pressure (mainly electron pressure) and temperature inside a polytrope for which $n=3$. σ^{I} is not significantly affected by H unless the latter be of the order of $1{\cdot}5 \times 10^5$ gauss. Thus currents of the above type seem quite feasible, crossing the sunspot's internal magnetic field at a depth depending on the strength of the latter, but in any case not far below the surface.

A complete conducting circuit can be formed by a tube of magnetic force in the atmosphere (one end of the tube passing into the sunspot, the other into the Sun's surface elsewhere), together with a return circuit through the wall of the sunspot. Alternately, a complete conducting circuit may be formed by two tubes of magnetic force in the atmosphere, along one of which the current passes into the sunspot; if inside the sunspot the resistance between the two tubes is small compared with that between either of the tubes and the wall of the sunspot, then the current may flow between the two tubes within the spot, while the body of the Sun, whose conductivity is high, can complete the circuit between the other ends of the tubes. The sense and order of magnitude of the current in the atmosphere are the same in the two cases, and we will therefore discuss only the latter case. Two such circuits are shown in Fig. 2. The current on one side of the dividing plane is all directed into the sunspot, while on the other side it is all directed out from the sunspot, the senses being the same as with neutral point currents.

We proceed to evaluate the resistances of the various elements of such circuits. For simplicity, a circuit is considered to consist of three sections, (*a*) the parts which are approximately radial from the sunspot, (*b*) the circuit through the sunspot itself, and (*c*) the remainder of the circuit. The resistance of (*c*) in fact may be neglected in comparison with those of (*a*) and (*b*).

For (*a*) we assume radial lines of force leaving the sunspot at $a=a_n/10$ extend to $a=a_n$. The resistance is $R_a = 18/\sigma_0 a_n \Delta X$, where ΔX is the solid angle of the

tube. The resistance R_b through the sunspot is difficult to estimate, but may be given in terms of the length s of a cylindrical conductor of constant conductivity equal to the value of σ_0 in the chromosphere, whose resistance equals that of the sunspot, and whose cross-section is constant and equal to that of the tube entering the sunspot, i.e. $a_n^2 \Delta X$, 100. If the spot funnels in rapidly so that the magnetic field increases by a factor of 10^3 just below the surface, and if the depth of the circuit into the sunspot is 10^9 cm., then $s = 2 \times 10^{12}$ cm. roughly. This value is little better than a guess. The total resistance R around a circuit is given by

$$R = (18 + 100s/a_n)/\sigma_0 a_n \Delta X.$$

As in the previous section, we shall discuss the case in which the external constant magnetic field is perpendicular to the axis of the bipolar group and inclined to the surface at an angle ψ.

The magnetic flux through a circuit of the type described above decreases as the spot grows, provided the circuit threads under the subsurface magnetic field of the toroid, and thus induced currents will flow around it. Some idea of their magnitude can be obtained from the following rough analysis.

Let AB (Fig. 2) be the locus of points on the sunspot, lines of magnetic force from which eventually meet the Sun's surface on the axis of the spot group, i.e. immediately above the subsurface toroid. Then the lines of magnetic force emanating from AB lie in the dividing plane, and on one side of this plane the direction of the current is into the sunspot; on the other side of the plane, it is out of the sunspot. To a first approximation, the current is symmetrical about this plane.

The value of s for current filaments close to the dividing plane will be less than for filaments well away from it, for the path across the magnetic field inside the sunspot will be least in the former case. Thus the current will be greatest close to this plane.

Before evaluating the currents, we must return to a problem previously left in abeyance, namely whether in the presence of a general field the magnetic field due to a sunspot can escape into the Sun's atmosphere in a reasonable time. We have seen earlier that the velocity of propagation of the electromagnetic field near a magnetic dipole is of the order of $3(2\omega/\mu\sigma)^{\frac{1}{2}}$. This expression may not be valid near the origin of a magnetic disturbance, but we shall assume here that it is valid everywhere.

At the dividing plane the electric field is perpendicular to the magnetic field and thus cannot give rise to any currents. (We here neglect Hall currents.) Thus the magnetic field is propagated rapidly in this plane. It is not so easy to predict the rate of propagation in other directions, but we shall suppose that this is governed by some effective value of σ. In an isotropic medium of conductivity σ_e, the current paths are parallel to the electric field and are concentric with the axis of the bipolar spot group, while the resistance of a current tube of cross-section ΔY, radius z, is $2\pi z/\sigma_e \Delta Y$. We assume the effective conductivity σ_e of the real atmosphere, at a point where the magnetic field and induced electric field are parallel (e. g. in a plane perpendicular to the dividing plane and containing the axis of the spot group, and at a distance z from the latter) to be such that the total resistance around a current tube having the same cross-section ΔY at this point also equals $2\pi z/\sigma_e \Delta Y$. Then if this point be distant b from the sunspot

through which the current passes, $\sigma_e = 2\pi z\sigma_0 a_n/(18 + 100s/a_n)b^2$. The values of σ_e/z for $b = a_n$ and the corresponding penetration velocities are given in Table IV.

TABLE IV

Circuits through Sunspots

s (cm.)	σ_e/z (e.m.u.)	Penetration velocity $\times z^{\frac{1}{2}}$ (cm.$^{\frac{1}{2}}$ sec.$^{-1}$)	E (e.m.u.)
10^7	10^{-18}	$3{\cdot}3 \times 10^6$	$2{\cdot}7 \times 10^5$
10^8	$8{\cdot}6 \times 10^{-19}$	$3{\cdot}6 \times 10^6$	$2{\cdot}3 \times 10^5$
10^9	$3{\cdot}8 \times 10^{-19}$	$5{\cdot}4 \times 10^6$	$1{\cdot}0 \times 10^5$
10^{10}	$5{\cdot}9 \times 10^{-20}$	$1{\cdot}4 \times 10^7$	$1{\cdot}6 \times 10^4$
10^{11}	$6{\cdot}3 \times 10^{-21}$	$4{\cdot}3 \times 10^7$	$1{\cdot}7 \times 10^3$
10^{12}	$6{\cdot}3 \times 10^{-22}$	$1{\cdot}4 \times 10^8$	$1{\cdot}7 \times 10^2$
10^{13}	$6{\cdot}3 \times 10^{-23}$	$4{\cdot}3 \times 10^8$	$1{\cdot}7 \times 10$

In the above table, s is the equivalent length of path through a sunspot, σ_e the effective conductivity at a point distant z from the spot group axis in a plane perpendicular to the dividing plane, the penetration velocity being measured at this point. The electric field E corresponds to a distance $a_n = 3{\cdot}5 \times 10^9$ cm. from the spot and for a circuit everywhere close to the dividing plane. E varies approximately inversely as the square of the distance from the spot, so that at the edge of the sunspot it may be one hundred times as great as indicated. E is computed for $\omega = 5{\cdot}6 \times 10^{-6}$ sec.$^{-1}$, $H_0 = 2000$ gauss, $\cos \omega t = 1$.

It is clear from these data that for filaments lying near the dividing plane, the field may escape in a time of 10^5 sec. even if s be small; but if $z = 10^9$ cm., s must be greater than 10^{13} cm. for the field to escape in this time.

Using the values originally adopted for the rate of spot growth, the current I in any tube not too far from the dividing plane will be given roughly by

$$I = 6 \times 10^{17}\Delta X/(18 + 2{\cdot}9 \times 10^{-8}s) \text{ e.m.u.};$$

the current density at a distance a will be

$$6 \times 10^{17}/a^2(18 + 2{\cdot}9 \times 10^{-8}s) \text{ e.m.u.};$$

and in the direction of the lines of magnetic force the electric field supporting this current density is

$$6 \times 10^{25}/a^2(18 + 2{\cdot}9 \times 10^{-8}s) \text{ e.m.u.};$$

values of the electric field for $a = 3{\cdot}5 \times 10^9$ cm. are also given in Table IV.

Discussion.—We have discussed the induced electromotive forces caused by the changing magnetic fields of sunspots and have shown that in certain neighbouring regions of the chromosphere and corona whose locations depend in part on the configuration of the total magnetic field near sunspots there will be both electric fields and electric currents. The electric fields may be of the order of 10^5 e.m.u., i. e. 10^{-3} volts per cm. Free electrons under the influence of such fields can readily acquire, owing to their long mean free paths, energy sufficient to cause excitation of hydrogen and other atoms. The localization of these phenomena in the neighbourhood of sunspots suggests a basis of an explanation of solar flares. A quantitative discussion, which will be published shortly, shows that many of the essential phenomena of flares can be so explained. The theory also leads to possible explanations of other observed phenomena, for example a certain type of prominence and the emission of radiation in the one-metre band.

Acknowledgments

It is with pleasure that I acknowledge the help obtained throughout from discussions with Dr G. H. Briggs, Mr J. Mackenzie, Mr A. F. A. Harper and other officers of the Council for Scientific and Industrial Research and, in the early development of this work, with Dr C. W. Allen and Dr D. F. Martyn of the Commonwealth Observatory, Canberra.

The above investigation has been carried out as part of the programme of the Commonwealth Council for Scientific and Industrial Research.

Commonwealth Council for Scientific and Industrial Research,
Division of Physics, National Standards Laboratory,
Chippendale, Sydney :

1946 *December* 2 *and* 1947 *December* 17.

References

(1) Chapman, S., *M.N.*, **103,** 117, 1943.
(2) Cowling, T. G., *Proc. Roy. Soc.*, **183** A, 453, 1945.
(3) Stratton, J. A., *Electromagnetic Theory*, 1st ed. p. 437 (McGraw-Hill, 1941).
(4) Stratton, J. A., *loc. cit.*, p. 334.
(5) Born, M., *Optik*, p. 486 (Julius Springer, 1933). See also Fletcher, A., Miller, J. C. P., and Rosenhead, L., *An Index of Mathematical Tables*, 1st ed. p. 230 (Scientific Computing Service Ltd., 1946).
(6) Giovanelli, R. G., *Phil. Mag.*, " Electron Energies Resulting from an Electric Field in a Highly Ionized Gas ", in the press.
(7) Townsend, *Proc. Roy. Soc.*, **86** A, 571, 1912. See also Chapman, S., and Cowling, T. G., *The Mathematical Theory of Non-Uniform Gases*, 1st ed. p. 328 (Camb. Univ. Press, 1939).
(8) Cillié, G. G., and Menzel, D. H., *Harvard College Observatory Circular* 410 (1935).
(9) Hale, G. E., *Astrophys. J.*, **38,** 27, 1913. See also *Observatory*, **67,** 10, 1947.
(10) Alfvén, H., *M.N.*, **105,** 3, 1945.
(11) Walén, C., *Ark. Mat. Astr. Fysik*, **30** A, No. 15, 1944.
(12) Cowling, T. G., *Observatory*, **66,** 245, 1946.
(13) Eddington, A. S., *The Internal Constitution of the Stars*, 1st ed. p. 83 (Camb. Univ. Press, 1926).

NEW WIDE-APERTURE CATA-DIOPTRIC SYSTEMS

C. G. Wynne

(Received 1947 March 14)

Summary

The inherent limitations of the Maksutov lens are examined, both as regards the higher orders of spherical aberration (and hence maximum relative aperture) and residual oblique aberrations. Two-meniscus spherical surfaced systems are described giving a good axial correction up to $f/0{\cdot}7$ with almost complete correction of all orders of oblique aberration, other than field curvature, for a 30° field. Very large glass masses may be avoided by " paraxial division " of the menisci, and considerable departure from symmetry leads to forms in which the small residual higher order spherical aberration terms may be balanced. The degree of correction attainable, and the influence of the probable glass inhomogeneity are discussed.

The systems described by Maksutov (1), in which the aberration of a spherical mirror is corrected by a single achromatic meniscus lens, give remarkably fine results for the astronomical work for which they were designed, where small angles of field and relative apertures are required. For purposes where larger angles of field are needed, it is clear from a consideration of the form of the third-order aberration coefficients that astigmatism and oblique colour cannot be corrected simultaneously with spherical aberration, coma and axial colour. Thus if A_1, A_2 and A_3 be the spherical aberration of the two meniscus surfaces and the mirror respectively, then for spherical aberration correction

$$A_1+A_2+A_3=0$$

and taking the stop at the centre of curvation of the mirror, the coma condition requires that

$$A_1B_1+A_2B_2=0,$$

where the factors B depend on the position of the stop relative to the surface; since A_3 is not zero, (A_1+A_2) must be finite, so that for coma correction, B_1 and B_2 must be unequal*; hence the Seidel coefficient for astigmatism, of the form $(A_1B_1^2+A_2B_2^2)$ must also be finite. Similarly, since the mirror has no chromatic aberration, axial colour correction requires that the first order aberrations of the two meniscus surfaces, $C_1+C_2=0$ and the oblique colour $(C_1B_1+C_2B_2)$ must be finite.

Moreover, the correction of first order coma requires equal and opposite coma terms on the two meniscus surfaces, with respect to a stop at the centre of curvature of the mirror; it necessarily follows from this that the meniscus must be so placed that the stop position is some way removed from the meniscus

* Except for the case $B_1=B_2=0$, where the two meniscus surfaces are concentric with the mirror; but this form does not satisfy the condition for axial achromatism.

centres of curvature, that the angles of incidence of the principal ray are appreciable, and that higher orders of coma than the first will be present.*

Field curvature is, of course, not corrected in simple Maksutov systems, nor in the modifications to be described later.

The size of the uncorrected residual oblique aberrations may be reduced by reducing the thickness of the meniscus lens, but this results in an increase of the higher-order spherical aberration, both since deeper curvatures and larger angles of incidence are then required for first order correction, and since a reduced thickness reduces the effect, characteristic of meniscus lenses, of a reduction of higher order over-correction arising from the effect of the aberration of the first surface on that of the second. In the systems described in detail by Maksutov, the thickness of the meniscus is maintained at one-tenth of the aperture, and for a relative aperture of *f* 1 (which is of course outside the range for which these systems are intended) the focal length must not exceed 1·37 mm. for the axial aberration to fall within the Rayleigh limit; the astigmatic focal distance is about 0·002 of the focal length at 15° from the axis and the ratio of image sizes for the C and F wave-lengths 1·0006. These uncorrected oblique aberrations are therefore comparatively small, but as the meniscus is thickened to give any appreciable improvement in the spherical zone, they are rapidly increased.

For purposes where systems of very large relative aperture, of the order of 1:1, are required, having excellent correction in fairly large focal lengths, the Maksutov system cannot therefore take the place of the Schmidt system. However, with present methods the difficulty of production of aspheric surfaces is so much greater than for spherical ones that it appears worth while to investigate the possibility of designing an effective substitute using spherical curves. The alternatives hitherto proposed either fail to give the required high degree of correction of spherical or chromatic aberration (**2**) or still require the use of figured surfaces of less asphericity than the Schmidt (**3**). Systems employing two spherical surfaced menisci have therefore been investigated, one concave and one convex to the mirror. This immediately results in a reduction of the zonal aberration of the Maksutov system to about one-tenth with the same thickness of meniscus, and in addition a number of quite new properties appear. In the first place there are two sets of solutions.

(*a*) There is a set of solutions having each meniscus substantially corrected for first-order coma, and standing in the same relationship to the mirror centre as in Maksutov's system; astigmatism may be corrected, but the oblique colour is of the same sign on each meniscus, and increases with meniscus thickness.

* In the Maksutov meniscus, A_1 and A_2 have opposite signs, so that B_1 and B_2 must have the same sign if $A_1B_1+A_2B_2=0$. Now B (which is invariant on refraction) may be written as

$$B=\frac{H}{nu^2}\cdot\frac{(x-r)}{(x-s)(s-r)},$$

where H is the Smith-Helmholtz constant, n the refractive index, u the angular semi-aperture, r the radius of the refracting surface, and x, s, the distances of the (intermediate) stop and image positions from the vertex of the surface, all to a paraxial approximation. From the achromatic condition, $Q_1h_1^2=Q_2h_2^2$ (Q being the Abbé invariant and h the incidence height of a marginal ray to paraxial accuracy), so that Q_1 and Q_2 have the same sign, and since for a meniscus r_1 and r_2 have the same sign, so have $(s_1'-r_1')$ and (s_2-r_2); in the glass space $(x_1'-s_1')=(x_2-s_2)$, so that considering B_1 and B_2 in that space, $(x_1'-r_1')$ and (x_2-r_2) have the same sign, i.e. the image of the stop in the glass space cannot lie between the centres of curvature; the meniscus index being greater than that of air, and the stop on its concave side, the actual stop must be further removed from the centres of curvature than its image in the glass space.

(*b*) In a second set of solutions, small coma terms of like sign on one meniscus are corrected by equal and opposite terms on the other, the effective stop being situated between the centres of curvation of the two surfaces of each meniscus (Fig. 1). With such a construction, the principal ray through the stop centre makes extremely small angles of incidence with all the surfaces, and is substantially coincident with the auxiliary axis for each surface (Table I), so that the higher-order oblique aberrations become very small. In addition astigmatism, oblique colour and distortion may be corrected, and thickening of the menisci is possible to give further improvement of the higher-order spherical aberrations without affecting the oblique corrections. The overall length is much less than for the first type.

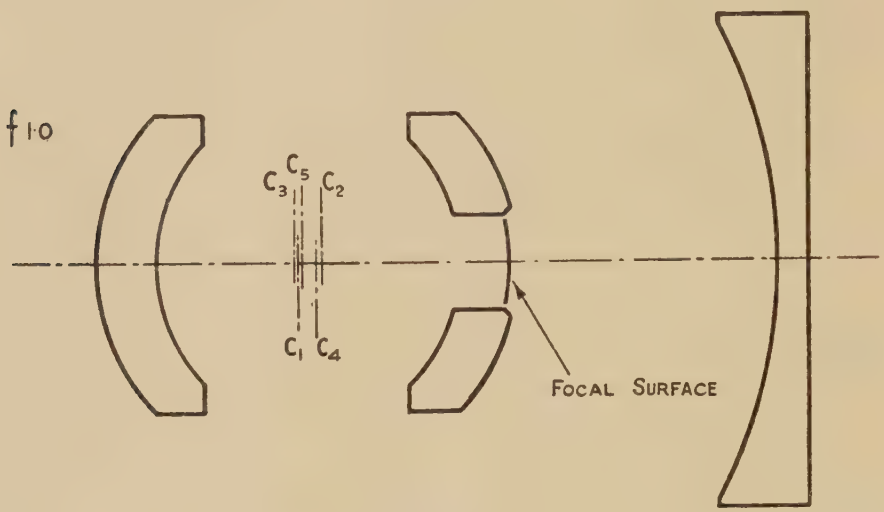

FIG. 1.

		n_d	ν
R_1	+0·9704		
		0·291	1·613	59·3
R_2	+0·7820		
		1·456		
R_3	−0·7820		
		0·281	1·613	59·3
R_4	−0·9704		
		1·232		
R_5	−2·268		

TABLE I

Angles of incidence for principal ray at 12° to axis

Surface 1	2° 08′
,, 2	0° 27′
,, 3	1° 25′
,, 4	1° 06′
,, 5	0° 00′

It is this second set of solutions which is considered in this paper. In the lens shown in Fig. 1, for an angle of field of 30°, the oblique aberrations in the meridional plane are identical with the axial to six-figure accuracy, while skew-ray traces show that in the secondary plane there is higher-order aberration producing about a 20 per cent improvement over the axial spherical aberration.

The axial spherical aberration for a relative aperture of $f/1$ produces a departure of the emergent wave-front from the spherical of about a quarter of a wave-length per 25 mm. of focal length.

Fig. 2 shows a similar design, having considerably thicker lenses, and hence better axial correction; in this case the emergent wave-front departs from the spherical form by about 1/7 of a wave-length for 25 mm. of focal length at a relative aperture of $f/1{\cdot}0$, and about one wave-length at an aperture of $f/0{\cdot}7$. The oblique aberrations at $f/1{\cdot}0$, as in the previous system, are substantially identical with the axial.

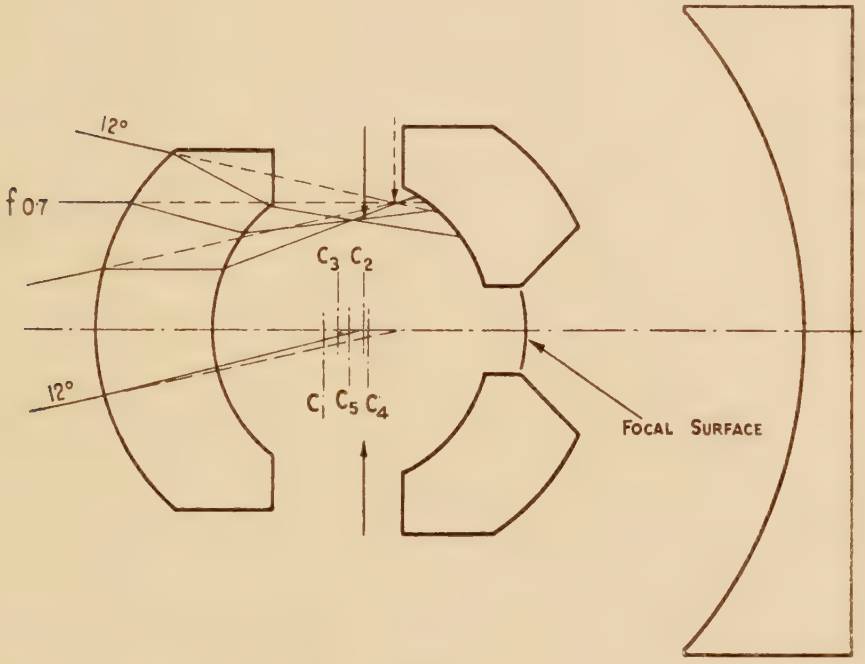

FIG. 2.

			n_d	ν
R_1	+1·237			
		0·609	1·613	59·3
R_2	+0·8378			
		1·443		
R_3	−0·8378			
		0·609	1·613	59·3
R_4	−1·274			
		1·103		
R_5	−2·466			

At the aperture of $f/0{\cdot}7$ another effect becomes significant; the axial point of the stop is virtually free from aberration, but the edges of the stop suffer from a higher order aberration which, in the meridional plane, is of symmetrical form, as shown in Fig. 2; this corresponds to a displacement of the effective stop position, variable with incidence angle. This means that, although at any angle up to 30° of field the coma is completely corrected, to six-figure accuracy, with respect to the stop position appropriate to that angle, the necessary use of a fixed stop introduces a higher order coma in the final image; with the original stop position, this may be completely eliminated for a field angle of 30°, by

introducing vignetting stops reducing the effective aperture by 6 per cent; or, by taking a new stop position which is a compromise between the positions required for different incidence angles, a much smaller vignetting factor is needed to give oblique correction equivalent to the axial.

At apertures much greater than $f/1{\cdot}0$ the chromatic difference of spherical aberration also becomes more significant, but by balancing this against a small first order chromatic term, the residual errors, from *d* to F, at a relative aperture of $f/0{\cdot}7$, are reduced to less than one (yellow) wave-length for 25 mm. of focal length, and less than half this from C to *d*.

It will be clear that in double meniscus lenses of these types the variables at the designer's disposal are more than are required to fulfil the conditions for the correction of the first-order aberrations. Regarding the ratio of the combined axial thicknesses of the menisci to the equivalent focal length as fixed by the degree of correction of zonal spherical aberration required, and disregarding the possibility of variation of refractive index (which has little effect on the performance of the systems *) the variables are five curvatures, one thickness and two separations, making eight in all; the conditions to be fulfilled are the determination of focal length, four Seidel conditions (neglecting field curvature) and two chromatic conditions, making seven.

Moreover, on account of the very small angles of incidence of the principal rays throughout the system, the distortion remains small for modifications of the system which maintain these small incidence angles. Neglecting distortion, therefore, the variables are sufficiently numerous to enable two other conditions to be fulfilled. This flexibility has been used in the example shown in Fig. 1 by making the curvatures of the concave and convex surfaces the same on each meniscus, the axial thicknesses being then slightly different for full correction; the uncorrected "pin-cushion" distortion amounts to 1·1 minutes of arc for the worst zone of a 30° field.

This possible adaptability of the system may also be employed in another way, to overcome the practical difficulties likely to be encountered in making lenses of great focal length and aperture having a high degree of correction. If such lenses were made, of the form shown in Fig. 2, for example, very large pieces of glass would be required, which would be disadvantageous on account of absorption, lack of homogeneity, and difficulty of supply. Now if, in a thick meniscus lens, a central air-lens be introduced, bounded by concentric surfaces centred on the paraxial focus in the glass space, then two thin lenses will result, having the same power, first-order spherical aberration, coma, axial and oblique chromatic aberrations as the original thick lens (Fig. 3). The higher-order spherical aberration introduced is of the correct sign to improve the correction of the system, but is quite small in amount; first-order astigmatism results, which may readily be corrected by small modifications in the separations of the

* In the lenses described in the earlier part of this paper, the calculated performance of lenses computed for different refractive indices is very nearly constant ; but lower indices lead to deeper curves and higher angles of incidence at large apertures, with consequent greater reflection losses ; moreover, the "blooming" of lens surfaces to reduce reflection is less efficient for low index glasses, due to the absence of film materials with very low indices. For small sized lenses, therefore, where difficulties of supply and the variation of probable inhomogeneity between glass types need not be considered, dense barium crowns have some slight advantage. For the lenses described later in the paper, with balanced high-order spherical aberration, lower indices lead to a rather more rapid loss of this correction as field angle is increased.

menisci and the mirror; the field curvature is very slightly improved; and distortion is introduced in an amount which though small is not wholly correctable without an undesirable departure from the near-concentricity of the original system. The higher-order coma introduced is small for an aperture of $f/0{\cdot}7$. This division of a single thick meniscus into two thin ones, with a great saving of size of glass could, of course, be applied to each meniscus in the systems already described, and this would provide the possibility of balancing the distortion, but it represents a considerable increase in the complexity of the system.

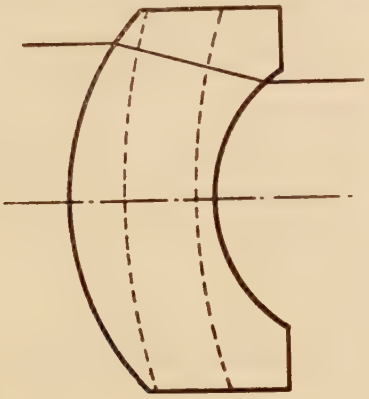

FIG. 3.

Alternatively, since the improvement of the spherical zone is achieved by an increase of thickness of either meniscus, a form may be chosen having one very thick meniscus, divided by an air-lens, and one thin meniscus (Fig. 4). This process of increasing the thickness of the front meniscus and decreasing that of the back necessarily requires, for full correction, a departure from separate achromatism of the menisci, and an increase of the relative contribution of the front to the correction of the spherical aberration of the mirror. Over a considerable range of change of relative thicknesses, the higher-order spherical aberration remains approximately constant for a given sum of axial thicknesses; this continues to be the case even after the total effect of the back meniscus on the spherical aberration of the system changes from over-correction to under-correction, but as the process is pushed further a point is reached at which the higher-order under-correction on the back surface of the back meniscus increases very rapidly, making possible a controlled balancing of the higher orders of aberration and hence a very great improvement in the axial correction. Thus in the lens shown in Fig. 4 with a relative aperture of $f/0{\cdot}75$ the emergent wave-front for *d* light on the axis departs from the spherical by less than $\pm 0{\cdot}09$ wave-length per inch of focal length.

This higher-order spherical aberration arises, of course, from the fact that to the Seidel degree of approximation the aberration on any surface is independent of the aberration of previous surfaces, and in this system light incident on the sixth surface is heavily over-corrected, this having the effect of increasing the higher-order aberration at that surface; and the angles of incidence for this surface being relatively and controllably large for large apertures, this increase is significant and controllable in magnitude. A similar effect arises in Gauss objectives, and is used in the design of wide-aperture double-Gauss photographic lenses.

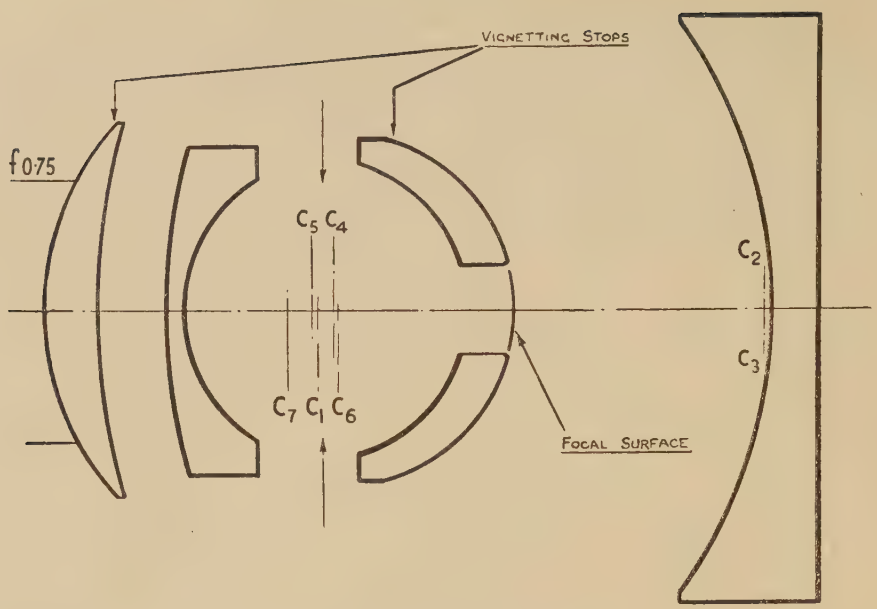

FIG. 4.—*Equivalent focal length* 1·00.

			n_d	ν
R_1	+1·4430			
		0·2748	1·613	59·3
R_2	+3·5222			
		0·3665		
R_3	+3·1557			
		0·0916	1·613	59·3
R_4	+0·8172			
		1·4468		
R_5	−0·7811			
		0·2639	1·613	59·3
R_6	−0·9143			
		1·4173		
R_7	−2·5280			

For points off the axis this higher-order spherical aberration affects the two sides of the aperture differently; and since the second meniscus is convergent, its thickness decreases away from the axis, with a consequent reduction in the under-correction with increasing angle of field, so that the advantage of this form decreases; but some advantage is retained over small field angles. Fig. 5 shows the departures of the wave-fronts from the spherical for different field angles, the spherical image surface having been chosen to give the best general result for a 31° field; for this image surface there is "barrel" distortion of 1·2 minutes of arc for the worst zone. If a smaller field were to be used, the best radius of image surface would be slightly different, giving rather less aberration for the smaller angles than that shown. For the larger angles of field, aberration increases very rapidly at the edge of the aperture, making it desirable to employ vignetting stops; these are shown in Fig. 4; they reduce the size of the nominal pupil area (neglecting the central obstruction) to 97·8 per cent of its axial value at $12\frac{1}{3}°$ from the axis.

This same method of higher spherical aberration control by the use of one thick and one thin meniscus does not of course depend on the thick one being

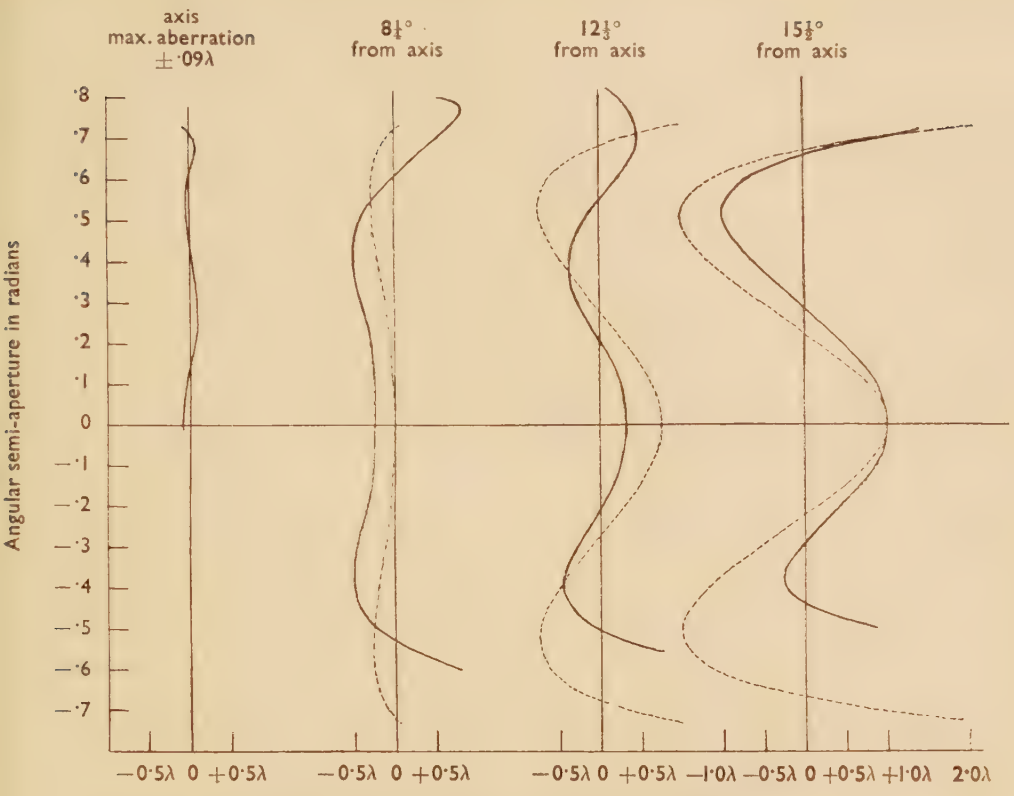

FIG. 5.—*f*/0·75 *system.* 1 *inch focal length.*

Departure of the emergent wave-front from a sphere centred on the spherical image surface.
Full line—Meridian section.
Dotted line—Sagittal section.

"paraxially divided" into two, and for smaller apertures the thicknesses involved may not require this. Fig. 6 shows a *f*/1·0 lens using two single menisci in which the axial aberration is less than ± 0·04 wave-length per inch of focal length, the aberration of the completely unvignetted emergent wave-fronts being shown in Fig. 7 for different field angles up to 30° (Fig. 7A shows, on the same scale, the aberrations of the meridional and sagittal sections for a semi-field of 12° of a *f*/1 Schmidt lens, having a corrector plate whose central and marginal thicknesses are equal). The effect of increase of angle is similar to that on the *f* 0·75 system. In all cases the wave-fronts are shown neglecting the necessary central obstruction, since the size of this depends on the field angle used. In both the *f*/1·0 and the *f*/0·75 systems, a small first-order axial chromatic aberration has been introduced to compromise the effects of chromatic difference of spherical aberration, and for the *f*/0·75 a small first-order oblique chromatic aberration is also required. The curves for the deviation of the C and F wave-fronts from that for *d* light for a meridian section is shown in Figs. 8 and 9. The virtual elimination of secondary spectrum characteristic of Maksutov systems is of course shared by all these meniscus lenses. It will be clear that, except when nearly monochromatic light is used, the residual chromatic aberrations are the limiting factor in the performance of both systems on the axis, and for the *f*/0·75 over most of the field. This is also true of the axial correction of Schmidt systems,

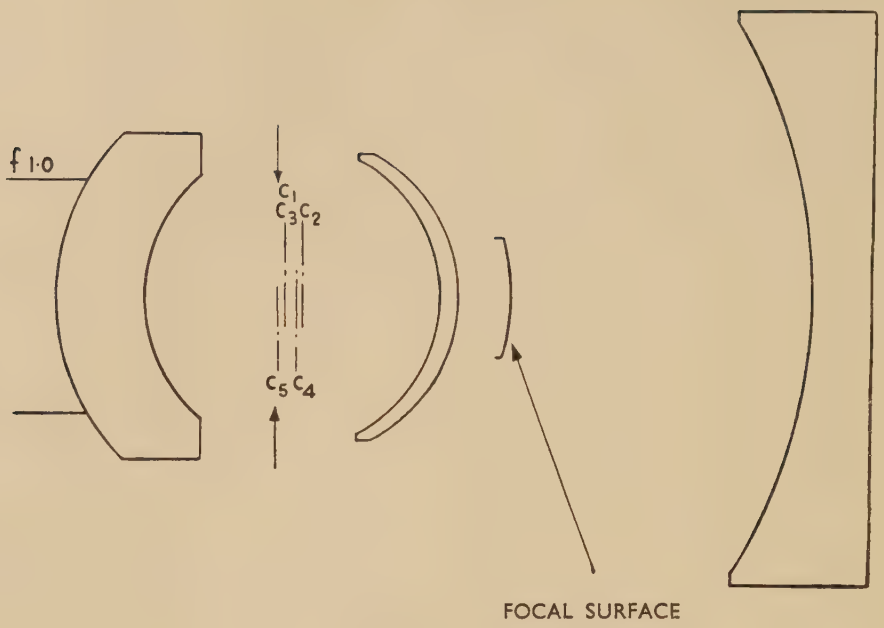

FIG. 6.—*Equivalent focal length* = 1·00.

			n_d	ν
R_1	+0·9676			
		0·3810	1·613	59·3
R_2	+0·6718			
		1·2529		
R_3	−0·6666			
		0·0762	1·613	59·3
R_4	−0·6837			
		1·4772		
R_5	−2·2455			

and the "Meniscus-Schmidt" systems described by Hawkins and Linfoot (3) *, and in all three systems the amount of the axial chromatic aberrations is similar. In the double meniscus and Schmidt systems the axial chromatic aberration curves are almost identical in form, but the errors are of opposite sign (Fig. 10). This may be expressed physically as the fact that the paraxially achromatic Schmidt plate, having the form $(n-1)x = ay^4 + by^6$ etc., has an effective glass thickness increasing for large values of the aperture y, whereas the paraxially achromatic meniscus lens decreases in effective thickness for large apertures in similar amount; these trends are unaffected by small departures from paraxial achromatism.

The similarity of form of the curves in the two cases is remarkable, and it is clear that the possibility exists of virtually complete corrections of the axial residual chromatic aberrations of the Schmidt by a combination of aspherized plate and meniscus lens correctors, in which the spherical aberration correction is divided appropriately between the two. The amount of figuring of the

* I am indebted to Dr Linfoot for the numerical data of the $f/1{\cdot}2$ Meniscus-Schmidt lens to which the curves of Fig. 10 relate; this was computed by him and Miss Hawkins after the publication of their paper (3) and departs slightly from the example given there. The plate glasses are changed to MBC 576594 and LF 575426, the front face of the plate is slightly convexed ($r = 39{,}000$ in.) and the interface radius $r_2 = -65{\cdot}83$ in. The effect of the changes is to improve the colour correction, which was incorrectly treated in (3) owing to a mistake in calculation. It is clear from the curves that the system was designed to give the optimum correction in the C–F range.

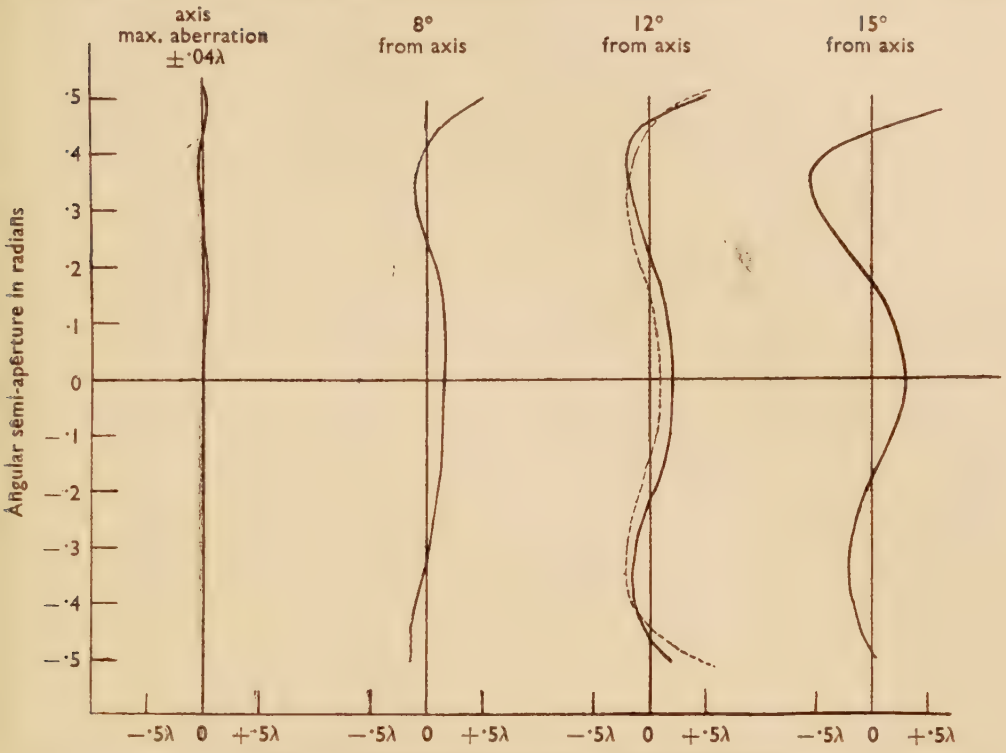

FIG. 7.—*Unvignetted f/1·0 system. 1 inch focal length.*

Departure of the emergent wave-front from a sphere centred on the spherical image surface for different angles of field.

Full line—Meridian section.

Dotted line—Sagittal section.

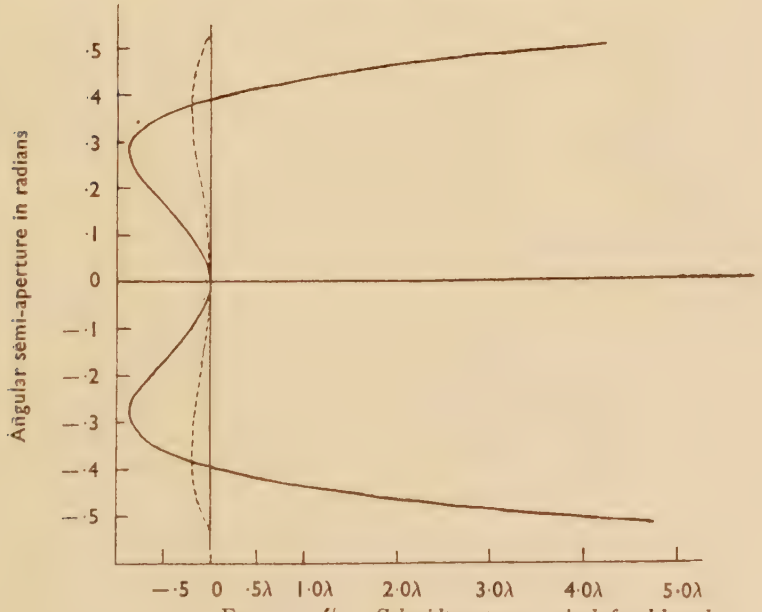

FIG. 7A.—*f/1·0 Schmidt system. 1 inch focal length.*

Departure of the emergent wave-front from a sphere for an object 12° from the axis.

Full line—Meridian section.

Dotted line—Sagittal section.

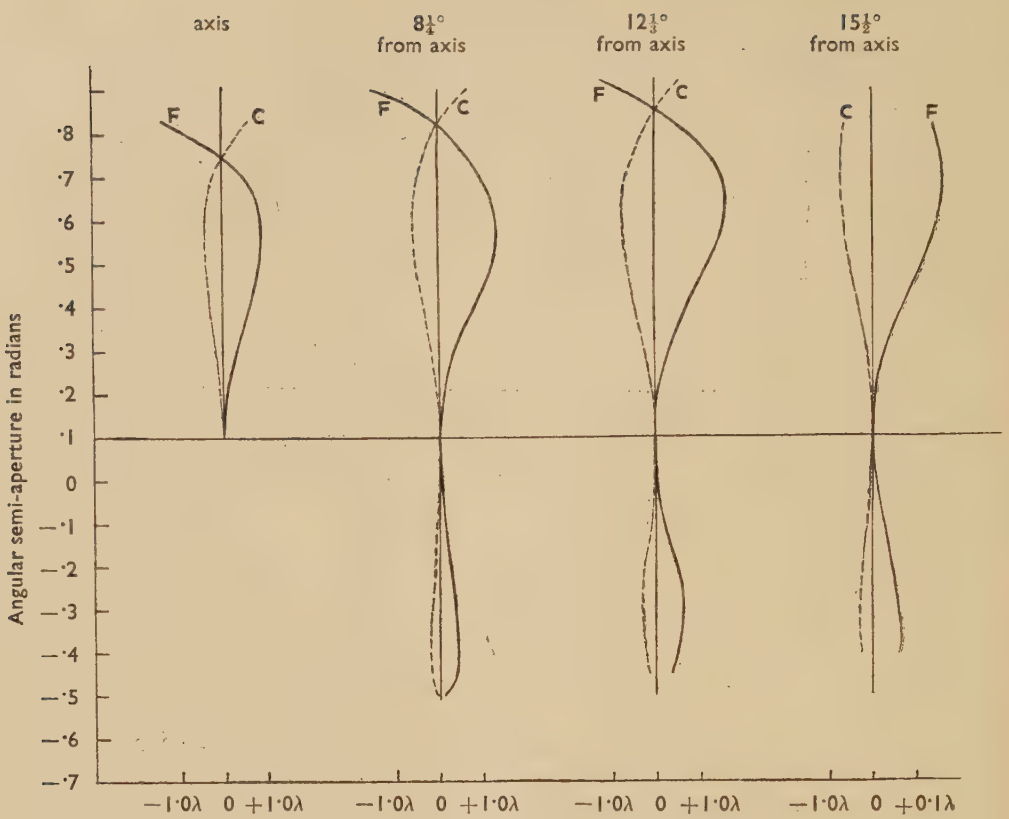

FIG. 8.—*f*/0·75 *system.* 1 *inch focal length.*
Aberration of the emergent wave-fronts for C and F with respect to the d wave-front.

Schmidt plate will of course be greater than in the "Meniscus-Schmidt" systems, and in consequence the oblique monochromatic corrections, arising from the inclination of the plate for oblique pencils, though superior to the Schmidt, will be inferior to those of either the "Meniscus-Schmidt" or double meniscus systems; but for small angles of field such systems offer the possibility of very wide aperture systems with perfection hitherto unapproached. Such combinations would seem to merit further investigation (**4**).

Although the slight figuring of the "Meniscus-Schmidt" lens is too small to produce this effect, it is interesting to observe that the chromatic difference of spherical aberration of the cemented doublet plate does, for C light, produce a considerable correction, but this is not maintained for all wave-lengths, due to the different relative partial dispersions of the crown and flint glasses used.

In comparing the performance of Schmidt and double meniscus systems, the axial corrections may be considered as effectively equal, since the chromatic aberration is almost identical, and in the presence of this the difference between the theoretically perfect monochromatic aberration of the Schmidt and that attained in the meniscus systems is clearly negligible; for oblique imagery the aberrations of the meniscus system are notably smaller.

Secondly, account must be taken of the probable vitiation of the calculated performance by the inhomogeneity of glass which must always be present to some extent. Unfortunately precise numerical information on this point does

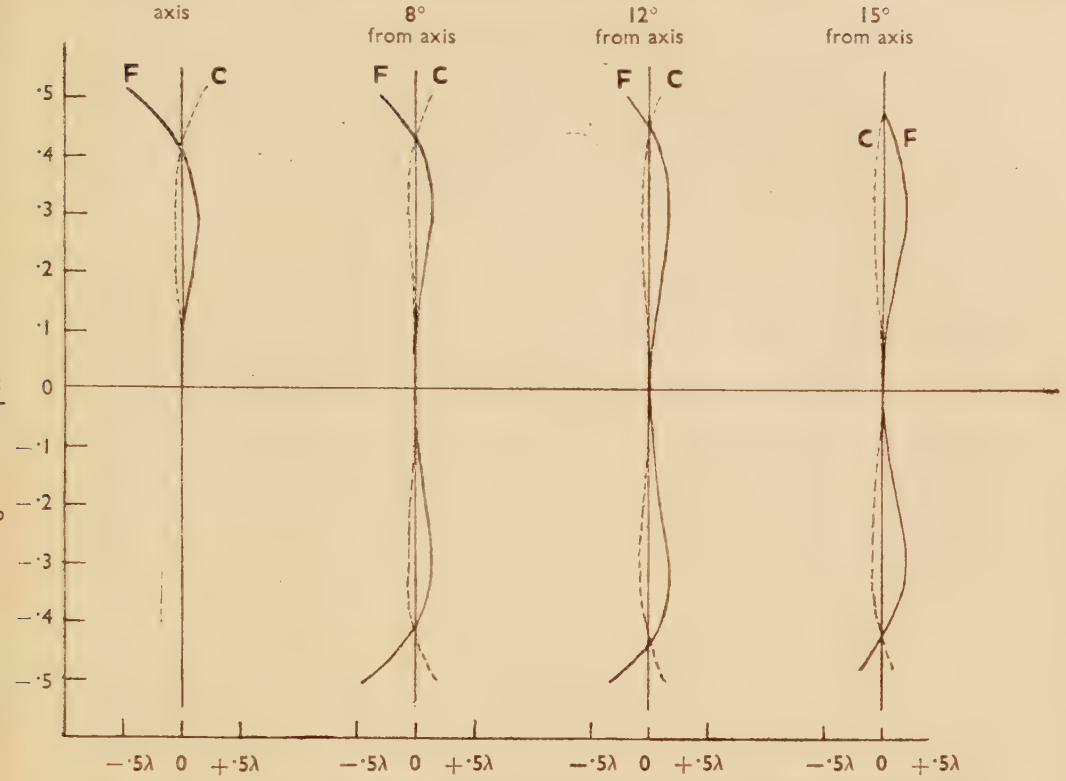

FIG. 9.—*f*/1·0 *system. Aberration per inch of focal length, of the C and F wave-fronts, with respect to the d wave-front.*

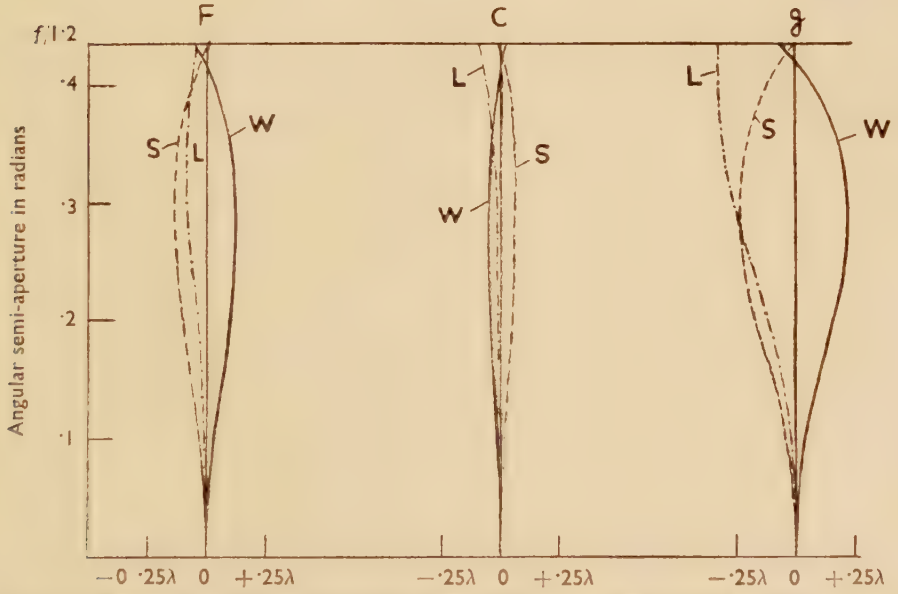

FIG. 10.—*Comparison, at f*/1·2*, of the axial chromatic aberrations for F, C and g with respect to d.*
S—Schmidt.
L—Linfoot's Meniscus-Schmidt.
W—Two Meniscus System.

not appear to have been published; but it is probable that the variation of refractive index increases with the size of glass block, and for lenses of considerable thickness it is obvious that quite small amounts of heterogeneity will introduce several wave-lengths of aberration. Inhomogeneity thus clearly sets a limit to the degree of correction that it is profitable to pursue in design. For very large systems, the Schmidt type will have a definite advantage from its smaller glass thickness despite the much greater difficulty of production.

Inhomogeneity errors may of course be corrected by the very laborious process of two-dimensional figuring, in any of these systems; but the diameter of the Airy-disk is 0·0014 mm. for an aperture of $f/1$ and 0·0010 mm. for $f/0{\cdot}7$ *, and in practice rather smaller than this, since an annular aperture is used, so that it appears probable that for many purposes other considerations, such as grain-size of photographic emulsions, would preclude the use of the calculated resolving power, even if this were attained. But for systems of fairly small focal length, say 100 mm., the optical inhomogeneity becomes of negligible importance, and it is possible that applications may be found for such lenses of relative aperture $f/1$ to $f/0{\cdot}7$, giving the full theoretical resolving power over a considerable angle of field.

52 *London Lane,*
Bromley, Kent:
1947 *March* 14.

References

(1) Maksutov, D. D., *J. Opt. Soc. Amer.*, **34**, 270, 1944.
(2) British Patent No. 544,694, 1941.
(3) Hawkins, D. G., and Linfoot, E. H., *Nature*, **157**, 445, 1946; and *M.N.*, **105**, 334, 1945.
(4) Wynne, C. G., *Nature*, **160**, 91, 1947.
(5) Hopkins, H.H., *Proc. Phys. Soc.*, **55**, 116, 1943.

* Dr H. H. Hopkins has shown (5) that the Airy-disk formula is substantially correct for a relative aperture of $f/0{\cdot}7$.

THE DAYLIGHT METEOR STREAMS OF 1947 MAY–AUGUST

J. A. Clegg, V. A. Hughes and A. C. B. Lovell

(Communicated by P. M. S. Blackett)

(Received 1948 March 9)

Summary

During the autumn and winter of 1946–1947 the well-known meteor showers were investigated by the radio echo technique on 4·2 m. wave-length. The results, both as regards activity and radiant areas, conformed closely to expectation from previous visual work. But during the investigation of the η Aquarids, which commenced on 1947 May 1 it was found that the well-known shower with its radiant near η Aquarii was not an isolated event, but merely the beginning of a great belt of meteoric activity extending towards the Sun observable only in daylight. Initially the main radiant of this new daylight shower was in Pisces, but the phenomena developed with great rapidity and by the end of June at least seven centres of considerable activity had been delineated, extending in the ecliptic up to $\alpha = 90°$. This daylight activity continued throughout July and August, and comparison with the known major showers indicates that it is without precedent in extent and duration.

1. *Introduction.*—The evolution of the radio echo technique for the study of meteors has enabled a systematic survey to be made of meteoric activity, unhampered by cloud or daylight. In this work the daylight investigations are of particular interest, since they yield information about the meteor streams falling on the sunlit side of the Earth. During the summer of 1945 Hey and Stewart * delineated two daylight radiants between June 6 and 13 and during the daylight hours of 1946 May, June and July, Prentice, Lovell and Banwell † found a high general level of meteoric activity. The real significance of these results was not immediately apparent, since little evidence existed as to the relation between the number of radio echoes and the number of visible meteors. During the autumn and winter of 1946–47 a careful survey was made of the known meteor showers from which it was apparent that, with the radio wave-lengths and apparatus constants used in this work, a close relation existed between the number of radio echoes and the number of meteors seen by a visual observer. After discussing these relationships this paper describes the investigation of the daylight activity from 1947 May to August, which was of a most extensive and unexpected character.‡

2. *The Relation between Radio Echoes and Meteors.*—The short duration radio echoes originating in the neighbourhood of 100 km. above the Earth's surface have been studied since 1929, and it was demonstrated in the early days of this work by Skellett §, Schafer and Goodall ‖ that meteors were, at least in part, responsible for these echoes.¶

* Hey, J. S. and Stewart, G. S., *Proc. Phys. Soc.*, **59**, 858, 1947.

† Prentice, J. P. M., Lovell, A. C. B. and Banwell, C. J., *M.N.*, **107**, 155, 1947.

‡ A preliminary announcement of the discovery of this daylight activity was made in *B.A.A. Circulars* Nos. 282 and 285, 1947.

§ Skellett, A. M., *Proc. Inst. Rad. Engr.*, **23**, 132, 1935.

‖ Schafer, J. P. and Goodall, W. M., *Proc. Inst. Rad. Engr.*, **20**, 1131; **20**, 1941, 1932.

¶ A review of the work on the transient echoes has been given by Lovell, A. C. B., *Phys. Soc. Rep. Progr. Phys.*, **11**, 1948 (in the press).

Until the work of Hey and Stewart * on wave-lengths in the 4 m. to 5 m. region, all previous investigators used much longer wave-lengths (~10 m. or above) and the real significance of the work to astronomy was obscured by the complexity of the echo phenomena which appeared to bear little resemblance to the main features of meteoric activity hitherto known to the astronomers. The phenomena on these longer wave-lengths are not yet properly understood, but it is now well established that on wave-lengths shorter than 6 m. the radio echoes observed are due only to the meteors which are clearly associated with the meteor streams of the type known to the visual observers. Also on these shorter wave-lengths the main radio echo is obtained only when the meteor crosses the perpendicular from the receiving station to the direction of the trail. † This aspect sensitivity leads to methods for the determination of the radiant points of the meteors ‡, and it is evident that contemporary radio technique on these short wave-lengths provides a powerful method for the investigation of the activity and radiant points of meteor streams free from the effects of cloud, daylight and the complex radio echo phenomena on the longer wave-lengths.

3. *Apparatus.*—The essential features of the apparatus have been described elsewhere.§ The wave-length used was 4·2 m.; peak power in the transmitter pulse 50 kw.; pulse recurrence frequency 150 c.p.sec. and pulse width 8 μsec. The receiver sensitivity was such that a signal of 2μV. at the receiver input doubled the signal/noise ratio. The large directional aerial system described previously ‖ was used throughout this work. Observations were made visually on a cathode-ray tube display from which the range, duration and amplitude of the radio echoes were observed.

4. *Observations of the Night-time Meteor Showers.*—The apparatus in the form described in Section 3 with the directional aerial system was first used during the Giacobinid shower of 1946 October 9–10. This work has been described previously ¶ and provided a very satisfactory proof that a high percentage of the radio echoes observed were associated with meteors from the major showers. Further experience on the well-known meteor showers also indicated that the hourly rate found on this particular apparatus was in reasonable agreement with the visual rate found by a single observer. Thus Table I shows the maximum hourly rate found by these radio echo observations compared with the maximum hourly rates predicted by Prentice ** for visual observers.

The duration of the above showers was also in good agreement with the durations predicted by Prentice. Further, when no showers are active, or when the aerial beam is directed away from its appropriate position at right angles to the direction of the radiant, the echo rate falls to approximately 1·5 per hour. It can therefore be assumed that the characteristics of new showers found by this apparatus under conditions not permitting visual observations (cloud or daylight) will be closely equivalent to the visual characteristics of the shower.

* *Loc. cit.*

† Hey and Stewart, *loc. cit.* ; Lovell, A. C. B., Banwell, C. J. and Clegg, J. A., *M.N.*, **107**, 164, 1947.

‡ Hey and Stewart, *loc. cit.* ; Clegg, J. A., in publication. (See footnote, p. 371).

§ Lovell, A. C. B., Banwell, C. J. and Clegg, J. A., *loc. cit.* ; Prentice, J. P. M., Lovell, A. C. B. and Banwell, C. J., *loc. cit.*

‖ Lovell, A. C. B., Banwell, C. J. and Clegg, J. A., *loc. cit.*

¶ Lovell, A. C. B., Banwell, C. J. and Clegg, J. A., *loc. cit.*

** *B.A.A. Handbooks*, 1946, 1947 and 1948.

TABLE I

	Radio Echo Maximum Hourly Rate			Visual Rate at Maximum	Duration of Visual Maximum
	1946	1947	1948	(after Prentice)	(days)
" No shower " rate	1·5	1·5	1·5		
Quadrantids, Jan. 3	*	50	100	40	1
Lyrids, Apr. 21	*	15	*	7 to 12	2
Perseids, Aug. 10–13	30	30	*	55	4
Orionids, Oct. 18–23	7	10	*	8 to 10	6
Taurids, Nov. 3–10	5	8	*	5 to 6	8
Leonids, Nov. 16–17	10	3	*	8	2
Geminids, Dec. 11–13	50	60	*	60	3

* Observations not made.

5. *Investigation of the η Aquarids and discovery of the New Radiant in Pisces.*— The investigation of the η Aquarid meteor stream commenced on 1947 May 1. For this purpose the radiant position was taken to be $\alpha = 333°$; $\delta = \pm 0°$, as found from previous visual observation *, and the aerial system directed accordingly.† The method of delineating the radiant points of a stream has been described by Clegg.‡

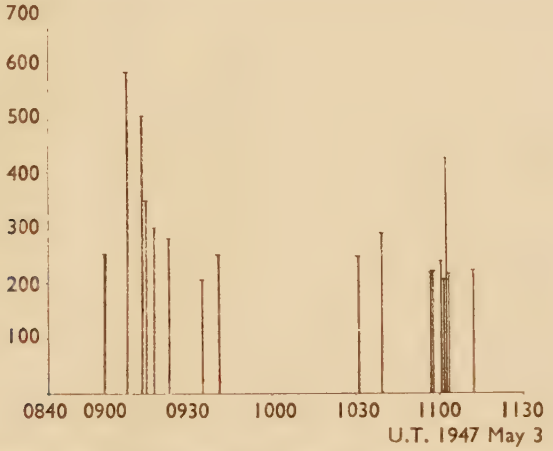

FIG. 1.—*Range/Time plots of echoes with aerial at azimuth* 110° *on* 1947 *May* 3. *Ordinates : Range in km.*

Fig. 1 shows the results obtained on 1947 May 3 between $8^h 40^m$ and $11^h 15^m$ with the aerial beam directed at azimuth § 110°. A single radiant corresponding to the η Aquarid stream passed through the beam between $9^h 00^m$

* Prentice, J. P. M., *B.A.A. Handbook*, 1948.

† In the following observations the elevation of the aerial beam was maintained constant at approximately 15°.

‡ Clegg, J. A. (in publication). The method is briefly as follows :—If the aerial azimuth is 90 , the first echoes from a given radiant will be received when this is on the meridian, owing to the aspect sensitivity of the trails. It can be shown that if the aerial is at a low elevation these initial echoes will appear at long range and that the ranges will steadily decrease as the radiant moves westwards, finally disappearing as the appropriate echo-region moves out of the beam. This gives the right ascension of the radiant, and in order to determine the declination the beam is then rotated through an angle θ to the south so that it is again in advance of the echo-region and the observations repeated. From the time interval between the first appearance of the long-range echoes in the two cases the declination can be calculated.

§ In this paper azimuth is taken as a bearing east of north.

and $10^h\,00^m$. During the next hour only two echoes were obtained (corresponding to the "no shower" rate) but between $10^h\,55^m$ and $11^h\,15^m$ a group of seven echoes appeared. This was the first indication that appreciable activity might exist well following the η Aquarid radiant. During the succeeding days this activity increased rapidly and the results with the aerial directed at 90° on May 7 between $7^h\,20^m$ and $13^h\,20^m$ are shown in Fig. 2. The η Aquarids transited

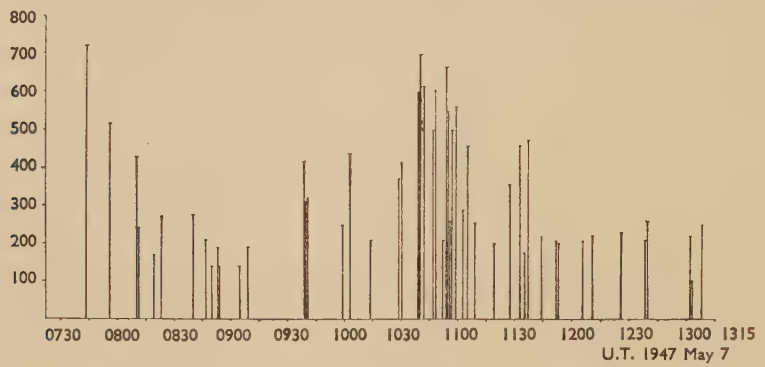

FIG. 2.—*Range/Time plots of echoes with aerial directed at azimuth* 90° *on* 1947 *May* 7. *Ordinates : Range in km.*

at $7^h\,40^m$, and after some scattered activity another clearly defined radiant passed through the beam at $10^h\,40^m$. It can be seen from Fig. 2 that the activity of this new radiant at this stage was 13 per hour, or twice the activity of the η Aquarids. The times of transit enable the right ascension of these radiants to be placed. The first is at $\alpha = 335° \pm 3°$ corresponding to the η Aquarid radiant and the new radiant at $\alpha = 20° \pm 2°$. Later observations on a different aerial azimuth enabled the declination of these radiants to be placed at $\delta = 0° \pm 3°$ and $\delta = +20° \pm 2°$. The first is thus verified to be the radiant in Aquarius already established by visual observation and the second to be a hitherto unknown radiant lying in the constellation Pisces. By twilight on this date a radiant in this position is just rising and hence cannot be seen visually.

6. *The Development and Radiants of the New Daylight Streams.*—After 1947 May 7, the daylight activity developed with great rapidity and became extremely complex. The events during the months of May to August were so unexpected and the general level of activity over a period of many weeks was so great compared with any previous events, that it became impossible with the single directional aerial to maintain a complete record. For example the situation on 1947 June 18 with the aerial directed at 90° is shown in Fig. 3. Compared with the results for May 7, illustrated in Fig. 2, it is evident that a stream of high activity transits similarly at $10^h\,30^m$ but in addition there is considerable scattered activity preceding and a series of new radiants extending on the following side for $3^h\,30^m$ in right ascension. Plots similar to those illustrated in Figs. 1–3 were obtained daily throughout May and June and check observations were then made until the commencement of work on the Perseid stream on 1947 August 1. The results of the analysis of this information are given in Table II. Columns 2, 3 and 4 of this table give the limits and duration of observation and the total numbers of echoes observed, and column 5 the principal radiants determined. The activity of ths streams cannot be directly derived from columns

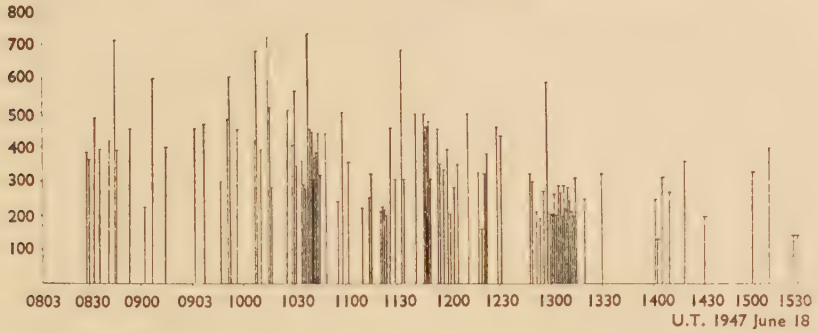

FIG. 3.—*Range/Time plots of echoes with aerial directed at azimuth 90° on 1947 June 18. Ordinates : Range in km.*

3 and 4 owing to the techniques used by which the aerial beam is set in advance of the radiant in order to observe the initial long-range echoes.* Entries in column 5 have been made only for the days on which marked radiants can be determined. Absence of entries does not necessarily imply that a particular radiant was not active but merely that the information obtained was either too confused or inadequate for a satisfactory delineation. Fig. 4 shows the areas of most intense activity on a Mercator projection of the heavens. (A B C D E F G corresponds to the tabulated radiants in Table II). During the latter part of July and August the situation became complicated by the presence of circumpolar radiants, and although the main streams of daylight activity still continued we are unable to delineate the radiant points with any precision. For example Fig. 5 shows the range-time plots for 1947 August 4 with the aerial directed at 90°. Two main daylight streams are still seen to be in transit at $10^h 20^m$ and $11^h 20^m$, but these are followed between $12^h 00^m$ and $14^h 30^m$ by an extensive series of echoes of gradually increasing range which corresponds with the lower culmination of a radiant in Lacerta. Similar range-time plots for August 26 are shown in Fig. 6. The activity was negligible until $10^h 50^m$ when a single radiant passed through the beam. After this date the daylight activity rapidly disappeared.

7. *The Activity of the Daylight Streams.*—Owing to the difficulties of resolution it is not possible to give the daily rates for each individual radiant. Fig. 7 shows the approximate mean daily rate per radiant. As shown in Table II a number of active radiants passed through the beam in succession on the majority of days. The equivalent overall visual rate would therefore have been determined by the sum of the activity for the individual radiants and hence would be considerably greater than the rates plotted in Fig. 7.

8. *Discussion.*—It is evident from the comparison of Tables I and II and Fig. 7 that the daylight meteor activity during 1947 May–August was of a different order from that of the regular night-time showers. The activity appears to have been caused by a number of very active radiants closely grouped in right ascension and declination and moving regularly in increasing longitude throughout the period. The phenomena were of great complexity and from the observations made it is only possible to describe the main features of the events as follows :—

(*a*) The η Aquarid stream (A in Table II and Fig. 4) conformed closely to predictions from previous visual observations. It existed from May 1 to 10

* See footnote, p. 371.

TABLE II

Date (1947)	Limits of Observation (U.T.)		Number of Hours	Number of Echoes	Principal Radiants* ($\alpha \pm \delta$)			
	h m	h m			A			
May 1	08 43	09 43	1·0	4				
2	09 30	10 30	1·0	12	**332±0**			
3	08 00	15 45	5·3	52	**341±0**		C	
4	05 50	15 40	8·4	67		*7+20*		*34+25*
5	03 04	13 25	8·0	45	**339±0**		**20+20**	
						B		
6	02 26	15 15	10·3	87		**354+5**	**21+20**	
7	05 30	15 40	9·6	88	**337±0**		**22+20** to	**41+20**
8	07 15	15 48	8·0	39				
9	05 38	16 20	10·4	130		**357+5**	**27+20** to	α=**38**
10	05 25	16 25	10·6	132	**343±0**		**28+29**	
11	08 44	14 37	5·5	50			**29+30** to	α=**36**
12	05 20	11 12	5·4	55			**30+30** to	**45+25**
13	04 33	15 40	10·5	133		**1+5**	**31+24**	
14	08 05	13 50	5·5	51			**32+28**	
15	07 03	12 08	5·1	52	α=*335*	**1+5**		
16	08 39	11 13	2·6	26				
17	08 20	10 30	2·0	14	α=*17, 47, 62*			
18	01 43	16 03	13·9	109				
19	08 23	13 21	5·0	22	α=*37, 68*			
20	08 13	16 11	6·1	64	α= *0, 9*			
21	07 55	14 15	6·1	62	α=*354, 19, 31*		*51+30*	
22	09 07	10 37	1·5	29				
23	08 09	14 05	6·6	96	*43+15, 50+20*			
24	07 33	13 00	4·2	53	α=*44, 51*			
25	09 40	14 06	4·4	46	*62+35*			
26	06 14	08 51	2·6	16				
27	09 03	13 30	4·1	31				
28	08 32	14 00	4·8	38	α=*35, 51*			
29	08 32	14 20	5·7	59	D		*36+30*	
30	06 33	13 30	6·4	54	**45+35**		*37+30*	
31	...	...	...	...		E		
June 1	...	...	...	...				
2	08 00	15 52	7·6	88	**45+25**	**52+15**	*39+30*	
3	08 00	13 36	4·9	40	**47+25**	**53+15**		
4	07 08	14 16	6·6	134	**47+25**	**54+15**		
5	07 20	14 56	7·5	98	**47+25**	**54+15**		
6	07 02	15 34	8·4	162	**48+30**	**57+15**		
7	11 40	16 16	4·5	50				
8	09 55	14 07	4·1	86	**49+28**			
9	07 54	15 15	7·2	149				
10	07 30	14 35	7·1	53	**51+28**			
11	07 18	14 10	6·6	110	**51+33**	**60+15**		
12	08 23	14 00	5·5	51	**53+30**	**61+15**		
13	07 10	14 00	6·7	118	**52+30**	**62+15**		
14	07 14	08 31	1·3	27	**53+35**			

TABLE II (*cont.*)

Date (1947)	Limits of Observation (U.T.)		Number of Hours	Number of Echoes	Principal Radiants * ($\alpha \pm \delta$)
	h m	h m			D E
June 15	11 00	13 11	2·1	40	
16	07 17	16 00	7·0	89	
17	07 53	14 00	3·9	141	α=**53** to **67**, δ=+**25** to +**35**
18	07 21	15 40	8·3	126	
19	07 44	16 00	8·2	88	
					G
20	07 24	15 28	8·0	111	**80**+**20**
21	12 05	16 00	3·9	37	**79**+**30**
22	11 04	12 04	1·0	34	F
23	07 35	15 57	5·7	122	**68**+**35**
24	07 25	16 08	7·6	163	**68**+**40**
25	07 26	15 30	6·4	85	**68**+**35** **83**+**25**
26	07 20	15 15	8·6	107	**66**+**30**, **67**+**35**, **84**+**25**
27	08 12	16 30	6·3	73	**68**+**30** **85**+**25**
28	09 30	12 00	2·5	56	
29	11 02	13 41	2·7	44	
30	08 36	15 07	6·1	101	
July 1	08 36	16 00	7·4	100	
2	08 45	15 30	6·7	86	α=*87* *88*+*10*
3	07 57	14 15	6·2	88	
4	09 52	14 00	4·1	72	α=*74*
5	10 40	13 20	2·6	45	*93*+*10*
7	09 15	12 20	3·1	31	α=*81*
8	09 31	10 33	1·0	13	α=*82*
10	09 17	11 20	2·1	26	α=*71*, *85*
11	11 15	12 15	1·0	8	α=*100*
12	10 40	12 35	1·9	28	
14	09 06	14 12	4·9	46	
17	09 29	14 20	4·9	58	α=*100*, *112*, *127*
21	08 37	15 18	6·4	77	
23	08 45	14 30	5·8	81	
25	10 52	13 00	2·1	33	
28	09 19	11 30	2·2	24	
30	11 00	12 30	1·5	26	
31	10 00	13 31	3·4	46	

After July 31 the programme was interrupted by work on the Perseids, and the only subsequent observations obtained were as follows :—

Aug. 1	11 00	12 00	1·0	11	
4	08 45	15 00	6·3	64	α=*103*, *120*
8	10 50	11 45	0·9	7	
19	10 13	11 43	1·5	12	
26	09 31	12 45	3·2	17	α=*134*
		Total	427·1	5298	

* The seven principal streams are indicated in heavy fount and lettered A to G corresponding with Fig. 4.

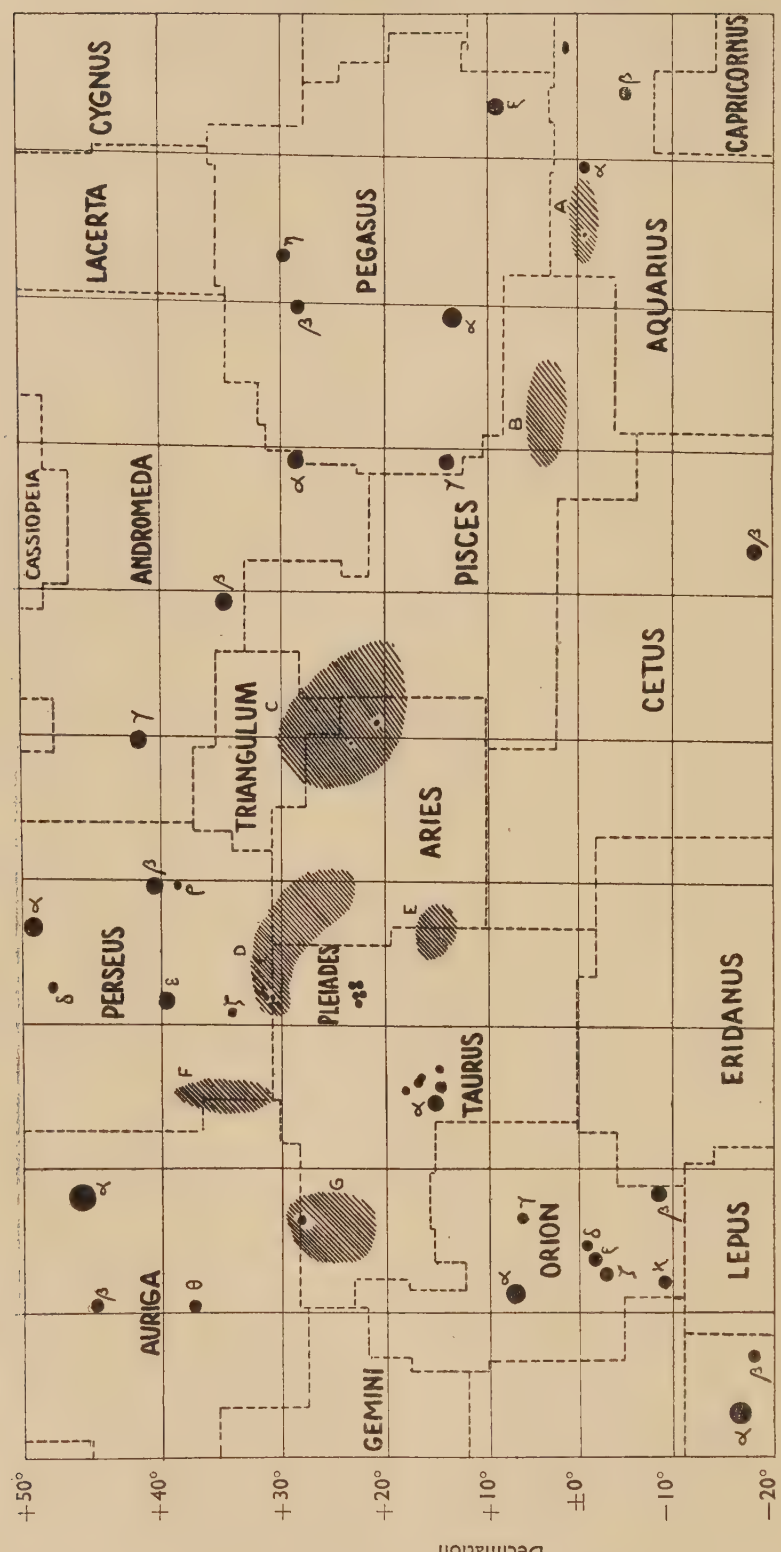

FIG. 4.—*Main Areas of Daylight Activity (Mercator Projection).*

Principal Periods of Activity :

A. *May* 1–10.
B. *May* 6–15.
C. *May* 3–15.
D. *May* 30–*June* 17.
E. *June* 2–13.
F. *June* 23→ ?
G. *June* 20→ ?

A, B, C, D, E, F, G *correspond to Table* II.

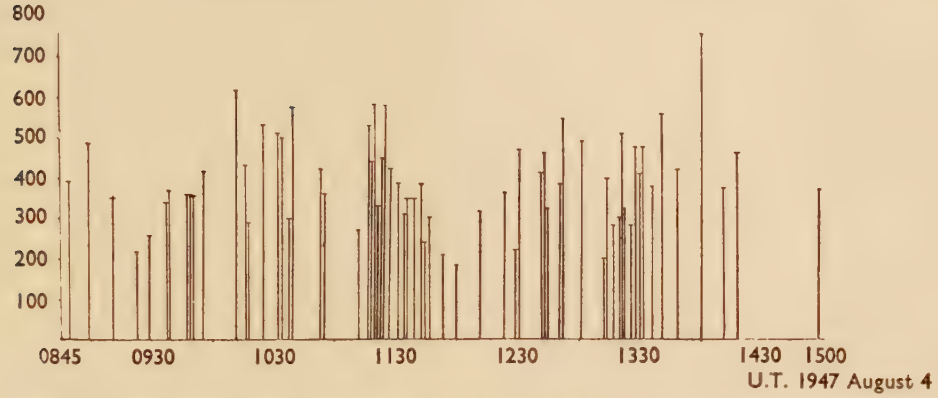

FIG. 5.—*Range/Time plots of echoes with aerial directed at azimuth* 90° *on* 1947 *August* 4. *Ordinates : Range in km.*

and possibly later; radiant $\alpha = 339°$, $\delta = \pm 0°$, hourly rate ≃12. Overlapping in date, there was a near following stream (B) with radiant approximately $\alpha = 355°$ to 5°, $\delta = +5°$, hourly rate ≃13.

(*b*) Simultaneously with the appearance of the η Aquarids, three more radiants were observed following these centres. The main new Piscid radiant (C in Table II and Fig. 4) at $\alpha = 20°$ to 32°, $\delta = +20°$ to $+30°$, with hourly rate ≃20 to 25, and minor radiants preceding and following.

(*c*) The radiant in Pisces and the two minor radiants were clearly delineated until May 15; then followed a period of confused activity. After May 29 even more active radiants, north preceding and south preceding the Pleiades, appeared at $\alpha = 45°$ to 55°, $\delta = +25°$ to $+35°$, hourly rate 20 to 25 (D), and $\alpha = 52°$ to 62°, $\delta = +15°$, hourly rate 20 to 40 (E).

(*d*) On June 20 the series was joined by a new centre of great activity near β Tauri at $\alpha = 80°$ to 85°, $\delta = +20°$ to $+30°$, hourly rate 20 to 30 (G).

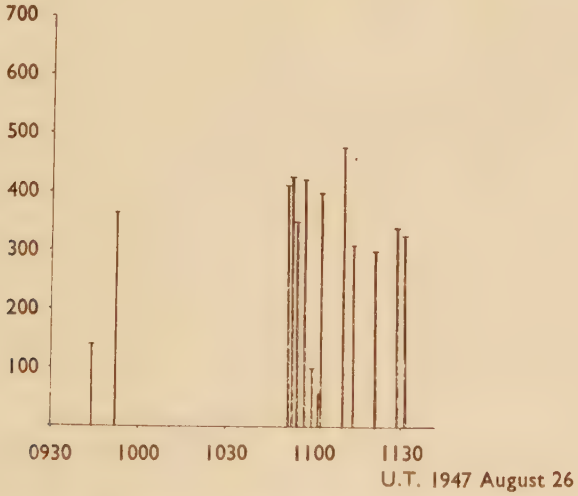

FIG. 6.—*Range/Time plots of echoes with aerial directed at* 90° *on* 1947 *August* 26. *Ordinates : Range in km.*

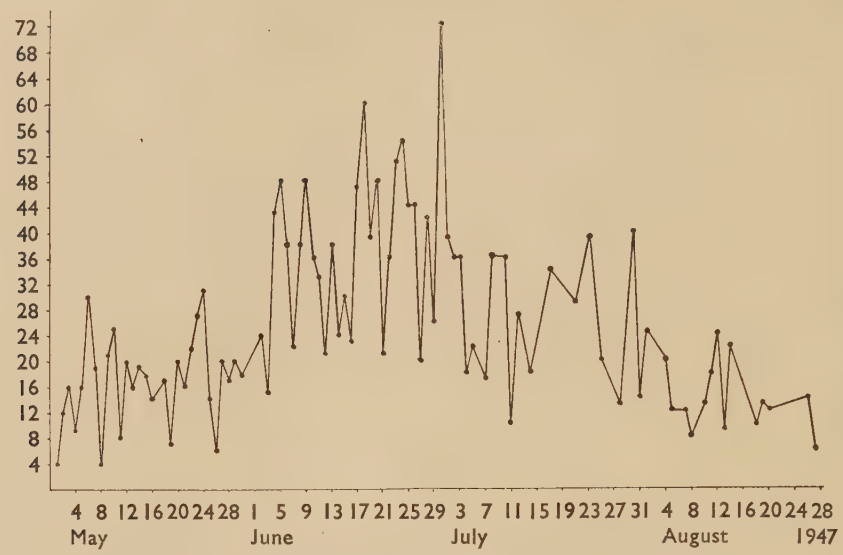

FIG. 7.—*Mean hourly rate per radiant* 1947 *May-August. Ordinates : Number of echoes/hour.*

(*e*) On June 23 a further prominent stream near 54 Persei was observed at $\alpha = 66°$ to $68°$, $\delta = +30°$ to $+40°$, hourly rate 20 to 45 (F).

(*f*) During July and August the observations were insufficient to delineate the radiants accurately but the indications are that the new radiants in Taurus and Perseus were mainly responsible for the activity during these months.

(*g*) The above analysis given in Table II refers only to the principal radiants. The situation was not always clearly defined and on many days the whole area between the main centres showed considerable activity.

In retrospect it seems justifiable to assume that the high daylight rate found by Prentice, Lovell and Banwell * in 1946 June–July must have been due to the above radiants. Thus there are good grounds for believing that the events detailed in this paper may be a recurrent phenomenon and that future observations will make it possible to give a more comprehensive account.

9. *Acknowledgments.*—The work described in this paper involved the recording of 5298 echoes during 427 hours of observation in 1947 May, June and July. This task could not have been accomplished without the willing help of our colleagues at the Jodrell Bank Experimental Station of the University of Manchester, and we wish to acknowledge our indebtedness to C. J. Banwell, J. G. Davies, C. D. Ellyett, D. R. H. Forsyth and F. Moran. We also desire to thank J. P. M. Prentice for his constant interest and for his help and advice in presenting these results.

Physical Laboratories,
University of Manchester :
1948 *March* 8.

* *Loc. cit.*

STELLAR PARALLAXES DETERMINED PHOTOGRAPHICALLY AT THE CAPE OBSERVATORY (SIXTEENTH LIST)

(Communicated by H.M. Astronomer)

(Received 1947 May 29)

This list is in the same form as previous lists, commencing in *M.N.*, **89**, 497, 1929.

A large proportion of the stars are from the Cape Astrographic Zone -40° to -52°,but a number of other interesting stars are included. A few of these are bright stars of early spectral type, but they are mostly faint stars of late type and rather large proper motion. The list contains a relatively large number of stars of M type.

No less than 5 stars have a parallax in excess of $0''\cdot100$ and for 3 others it is only slightly less. No. 1426 is a white dwarf. The spectral type, wA, is by Kuiper. Luyten gave the colour class as b. The photographic magnitude is probably not fainter than 12·0.

NOTES

1401. These results depend on 3 reference stars only. The plates were originally measured with a fourth reference star which proved to have a very large proper motion and was CPD -63° 51=LPM 26. This star had a dependence factor of ·233 and when it was included the results for the two stars were $\pi=+''\cdot004\pm''\cdot008$, $\mu=-''\cdot054\pm''\cdot004$ and $\pi=+''\cdot016\pm''\cdot0\cdot8$, $\mu=-''\cdot029\pm''\cdot004$. These results indicate that the p.m. of CPD -63° 51 in R.A. is $+''\cdot510$.

146. The determination is from a new set of plates with three early plates and relative to only four comparison stars on a new reference plate. From the two determinations we derive a parallax of $+''\cdot018\pm''\cdot006$.

1415. The Astrographic proper motion—the star is in the end zone—is spurious.

32. This is a difficult double star, the companion only shows with fair definition. This solution is from a new reference plate with only four reference stars. Three plates from the early series were re-measured. The original solution was $\pi=+''\cdot065\pm''\cdot013$, $\mu=-''\cdot502\pm''\cdot013$. The weighted mean is $\pi=+''\cdot082\pm''\cdot009$, $\mu=-''\cdot497\pm''\cdot002$.

404. This star was accidentally re-observed and measured against a new reference plate. The new solution includes 4 early plates. The weighted mean result of the two series is $\pi=+''\cdot038\pm''\cdot004$, $\mu=-''\cdot402\pm''\cdot001$.

1460. The separation in R.A. of the two stars is $6''\cdot160+''\cdot014$ (T$-$1942·0).

1477. LPM 691 is given as CoD -48° 12822. This star was observed as No. 576 in our sixth list. The proper motion in R.A. was found to be $+''\cdot031\pm''\cdot008$. The star with large proper motion is CoD -48° 12818 and is now about 2′ n.p to -48° 12822. It is slightly fainter photographically.

The unit for the last four columns is 0″·001

No.	Name and D.M. No.	Mag. Vis. Phot.	Type	R.A., Dec. (1900·0)	Proper Motion R.A.	Proper Motion Dec.	P.E. Unit Weight	Parallax	P.E.
				h m s					
1401*	PGC 100–101*	4·52	B9	0 26 58	+ 89	− 54	±37	+ 6	± 9
	β Tucn	4·50		−63° 30′·5	+ 64				± 5
		4·48	A2	0 26 58	+ 100	− 56	±36	+ 22	± 9
		4·54		−63° 31′·0	+ 91				± 5
	Mean							+ 14	± 7
1402	ZC 397	9·9	Go	0 48 29	+ 401	−126	±36	+ 9	±10
	−44° 229	10·2		−44° 18′·7	+ 415				± 6
1403	GC 1239	6·86	Go	0 57 12	+ 87	+104	±23	+ 8	± 6
	−61° 58	7·4		−61° 24′·1	+ 70				± 5
1404	GC 1748	7·9	G5	1 21 53	+ 301	−353	±29	+ 19	± 8
	−0° 229	8·7		−0° 40′·0	+ 300				± 3
1405	FS 470	...	K5	1 36 39	+ 293	+158	±25	+ 16	± 8
	−49° 470	11·4		−49° 44′·5	+ 282				± 3
1406	FS 477	...	...	1 38 35	+ 650	−130	±36	+ 29	± 9
	CAZ −43° 99	13·4		−42° 42′·2	+ 655				± 3
1407	Ci 20 129	...	...	1 45 57	+ 530	+ 60	±32	+ 29	± 9
	Ross 554	13·0		−12° 42′·2	+ 418				± 3
1408	LPM 88	...	M4	1 46 49	+ 570	−570	±36	+ 77	±11
	Ross 555	13·4		−11° 17′·0	+ 562				± 4
1409	FS 514	...	...	1 48 03	+ 444	+135	±32	+ 26	± 8
	CAZ −43° 111	13·6		−42° 05′·5	+ 441				± 3
1410	R Horo	Var.	Md	2 50 33	+ 132	+ 20	±24	+ 8	± 7
	FS 775			−50° 17′·9	+ 161				± 5
1411	GC 4139	8·4	Go	3 23 24	+ 353	−205	±36	+ 20	±10
	−7° 603	9·0		−6° 52′·3	+ 368				± 4
146*	LPM 194	9·6	Go	4 37 38	+ 662	+1307	±32	+ 19	± 8
	−65° 361	10·2		−65° 38′·8	+ 708				± 1
1412	ZC 2694	...	Go	5 04 59	+ 4	−180	±27	+ 9	± 9
	−46° 1698	10·3		−46° 53′·1	+ 9				± 4
1413	FS 1747	...	K7	5 22 30	+ 57	−108	±25	+ 18	± 6
	CAZ −42° 376	11·7		−41° 04′·9	+ 51				± 3
1414	FS 1792	...	K7	5 30 36	+ 85	+ 44	±22	+ 28	± 6
	−47° 1914	10·7		−47° 09′·50	+ 82				± 3
1415*	FS 1796	...	...	5 31 31	(+ 147	−190)	±33	+ 1	±11
	CAZ −41° 83	12·9		−40° 34′·4	+ 18				± 6
1416	GC 7604	8·54	Go	5 56 28	+ 195	+185	±21	+ 44	± 6
	−37° 2534	9·3		−37° 04′·0	+ 213				± 5
1417	GC 7611	8·21	Go	5 56 59	− 56	−208	±24	+ 12	± 6
	−37° 2539	8·8		−37° 02′·2	+ 17				± 5
1418	ZC 3448	8·4	K2	6 13 17	+ 107	+190	±26	+ 23	± 7
	−40° 2356	9·2		−40° 30′·1	+ 124				± 4

No.	Name and D.M. No.	Mag. Vis. Phot.	Type	R.A., Dec. (1900·0)	Proper Motion R.A.	Proper Motion Dec.	P.E. Unit Weight	Parallax	P.E.
				h m s					
1419	GC 8191	8·4	G5	6 17 50	+ 173	+ 76	±23	+ 22	± 6
	−44° 2600	8·6		−44° 44′·7	+ 185				± 2
1420	FS 2249	...	...	6 26 06	+ 214	−299	±20	+ 36	± 5
	−45° 2540	11·5		−45° 17′·5	+ 198				± 2
1421	ZC 4330	9·4	G5	7 11 34	− 152	+240	±31	+ 10	± 8
	−51° 2376	9·7		−51° 18′·1	− 144				± 4
1422	FS 3206	...	...	7 31 12	− 103	+156	±36	− 1	± 9
	−51° 2561	11·1		−51° 55′·0	− 97				± 5
1423	PGC 2060	5·11	B3	7 43 53	− 14	− 2	±39	− 8	±11
	GC 10523	4·94		−38° 15′·8	+ 9				± 5
1424	PGC 2111	3·60	B3	7 54 14	− 34	+ 20	±30	0	± 8
	χ Cari	3·43		−52° 42′·8	− 39				± 3
1425	FS 4575	...	Ko	8 33 05	− 161	+144	±29	− 16	± 7
	−42° 4435	11·0		−42° 35′·1	− 161				± 4
1426	LPM 297	11·5	wA	8 37 39	−1034	+1324	±26	+107	± 6
	−32° 5613	12·0		−32° 37′·3	−1047				± 4
1427	ZC 6739	8·6	G5	8 50 56	+ 200	−162	±36	+ 15	± 9
	−51° 3323	9·0		−51° 12′·0	+ 189				± 4
1428	GC 12588	7·43	Go	9 02 58	+ 53	+168	±32	− 15	± 8
	−42° 4968	7·6		−43° 05′·7	+ 50				± 3
1429	FS 5618	...	...	9 05 54	− 137	+222	±27	+ 26	± 7
	−41° 4851	11·0		−41° 42′·6	− 73				± 3
1430	ZC 7131	8·4	Go	9 10 00	− 153	− 53	±32	+26	± 8
	−41° 4907	7·9		−41° 53′·7	− 142				± 3
1431	ZC 7144	9·0	F8	9 10 34	− 158	+ 87	±23	+ 14	± 6
	−44° 5269	8·6		−44° 39′·3	− 149				± 3
1432	PGC 2483	5·15	B3	9 10 41	− 27	+ 7	±24	+ 7	± 6
	−42° 5086	4·98		−42° 48′·8	− 28				± 3
1433	FS 20558	...	...	9 35 51	− 532	+373	±28	+101	± 8
	−40° 5404	12·5		−40° 37′·5	− 519				± 3
1434	ZC 7703	9·8	Go	9 39 20	− 126	+ 98	±30	+ 8	± 8
	−51° 4094	9·2		−51° 34′·9	− 117				± 3
1435	FS 6926	...	...	9 52 45	− 110	+ 40	±25	+ 18	± 6
	−43° 5766	10·7		−43° 50′·4	− 104				± 3
1436	PGC 2723	4·09	A2	10 10 32	− 152	+ 31	±25	+ 28	± 6
	GC 14076	4·15		−41° 37′·6	− 134				± 3
1437	FS 7665	...	...	10 16 19	− 177	+ 48	±25	+ 34	± 7
	−43° 6163	11·3		−43° 24′·7	− 172				± 4
1438	FS 8083	...	Ko	10 35 43	− 73	+104	±24	+ 6	± 6
	−44° 6705	10·7		−44° 46′·5	− 75				± 3

No.	Name and D.M. No.	Mag. Vis. Phot.	Type	R.A., Dec. (1900·0)	Proper Motion R.A.	Proper Motion Dec.	P.E. Unit Weight	Parallax	P.E.
				h m s					
1439	GC 15049	8·49	Go	10 52 11	− 141	− 87	±27	+ 19	± 7
	−39° 6797	8·2		−40° 02′·2	− 152				± 3
32*	LPM 385	7·4	K5	11 20 20	− 507	+ 70	±47	+ 97	±12
	−60° 2911	9·0		−61° 06′·1	− 497				± 2
1440	FS 9094	...	G5	11 28 43	− 165	−113	±29	+ 2	± 8
	−40° 6796	11·7		−41° 06′·5	− 156				± 5
1441	GC 16351	6·68	A3	11 52 18	− 179	− 9	±25	− 11	± 7
	−48° 6984	7·7		−48° 48′·2	− 167				± 4
1442	FS 9622	...	...	12 00 33	− 306	+ 58	±32	− 8	± 8
	CAZ −50° 453	12·6		−49° 55′·0	− 293				± 4
1443	PGC 3176	4·20	B3n	12 06 25	− 40	− 26	±34	+ 29	± 8
	ρ Cent	4·03		−51° 48′·7	− 26				± 4
1444	FS 9866	...	K5	12 15 33	− 390	+ 32	±27	+ 18	± 7
	−41° 7123	11·9		−41° 15′·5	− 382				± 4
1445	PGC 3292	4·02	A2	12 32 14	− 190	− 15	±32	+ 20	± 7
	τ Cent	4·08		−47° 59′·4	− 180				± 4
1446	PGC 3302	2·38	Ao	12 36 00	− 196	− 15	±28	+ 20	± 7
	γ Cent	2·38		−48° 24′·6	− 175				± 4
1447	−30° 10073	9·0	Ko	12 38 12	− 247	− 13	±23	+ 11	± 6
		9·2		−30° 50′·2	− 243				± 3
1448	Ross 975	...	...	12 57 44	− 380	− 50	±28	+ 32	± 8
	AJ 1073	13·0		−02° 07′·4	− 284				± 4
1449	ZC 11706	8·9	G5	13 43 12	− 224	+ 46	±35	+ 3	± 8
	−40° 8181	9·7		−40° 22′·9	− 236				± 5
1450	PGC 3615	0·86	B1	13 56 46	− 21	− 28	±27	− 10	± 6
	β Cent	0·64		−59° 53′·4	− 25				± 3
1451	FS 12132	...	K5	14 22 49	− 47	−205	±26	+ 44	± 6
	−45° 9206	11·9		−46° 00′·7	− 38				± 4
1452	GC 19851	8·78	Go	14 39 11	− 191	− 68	±20	+ 5	± 5
	−45° 9398	8·9		−45° 27′·4	− 179				± 3
1453	FS 12725	...	Mo	14 59 15	− 103	− 59	±30	+ 23	± 7
	−46° 9785	12·2		−46° 23′·1	− 83				± 4
1454	FS 12800	...	Mo	15 04 01	− 338	−294	±26	+ 30	± 6
	−42° 10084	12·0		−42° 35′·3	− 310				± 3
1455	FS 12900	...	K5	15 09 10	− 239	− 36	±31	+ 25	± 8
	−41° 9674	12·2		−41° 19′·3	− 235				± 4
404*	FS 13856	...	K	15 39 29	− 411	−424	±25	+ 30	± 6
	−46° 10351	12·4		− 46° 54′·5	− 402				± 1
1456	FS 13969	...	M	15 42 29	+ 65	−390	±34	+ 34	± 8
	CAZ −48° 581	13·1		−47° 17′·5	+ 72				± 5
1457	FS 14011	...	...	15 43 40	+ 280	− 76	±29	+ 48	± 6
	−50° 9903	11·1		−50° 22′·9	+ 267				± 3

No.	Name and D.M. No.	Mag. Vis. Phot.	Type	R.A., Dec. (1900·0) h m s	Proper Motion R.A.	Proper Motion Dec.	P.E. Unit Weight	Parallax	P.E.
1458	PGC 4134	3·03	Ma	16 09 06	− 46	−149	±29	+ 2	± 7
	δ Ophi	4·38		−03° 26′·2	− 40				± 3
1459	FS 14586	...	G5	16 11 03	− 179	−170	±23	+ 7	± 5
	CAZ −41° 14	11·7		−40° 41′·8	− 167				± 3
1460*	FS 15003	...	...	16 23 52	− 107	−108	±40	− 1	±11
	CAZ −48° 795	13·0		−47° 43′·8	− 93				± 6
	FS 15004	...	...	16 23 53	− 101	−102	±31	+ 17	± 9
	CAZ −48° 796	12·9		−47° 43′·9	− 78				± 5
	Mean							+ 10	± 8
1461	PGC 4206	4·57	Fo	16 26 12	+ 13	+ 30	±28	+ 8	± 8
	ω Ophi	4·85		−21° 15′·2	+ 40				± 4
1462	ZC 15446	10·1	Go	16 46 10	− 115	− 87	±22	+ 6	± 4
	−46° 11085	9·7		−46° 09′·7	− 112				± 3
1463	ZC 15447	10·6	F8	16 46 11	− 183	− 82	±25	− 1	± 6
	−47° 11113	9·5		−47° 21′·7	− 175				± 3
1464	PGC 4361	3·44	F2	17 04 59	+ 19	−292	±27	+ 50	± 6
	η Scor	3·78		−43° 06′·4	+ 27				± 3
1465	FS 16337	...	Ko	17 12 15	− 113	−271	±38	+ 8	± 8
	−43° 11581	10·8		−43° 58′·3	− 104				± 5
1466	FS 16782	...	K5	17 24 34	+ 133	−101	±24	+ 1	± 5
	−40° 11550	10·7		−40° 31′·4	+ 125				± 4
1467	FS 16786	...	K7	17 24 42	− 62	−201	±28	− 3	± 6
	CAZ −49° 81	12·2		−48° 22′·7	− 60				± 4
1468	GC 23898	7·29	G5	17 31 50	− 230	−191	±23	+ 3	± 5
	−43° 11901	8·2		−43° 04′·9	− 231				± 3
1469	Ci 20, 1052	...	...	17 33 26	− 100	−510	±23	+ 18	± 5
	Ross 132	12·8		−22° 37′·8	− 86				± 3
1470	GC 24268	6·35	F8	17 45 44	+ 149	−201	±36	+ 23	± 8
	−41° 12139	7·1		−41° 57′·9	+ 144				± 4
1471	PGC 4544	4·60	Fo	17 55 12	+ 144	− 48	±32	+ 36	± 7
	ζ Serp	4·88		−03° 41′·0	+ 149				± 4
1472	FS 17710	...	G5	17 57 41	− 3	−215	±27	+ 25	± 6
	−44° 12307	11·0		−44° 45′·1	− 6				± 4
1473	FS 17924	...	...	18 10 56	− 12	−175	±29	− 3	± 7
	−50° 11840	11·6		−50° 46′·9	− 5				± 4
1474	GC 25095	6·62	F8	18 16 49	+ 34	−147	±29	+ 36	± 6
	−49° 12105	7·0		−49° 41′·9	+ 29				± 3
1475	FS 18095	...	...	18 23 01	− 241	− 87	±34	+ 18	± 8
	−47° 11324	11·5		−47° 20′·3	− 231				± 5
1476	FS 18216	Var.	M5e	18 35 53	+ 22	− 85	±27	+ 6	± 6
	−45° 12699	...		−45° 52′·5	+ 15	− 74			± 4

No.	Name and D.M. No.	Mag. Vis. Phot.	Type	R.A., Dec. (1900·0)	Proper Motion R.A.	Proper Motion Dec.	P.E. Unit Weight	Parallax	P.E.
				h m s					
1477*	FS 18398	...	m	18 51 33	+ 142	−489	±19	+ 93	± 4
	−48° 12818	13·7		−48° 23′·7	+ 149				± 1
1478	FS 18543	...	M	19 08 47	− 49	−333	±34	+ 28	± 8
	CAZ −48° 192	13·5		−47° 26′·3	− 49				± 3
1479	FS 18698	...	M	19 22 55	− 20	−102	±23	+ 4	± 6
	CAZ −50° 295	12·2		−49° 19′·5	− 39				± 4
1480	ZC 18221	9·7	Go	19 23 40	− 154	−174	±26	+ 2	± 6
	−47° 12942	10·2		−47° 52′·9	− 151				± 3
1481	FS 18798	...	Mo	19 35 39	+ 40	− 46	±28	+ 5	± 7
	−41° 13639	10·8		−41° 28′·5	+ 32				± 5
1482	LPM 712	...	m	19 46 42	− 90	−1050	±22	+ 96	± 6
	UOC 58, 43	14·0		−48° 02′·2	− 153				± 3
1483	ZC 18553	8·6	K2	19 55 05	+ 353	−371	±27	+ 45	± 6
	−50° 12780	10·2		−50° 19′·1	+ 377				± 4
1484	PGC 5166	5·34	K5p	20 04 38	+ 448	−1570	±37	+169	± 9
	GC 27992	7·1		−36° 21′·1	+ 453				± 4
1485	GC 28057	7·78	K5	20 06 45	+ 768	−137	±24	+171	± 5
	−45° 13677	9·6		−45° 27′·6	+ 775				± 3
1486	GC 28213	6·34	F5	20 12 07	+ 178	−207	±22	+ 22	± 5
	−47° 13340	6·8		−47° 53′·2	+ 192				± 3
1487	ZC 18813	8·2	Go	20 20 36	− 143	− 17	±28	+ 8	± 7
	CPD −52° 11692	9·4		−51° 59′·5	− 141				± 4
1488	ZC 18881	8·5	Go	20 28 04	+ 126	−130	±34	+ 19	± 8
	−50° 13038	9·8		−50° 05′·6	+ 105				± 5
1489	LPM 747	10·4	M1	20 37 10	+ 650	−890	±33	+ 68	± 8
	−19° 5899	11·8		−19° 15′·2	+ 582				± 4
1490	FS 19352	...	K2	20 56 09	+ 235	−430	±26	+ 30	± 6
	−47° 13670	12·4		−47° 06′·3	+ 211				± 3
1491	FS 19481	...	Ko	21 16 02	− 41	−194	±22	+ 4	± 5
	−44° 14433	11·4		−44° 00′·4	− 31				± 2
1492	LPM 786	11·5	M4e	21 25 51	+1210	+ 20	±34	+137	± 8
	Wolf 922	13·8		−10° 13′·7	+1197				± 3
1493	FS 19583	...	...	21 33 49	− 195	− 64	±23	+ 8	± 7
	CAZ −50° 162	12·7		−49° 43′·9	− 194				± 4
1494	ZC 19584	8·8	Go	21 42 56	− 102	−354	±33	+ 4	± 8
	−48° 14016	9·1		−48° 26′·0	− 107				± 4
1495	FS 19726	...	M	21 52 07	+ 66	− 7	±32	+ 25	± 8
	CAZ −51° 112	13·8		− 51° 02′·3	+ 70				± 3
1496	FS 19758	10·0	Go	21 57 11	+ 232	+ 34	±19	+ 6	± 5
	−51° 13155	10·8		−51° 41′·3	+ 204				± 2

No.	Name and D.M. No.	Mag. Vis. Phot.	Type	R.A., Dec. (1900·0)	Proper Motion R.A.	Proper Motion Dec.	P.E. Unit Weight	Parallax	P.E.
				h m s					
1497	ZC 20430	9·4	G5	23 15 18	− 97	−185	±38	+ 4	±10
	−49° 14120	11·2		−48° 57′·7	− 111				± 6
1498	FS 20445	...	Ko	23 38 01	+ 186	− 92	±25	− 10	± 6
	−40° 15225	11·6		−40° 31′·9	+ 182				± 3
1499	FS 20478	10·1	Go	23 44 07	+ 146	+ 5	±29	− 3	± 5
	−46° 14782	11·1		−46° 24′·1	+ 136				± 8
1500	−12° 6598	8·3	Go	23 55 48	+ 410	− 70	±27	− 13	± 8
		8·9		−12° 22′·7	+ 406				± 4

Royal Observatory,
Cape.
1947 *April* 15.

SOLAR RADIO-NOISE OF 200 MC./S. AND ITS RELATION TO SOLAR OBSERVATIONS

C. W. Allen

(Communicated by the Commonwealth Astronomer)

(Received 1947 May 7)

Summary

The solar radio-noise observing programme on Mount Stromlo is described. Daily means of (*a*) steady flux, and (*b*) number of bursts per hour have been plotted against sunspot and geomagnetic data. Both flux level and burst frequency increase during a solar radio-noise storm, and both are closely related to the central meridian passage of sunspots. However, some large sunspot groups do not produce solar noise. No close relation has been found between the emission from the Sun of (*a*) radio-noise, and (*b*) those particles which produce geomagnetic storms.

No close correlation has been found between short period radio-noise phenomena and solar observations, but there are occasional outbursts of solar noise accompanying the commencements of flares. It is suggested that the noise source is located rather high in the corona. The observation of a noise outburst caused by a flare 37° from the main spot group can be explained if the source is more than 120,000 km. above the Sun's surface. Physical arguments lead to a similar height.

1. *Introduction.*—From the time it was announced that solar radiation in certain ultra-short wave radio was far more intense than black body radiation (**1**) at the accepted solar temperature (6000 deg. K.), and that increases were associated with sunspot activity (**2**) it was realized that a mass of important information would become available from extended and detailed solar radio intensity measurements at the appropriate wave-lengths. This paper describes the Commonwealth Observatory programme initiated in 1946 to investigate the relation between the incidence of the solar radio-noise (**3**) and other solar phenomena of the type that can be observed with optical instruments. Radio equipment for the purpose was prepared and erected by the Radiophysics Laboratory of the Council for Scientific and Industrial Research.

It was regarded as essential to have the radio and astronomical equipment in as close association as possible, so that the two sets of phenomena, both of which exhibit rapid changes, could be studied together. As the spectrohelioscope was thought to be the most promising astronomical tool for the purpose, the recorder of a 200 Mc./s. receiver was placed inside the spectrohelioscope hut on Mount Stromlo.

2. *Observations on* 200 *Mc./s. Solar Radio-noise.*—The receiving equipment, consisting of a 200 Mc./s. receiver and a four Yagi aerial array, has already been described by Pawsey, Payne-Scott and McCready (**4**). The receiver output is applied to an Esterline-Angus recording chart operating at three inches per hour. Full chart deflection is equivalent to 1000 microamps, and the set noise is normally adjusted by means of the gain to read 500 microamps. For this purpose the aerial system is turned to the sky at least 40° from the Sun and away from the

Galaxy. The solar radio-noise is superimposed on the set noise when the aerial is directed towards the Sun, and at normal quiet periods, the increase due to the Sun is of the order of 10 microamps and just detectable. The increase of the recorder deflection due to the Sun at periods of great activity may bring the needle to full scale deflection, and hence at such times the practice is to reduce the gain of the receiver. As power in the receiver is proportional to the square of the recorder current, the power ratio R of the solar component in terms of the set noise is $(d^2_{\text{sun}} - d^2_{\text{sky}})\, d^2_{\text{sky}}$, where the d's are recorder deflections. The evaluation of the solar radio-noise flux depends on the noise factor of the set and the effective area of the aerial. The noise factor N (as defined by Pawsey, Payne-Scott and McCready (**4**)) is determined daily from a signal generator using a nomogram prepared by the Radiophysics Laboratory. It has varied between 7 and 30 since 1946 April. The Radiophysics Laboratory has also determined the effective area A of the aerial as 8·5 square metres. The flux of solar noise is then $8{\cdot}2 \times 10^{-15}\ RN/A$ watts metre^{-2} (Mc./s.)$^{-1}$. All values in this paper are reduced to the flux unit 10^{-15} watts metre^{-2} (Mc./s.)$^{-1} = 10^{-18}$ ergs/cm.^{2}.

The aerial is mounted on a manual polar axis, and is directed towards the Sun, or a few degrees ahead of the Sun, about every hour. The acceptance cone of the aerial is nearly 30°, and very little intensity is lost if the aerial is adjusted hourly.

Owing to the instability of the set, and to the fact that in normal times the measurement is of a very small difference, it is necessary to turn the aerial away from the Sun and back again at frequent intervals. In order to supplement the recorder on quiet days, the flux intensity is also determined visually on a backed-off microammeter by noting the variation as the aerial is turned on and off the Sun. This is done three times a day.

The general nature of 200 Mc./s. solar radio-noise records has already been described (**4**), and some examples are shown in Fig. 1. On the quietest days, there has always been a detectable amount of radiation which appears to be quite variable. Even on quiet days there are occasional sudden "bursts" of solar radio-noise which last for periods of the order of 1 sec. The peak intensity of bursts is usually between 1 and 10 flux units (i.e. $\times 10^{-15}$ watts metre^{-2} (Mc./s.)$^{-1}$). However, set instability and thunderstorms also provide occasional peaks which look like bursts, and it is not always possible to recognize the true bursts. During a radio-noise "storm" there is usually a high steady or slowly varying flux which has reached as high as 400 units. Furthermore, bursts are far more frequent during a storm and have sometimes reached the frequency of several per minute. Their intensity occasionally reaches the limit of the recorder at 50 units, and sometimes when the gain has been turned down have been observed over 100 units.

Besides steady noise and bursts, one can detect, rather rarely, sudden outbursts of radio noise, which last for a few minutes, fluctuating violently, and then disappear. In Section 5 we will see that such outbursts have a physical significance although they cannot be recognized with certainty from the records.

For tabulation purposes, the data can be described by (*a*) hourly values of steady flux, (*b*) hourly frequencies of bursts above a selected intensity, (*c*) time and intensity of the main bursts, and (*d*) time and maximum smoothed flux of all outbursts. The hourly values can also be averaged to give daily values of

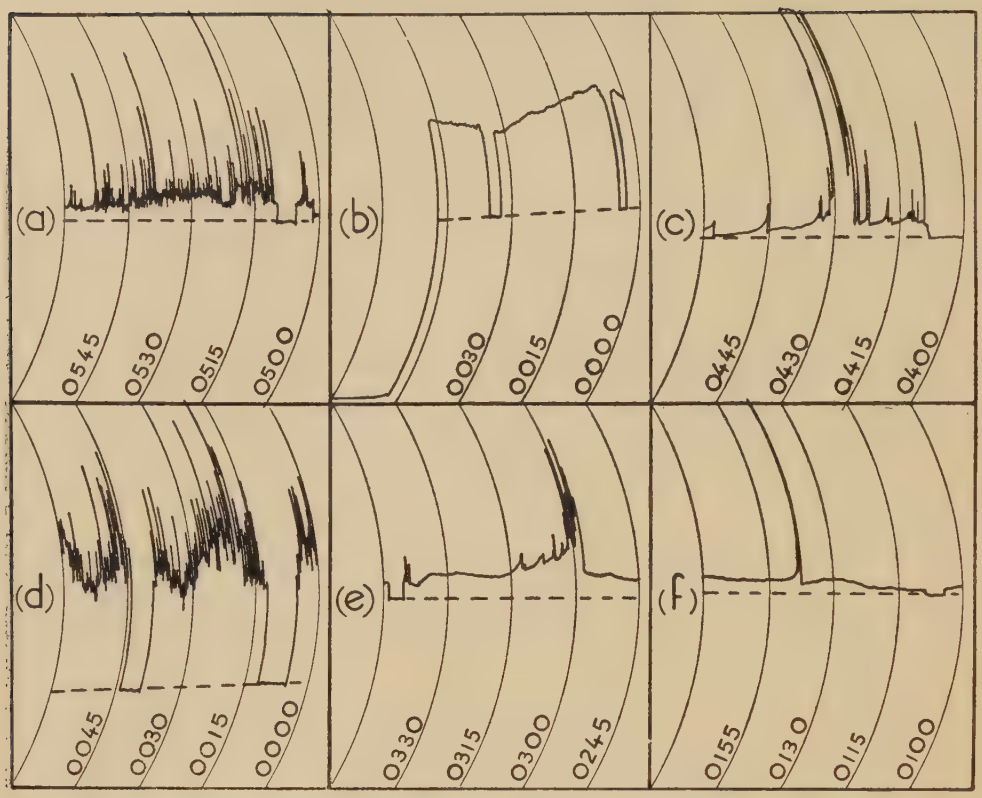

FIG. 1.—*Examples of solar radio-noise recordings. Set noise level is indicated by broken line. Note that timing is from right to left.*

(a) 1946 *September* 14. *Frequent bursts and low noise level.*
(b) 1946 *September* 20. *No bursts and high noise level.*
(c) 1947 *March* 8. *Large outburst.*
(d) 1947 *March* 10. *Frequent bursts and high noise level.*
(e) 1947 *March* 14. *Small outburst.*
(f) 1947 *March* 18. *One burst and fairly quiet.*

the steady flux and the frequency of bursts per hour. We have divided the burst data into large bursts, over 5 units; and small bursts, from 1 to 5 units. Bursts smaller than one unit could not be detected with certainty on our records. The normal recording period on Mount Stromlo is 00.00 to 06.00 U.T.

It should be mentioned that recordings on frequencies other than 200 Mc./s. might not have the same characteristics, and that the form of tabulation here adopted may not be suitable for all solar radio-noise analyses.

3. *Daily Correlations.*—The solar radio-noise recorder commenced fairly regular daily operation in 1946 April, and the data for the twelve months 1946 April–1947 March, are plotted against sunspot and magnetic data in Figs. 2 and 3. The radio-noise values are plotted on a square root scale in order to compress the variations and keep them similar to the sunspot and magnetic data. All values above what may be regarded as the disturbance level are blocked in for emphasis. Both visual and recorded readings for the steady flux are included, although they cannot always be distinguished on the diagram. From 1946 April to August, values below 0·8 units could not be detected on the recorder,

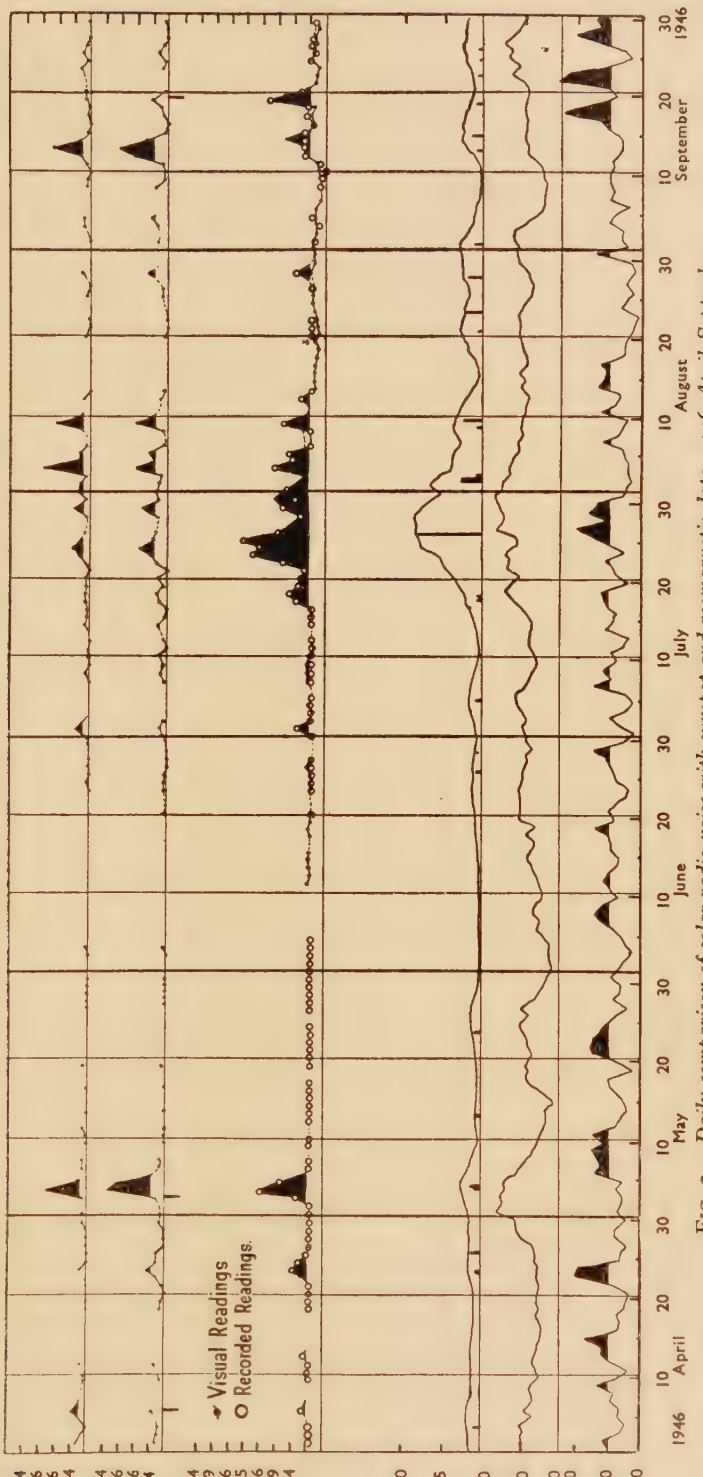

FIG. 2.—*Daily comparison of solar radio-noise with sunspot and geomagnetic data, 1946 April-September.*
From April to August recorded values below 0·8 units could not be detected, and such days are all plotted as 0·8.

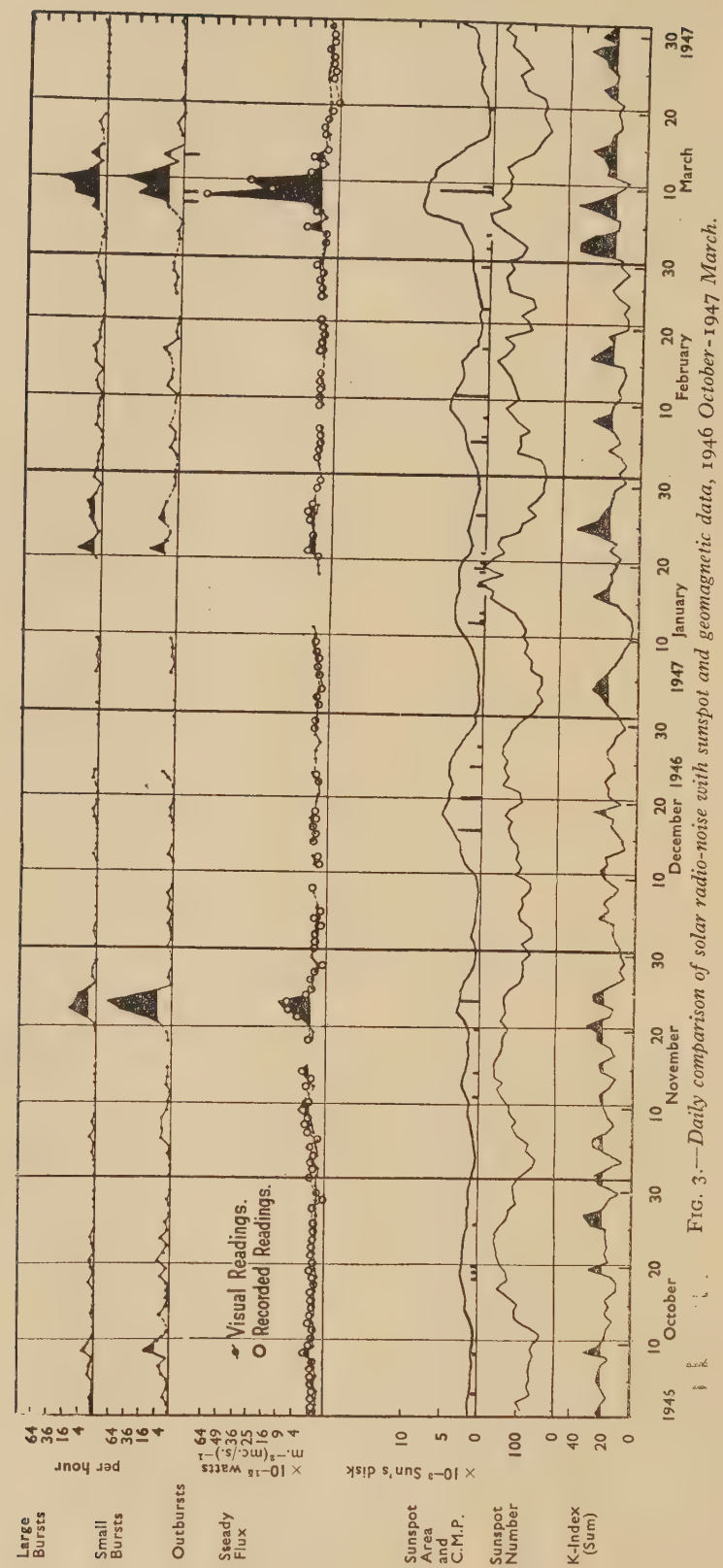
Large Bursts
Small Bursts
Outbursts
Steady Flux
Sunspot Area and C.M.P.
Sunspot Number
K-Index (Sum)
per hour
64 36 16 4
× 10⁻¹⁵ watts m⁻²(mc./s.)⁻¹
64 49 36 25 16 9 4
Visual Readings.
Recorded Readings.
× 10⁻³ Sun's disk
10 5 0
100 0
40 20 0
1945 October 10 20 30 November 10 20 30 December 1946 10 20 30 1947 January 10 20 30 February 10 20 March 30 1947

FIG. 3.—*Daily comparison of solar radio-noise with sunspot and geomagnetic data, 1946 October-1947 March.*

and all such days are plotted as 0·8. The visual readings are always more accurate than recorded readings for the low values.

The sunspot and magnetic data are taken, where possible, from *Terrestrial Magnetism* and after 1946 October are either from the Interservice Radio Propagation Laboratory publications or from observations made in Australia. Projected sunspot areas are used, measured from the Observatory spot sketches. As the K-indices are summed for Greenwich days, the points are located on the centre of each day. Other data are located at the time to which the observations actually refer. Any systematic lags detectable in the diagram should therefore be real. The central meridian passages and maximum areas of all spots whose projected areas exceeded 500×10^{-6} of the visible disk are shown beneath the spot area curve.

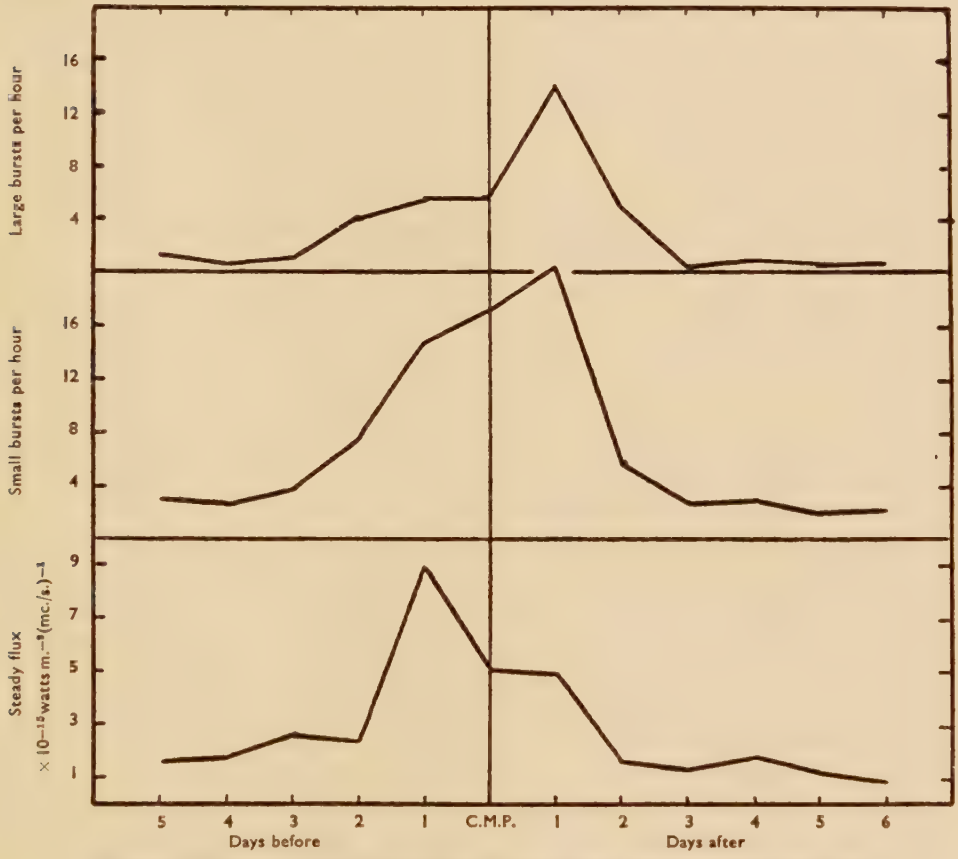

FIG. 4.—*Variation of solar radio-noise as large sunspots pass the central meridian.*

The general relation between solar radio-noise and sunspots is clearly demonstrated. The sunspot area is seen to be a better correlation index than sunspot number, and a still better index is the central meridian passage of the great sunspots. However, as Hey has remarked (**5**), there is no strict proportionality between spot area and noise flux. All solar noise storms or periods of activity in Figs. 2 and 3 coincide with near meridian passage of spots (possible exception on 1946 July 2), but the meridian passage of large spot groups is not necessarily accompanied by an appreciable noise increase.

There is a strong tendency for radio-noise to be received from the Sun only when the spot is not more than one day from the central meridian. This tendency had already been noticed in the observations made in Sydney (4) and is now well confirmed by independent data. For the 24 spot groups whose areas exceeded 1000×10^{-6} of the Sun's visible disk, the mean noise flux and burst frequency from five days before to six days after central meridian passage of the spots is shown in Fig. 4. The concentration of solar noise as the spot passes the meridian implies that the noise is emitted in an approximately radial beam. Noise has been received from the greatest spots when four days or more from the central meridian, but such noise has always been weaker than near the meridian.

Fig. 4 demonstrates some tendency for the steady noise to precede, and the bursts to follow, the central meridian passage of spots, but this tendency may be changed as more data becomes available.

A close relation between frequency of bursts and flux of steady noise is readily seen in Figs. 2 and 3, but some radio-noise storms, e.g. 1946 September 14, consist mainly of bursts, while others, e.g. 1946 September 20, are mainly high steady noise. On September 14, the main spot group was developing rather rapidly, while on September 20, the main spot group—mostly small spots was on the decline. A search through the data gives some support for the generalization that bursts are relatively more frequent in the early stages of sunspot development and steady noise in the later stage.

No significant difference between the distribution of large bursts and small bursts has been detected.

There is a good general correlation between noise and geomagnetic activity, as might have been expected, since both are associated with great sunspots. However, the details of the correlation do not suggest that radio-noise and geomagnetic particles are necessarily emitted from a sunspot at the same time. The lag between radio-noise emission and the apparently associated magnetic storm varies between 0 and 3 days.

4. *Short Period Correlations.*—Since solar radio-noise and spectrohelioscope features both vary with periods much shorter than a day, it was hoped that the daily correlation just mentioned would be amplified by detailed correlation of some of the more rapid features. A visual observing programme, particularly aimed at detecting such relations, has been carried out since 1946 April.

As was expected, no solar features whatever could be detected with periods of the order of 1 sec., and hence correlation with individual bursts, when frequent, was at once ruled out.

The next attempt was to search for any features in the spectrohelioscope or spectroscope which might vary in a systematic fashion with the coming and going of solar radio-noise. The following features were studied visually: (*a*) bright $H\alpha$ flocculi, (*b*) dark $H\alpha$ flocculi, (*c*) dark flocculi with high sight-line velocities, (*d*) flares, (*e*) changing width of $H\alpha$ in flares, (*f*) general appearance in spectrohelioscope, (*g*) appearance of $H\alpha$ in spectroscope, (*h*) bright $H\alpha$ "bombs", (*i*) incidence and density of the D3 line of *He*, (*j*) incidence and brightness of emission in 5169 A. of Fe^+. Generally, the procedure was to become familiar with these features on normal days, and then to seek for anything unusual during periods when solar radio-noise was being received. Nearly all the features were found to vary so closely with the size and general activity of sunspot groups that they gave no new information. *We could find no chromospheric or photo-*

spheric features which appeared to have an invariable physical connection, or high short period correlation, with the solar radio-noise.

This rather disappointing result has led us to suspect that the location of the noise source was not near the photosphere or chromosphere, but probably high in the corona. This suggestion has been made elsewhere (**6**, **7**), and is supported by an observation in Section 5.

It should be remarked that a search for a correlation between radio-noise and visible features might be confused by the geometrical conditions affecting the direction of the solar noise beam. The fact that nearly all noise is received when a sunspot is within a day of the meridian, shows that there is a directional control which concentrates the radiation in an approximately radial direction. However, the exact direction of the beam might well depend on equidensity contours of the corona and this would cause a variation in the received noise which would be rather independent of the actual emission.

The situation with regard to flares differs from other chromospheric observations, in that, while there is no general correlation, there are occasions when there appears to be a physical connection between an outburst of noise and the onset of a flare.

5. *Flares and Outbursts of Radio-noise.*—Interest in the association of flares and solar radio-noise was first aroused by Appleton's remark (**1**) that "the noise . . . . was often the precursor of a catastrophic fade-out associated with a bright eruption (flare) on the Sun". Hey (**5**) and Ellison (**8**) have described the coincidence of an outburst of radio-noise with the onset of a great flare on 1946 July 25, and similar observations are mentioned in the report by Reber and Greenstein (**7**).

Since 1946 July, 130 flares or fade-outs have been observed in Australia at times when the radio-noise set was in operation. Most of these showed no influence at all on the noise record, whether noise was being emitted at the time or not. For only 31 of them was there any evidence of change in the solar noise record that might possibly be attributed to the flare, and for only five of them could one be reasonably sure of a physical connection between the flare and the noise change. The conditions for the five occasions were as follows:

(1) On 1946 August 29, a flare of importance 1 in a spot group at lat. 30° S., long. 22° E., was seen to commence at 01.38 U.T. and finish at 01.58. The intensity was greatest at 01.40, at which time the $H\alpha$ emission was somewhat broader than normal—the flare could be seen at $\pm 1{\cdot}0$ A. from the centre of $H\alpha$. At 01.41, the recorder showed a burst of about 20 units (the highest for the day). After the burst the steady flux decreased a little, until about 02.01 when, with a small burst, it returned to the earlier value—about 1 unit.

(2) An active flare was seen in lat. 11° N., long. 29° E. at 04.40, 1947 March 8. It was decreasing when first noticed and gone by 04.50. A fade-out was observed on the ionospheric recorder at 04.30, and strongly suggests that this flare started rather violently about that time. From 04.26 to 04.30 there was a very remarkable outburst of solar noise, exceeding the recorder limit of 68 units (see Fig. 1). The noise then returned to normal while the flare was still in progress.

(3) On 1947 March 9, at 05.13, a rush of noise was heard in the loud speaker attached to the noise recorder. The flux had been steady at about 26 units, but without bursts, for about an hour. A rapid scan of the Sun with the spectrohelioscope revealed that a flare of importance 2 was commencing at lat. 14° N.,

long. 11° E. The *Hα* line was fairly wide, about ±1·0 A., during the first few minutes. In the period 05.13–05.16 there were two bursts and an increase of flux, which we have listed as an outburst although not very typical. The radio noise then decreased to about 19 units, until the flare was over at 05.29, after which there was an increase to 33 units.

(4) On 1947 March 9, at 06.57, a flare of importance 2 was seen to commence at 26° S., 15° E. It developed very rapidly in the first five minutes, during which time *Hα* extended to 2·4 A. to red and 2·0 A. to violet. The solar noise had been fairly steady at about 24 units for over an hour. With the incidence of the flare the steady noise remained the same, but a series of bursts commenced rather suddenly and continued for a half hour during the intense part of the flare. There was some evidence of outbursts at 06.59 and 07.02, when two different sections of the flare were at their widest in *Hα*.

(5) At 04.00 on 1947 March 14, a flare was found to be in progress at 25° S. and 58° W., and continued until 04.35. The flare was rated importance 1, but from the glowing appearance in the spectrohelioscope it was judged to be the end of a flare of importance 2 or 3. There was an outburst from 02.58 to 03.02 (see Fig. 1), followed by a rather quiet period. Bursts and steady noise increased again at about 04.15. Three ionospheric stations reported fades beginning between 02.45 and 03.00, but all reported a maximum fade intensity at 03.00, in good synchronization with the outburst.

If we ignore the fourth case this information suggests that a normal accompaniment of a vigorous flare is an outburst of noise during the initial stages when *Hα* is wide, followed by a small decrease in flux during the life of the flare. Individual flares, however, differ widely in detail.

It is this correlation between flares and outbursts that shows that an outburst has a particular physical significance. Outbursts cannot be recognized with certainty on the noise records, but a list of occasions which appear to be genuine outbursts has been extracted from our recordings, as in Table I.

TABLE I

List of Outbursts from 1946 *April*–1947 *March*

Time	Date	Maximum Flux
05.15 U.T.	1946 April 6	8 units
06.30 ,,	,, May 3	11 ,,
07.26 ,,	,, Sept. 20	28 ,,
04.28 ,,	1947 March 8	68 ,,
05.14 ,,	,, March 9	32 ,,
03.00 ,,	,, March 14	26 ,,

The outbursts are shown in Figs. 2 and 3, but they are not sufficiently complete or numerous for correlating with other phenomena. They may prove to have a connection with magnetic storms.

It is important to notice that only a small percentage of solar radio-noise is associated with flare commencement, and that, therefore, flares are not a necessary part of the physical mechanism that produces the radio noise. The conditions that obtain in the corona might be rather delicately balanced, so that the corona could be stimulated into noise production by the ultra-violet radiation from a flare. Whether or not a flare would be accompanied by a noise outburst would then depend on whether (*a*) the corona was already in the condition to emit

noise, (*b*) the flare was sufficiently vigorous, and (*c*) the radio-noise beam was directed towards the Earth.

In the above list of examples, the flares of 1947 March 8 and 9, are of special interest, since they took place in a spot that was 37° from the great spot. The close relation between noise and great sunspots suggests that the noise source in this case was in the region of the great spot. If the noise was stimulated by radiation emitted from the Sun's surface near the small spot, it can readily be seen from Fig. 5 that the source of the radio-noise must have been at least

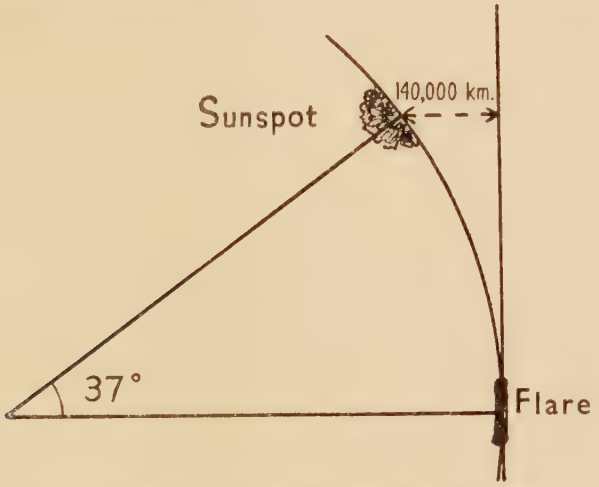

FIG. 5.—*Illumination of sunspot neighbourhood by a flare.*

140,000 km. from the centre of the great spot, and at a height of at least 120,000 km. above the Sun's surface.

Such a height is reasonably consistent with Appleton's theory of reflection and absorption in ionized layers (**9**) for 200 Mc./s. waves, particularly if, as Martyn has shown (**10**), the radiation is the extraordinary polarized ray. In that case the height of the reflection layer is dependent on the electron concentration in the corona and the magnetic field from the spot. Using Baumbach's electron concentrations (**11**), Martyn's method of analysis (**12**), and reasonable values for the spot field, the 200 Mc./s. extraordinary reflection layer is at a height of 130,000 km., in good agreement with that deduced from Fig. 5. For lower frequencies, the height would be greater.

Since the bursts at different wave-lengths show very little detailed agreement (**13**), it might further be inferred that they are not produced at the same level. Presumably, the lower frequencies would be produced at a higher level. Rather definite information on the heights of the sources would be provided if a flare from a distant spot group were to produce a noise outburst at one frequency and fail to produce an outburst at a higher frequency.

Routine observations such as those described in this paper, if made at more than one frequency, should settle such questions in due course.

Acknowledgments

The observations described were made at the Commonwealth Observatory. The radio equipment was prepared and erected by the Radiophysics Laboratory

of the Council for Scientific and Industrial Research, Sydney; and operated by Mr L. H. Heisler and Mr R. O. Errey of the Radio Research Board, also of the Council for Scientific and Industrial Research, Sydney. Solar observations were made by Miss F. J. Daly and the author. The author is indebted to Drs R. v. d. R. Woolley, D. F. Martyn and J. L. Pawsey for helpful discussion.

Addendum, 1948 *March*

More recent checks on the constants of the aerial and receiver show the system to be 6 D.B. less sensitive than formerly estimated. As a result all noise levels quoted in the paper should be increased by a factor of 4, and the flux unit becomes 4×10^{-15} watts metre^{-2} (Mc./s.)$^{-1}$.

Commonwealth Observatory,
Mount Stromlo,
Canberra, A.C.T.:
1947 *May* 2.

References

(1) Appleton, E. V., *Nature*, **156**, 534, 1945.
(2) Pawsey, J. L., Payne-Scott, R., and McCready, L. L., *Nature*, **157**, 158, 1946.
(3) As the radiation appears as an increase of noise level in a radio receiver, it will often be referred to in this paper as solar radio-noise.
(4) Pawsey, J. L., Payne-Scott, R., and Mc Cready, L. L., *Proc. Roy. Soc.*, A., **190**, 357, 1947.
(5) Hey, J. S., *Observatory*, **66**, 360, 1946.
(6) Martyn, D. F., *Nature*, **158**, 632, 1946.
(7) Reber, G., and Greenstein, J. L., *Observatory*, **67**, 15, 1947.
(8) Ellison, M. A., *M.N.*, **106**, 500, 1946.
(9) Appleton, E. V., and Builder, G., *Proc. Phys. Soc.*, **45**, 208, 1933.
(10) Martyn, D. F., *Nature*, **158**, 308, 1946.
(11) Baumbach, S., *A.N.*, **263**, 121, 1937.
(12) Martyn, D. F., Private communication.
(13) Unpublished observations from the Radiophysics Laboratory.

FAINT STARS WITH PROPER MOTIONS EXCEEDING 0″·15 PER ANNUM IN HYDERABAD ASTROGRAPHIC ZONES, LIST V.

(Communicated by the Director)
(Received 1947 May 16)

Summary

This paper gives a list of 100 faint stars with relative proper motion exceeding 0″·15 per annum.

The present list is a continuation of the four lists previously published in the *Astronomische Nachrichten.** The Hyderabad Serial number is continued from the fourth paper of this series. The annual proper motion of each star in both R.A. and declination is given in seconds of arc instead of the resultant P.M. given in the previous papers. The proper motions have been generally derived from one pair of plates, the average interval between the plates being 20 years. Numbers marked with an asterisk show that two pairs of plates were used in determining the P.M., and the mean value of $\Delta\alpha$ and $\Delta\delta$ was adopted.

For details of method of comparison and reduction of proper motions, reference may be made to the above cited papers. The proper motions of the bright stars in the Hyderabad Catalogues were compared with the corresponding ones in the general catalogue of Boss and the general accordance was found to be good. The average of the differences without regard to sign is about 0″·03.

The plates were blinked mainly by Mr S. Aravamuthan and measured by Mr U. S. Rao; the reductions were carried out by Messrs M. V. V. Sastry and S. Aravamuthan.

The proper motions of 39 stars (numbers 186–224) derived during the time of Mr T. P. Bhaskaran, the former Director of the Observatory, have also been included in the present list.

Proper motions exceeding 0″·15 per annum in Hyderabad Astrographic Zones :—V

Serial No.	Ptg. Mag.	R.A. (1900)	Decl. (1900)	μ_α	μ_δ
		h m s	° ′	″	″
142	10·1	0 12 46	−20 3·6	+0·086	−0·157
143*	11·4	0 25 28	−19 8·8	+0·193	−0·007
144*	10·6	0 43 50	−21 5·7	+0·134	−0·127
145	11·1	0 49 16	−20 12·7	+0·135	−0·150
146*	10·4	0 51 39	−19 24·3	+0·191	−0·022
147	12·6	1 28 15	−20 21·4	+0·270	+0·156
148*	11·0	1 36 42	−18 21·4	−0·100	−0·100
149	10·8	1 51 36	−20 12·2	+0·156	−0·114
150	10·0	1 53 57	−20 14·9	+0·455	−0·100
151	10·8	1 58 58	−19 12·7	−0·137	−0·068
152	12·6	2 03 37	−19 13·9	+0·164	+0·014
153	10·5	2 27 20	−19 35·3	−0·043	−0·143
154	12·3	2 30 04	−19 13·9	+0·128	+0·200
155	10·9	2 33 07	−18 58·2	+0·156	0
156*	11·3	2 39 54	−19 14·5	−0·043	−0·178

* *A.N.*, **267**, 26, 1939 ; *A.N.*, *B.Z.*, **21**, 4, 1939 ; *A.N.*, *B.Z.*, **21**, 27, 1939.

Serial No.	Ptg. Mag.	R.A. (1900) h m s	Decl. (1900) °	μ_α ″	μ_δ ″
157	12·0	3 13 12	−19 59·0	−0·028	−0·199
158	9·5	3 23 38	−20 6·0	+0·014	−0·171
159	11·8	3 48 08	−18 59·6	+0·057	+0·142
160*	12·3	4 06 20	−19 26·4	+0·098	−0·116
161	11·3	4 17 09	−19 59·1	−0·142	−0·397
162	12·3	4 20 42	−19 5·1	+0·213	0
163	10·5	4 21 31	−18 26·6	+0·241	+0·014
164	11·4	4 46 55	−19 29·2	+0·213	+0·099
165	12·3	5 17 06	−19 21·3	+0·140	−0·070
166	10·6	5 26 53	−18 38·0	+0·105	−0·105
167	12·5	5 41 56	−19 40·2	+0·070	−0·158
168	10·6	5 45 26	−18 36·0	−0·122	−0·087
169	11·1	6 04 22	−18 1·7	+0·070	−0·193
170	12·0	6 05 23	−19 32·1	+0·035	−0·158
171	12·9	6 23 26	−19 15·2	−0·018	+0·175
172	11·0	7 15 51	−19 37·7	+0·035	−0·159
173*	11·0	7 20 12	−19 21·7	−0·036	−0·282
174	12·6	7 30 20	−19 7·3	−0·035	−0·176
175	12·3	7 46 53	−18 25·5	+0·088	−0·211
176	10·3	7 55 17	−19 59·4	+0·105	−0·123
177	11·2	8 00 05	−18 27·9	+0·264	0
178	12·3	8 16 13	−18 23·1	−0·176	−0·053
179	13·1	8 16 22	−19 26·2	−0·193	−0·105
180	11·8	8 37 14	−18 17·6	+0·156	−0·028
181	12·9	8 39 14	−18 29·8	−0·370	+0·327
182	12·6	8 43 00	−18 37·6	−0·170	+0·014
183	13·0	8 48 08	−18 45·3	−0·142	−0·085
184	12·6	8 49 56	−19 23·8	−0·156	0
185	10·7	8 56 26	−19 35·6	−0·142	+0·043
186*	12·0	11 02 33	−18 45·0	−0·286	+0·142
187	11·2	11 03 45	−16 59·2	−0·149	+0·054
188	12·6	11 09 09	−18 08·2	−0·095	+0·136
189	11·9	11 10 20	−17 34·7	+0·122	−0·721
190	11·9	11 10 21	−17 34·6	+0·190	−0·761
191	12·0	11 15 00	−17 46·4	+0·122	+0·204
192	10·8	11 28 59	−17 29·1	−0·096	−0·136
193	11·7	11 54 55	−17 51·1	−0·257	+0·054
194	12·4	12 17 50	−17 06·3	−0·027	−0·246
195	12·4	12 39 26	−18 27·7	+0·142	+0·071
196	12·6	12 39 36	−18 28·7	−0·043	+0·156
197	12·7	12 42 26	−19 8·1	+0·114	−0·100
198	12·6	12 43 19	−19 1·6	+0·156	−0·114
199	10·6	12 43 45	−19 0·9	+0·142	−0·071
200	10·8	13 06 43	−16 57·1	−0·123	−0·096
201*	12·1	13 10 25	−18 57·4	−0·149	−0·026
202	10·6	13 35 24	−18 0·3	−0·163	+0·082
203*	10·2	13 48 31	−17 26·8	+0·156	−0·122
204	10·1	13 52 02	−17 25·9	−0·068	+0·136
205*	10·8	14 27 34	−17 35·6	−0·046	−0·157
206	11·1	14 31 02	−17 53·3	+0·026	−0·183
207	10·8	14 45 27	−18 43·0	−0·157	−0·026
208	10·5	14 45 36	−17 35·1	+0·013	−0·209
209	12·8	15 09 14	−18 14·8	−0·341	−0·301
210	12·7	15 12 55	−18 15·0	+0·550	−0·301
211	12·7	21 00 50	−19 7·9	−0·096	−0·123
212*	11·9	21 07 29	−17 53·6	+0·070	−0·139

Serial No.	Ptg. Mag.	R.A. (1900) h m s	Decl. (1900) ° ′	μ_α ″	μ_δ ″
213	11·6	21 09 33	−18 38·3	+0·129	−0·157
214	9·6	21 17 52	−17 31·3	−0·029	−0·157
215	11·8	21 20 44	−17 15·2	−0·157	+0·114
216	11·0	21 20 58	−17 52·4	+0·114	+0·129
217	10·6	21 28 29	−18 1·4	+0·243	+0·071
218	12·2	21 33 56	−17 6·2	+0·100	−0·114
219	11·0	21 34 12	−17 1·0	+0·085	−0·213
220	10·3	21 34 37	−18 23·4	−0·156	−0·156
221	11·2	21 46 09	−18 14·2	+0·177	−0·068
222	12·8	21 50 30	−17 58·5	−0·043	−0·142
223	11·2	21 51 35	−18 28·6	−0·171	−0·299
224	12·7	21 52 21	−18 15·1	−0·185	−0·355
225	12·3	22 02 09	−17 26·1	−0·255	−0·180
226	12·3	22 06 36	−18 38·9	−0·171	+0·014
227	10·9	22 16 15	−17 39·5	+0·369	−0·219
228	11·8	22 21 32	−17 56·1	+0·380	+0·160
229	11·8	22 23 45	−17 49·3	+0·200	−0·040
230	11·6	22 24 21	−17 45·9	−0·100	−0·140
231*	11·3	22 25 12	−18 27·4	+0·162	−0·102
232	10·9	22 29 41	−16 58·6	+0·229	−0·057
233*	11·6	22 32 55	−18 41·8	−0·154	−0·106
234*	11·2	22 32 58	−18 37·4	+0·154	−0·022
235	10·5	22 40 42	−17 48·5	+0·110	+0·096
236	12·3	22 45 54	−18 49·0	+0·071	−0·171
237	10·5	22 53 54	−17 39·2	−0·115	+0·129
238*	12·4	22 55 47	−19 8·8	+0·544	−0·222
239*	12·0	23 02 54	−18 30·6	−0·121	−0·079
240	10·8	23 03 22	−16 55·5	+0·214	+0·086
241	10·9	23 18 08	−17 4·3	+0·156	+0·057

Nizamiah Observatory,
Hyderabad, Deccan, India :
1947 *April* 20.

OCCULTATIONS OF STARS BY THE MOON OBSERVED AT THE NIZAMIAH OBSERVATORY, HYDERABAD, DURING THE YEAR 1946

(Communicated by the Director)

(Received 1947 May 16)

TABLE I

No.	Star	Mag.	Phase	Date 1946	U.T. h m s	Obs.
1	B.D.+1° 223	6·8	D	Jan. 10	16 06 15·3	V.
2	148 B Tauri	6·0	D	,, 13	12 55 09·3	V.
3	163 B Tauri	5·8	D	,, 13	18 05 08·9	M.G.
4	B.D.+12° 2284	6·4	R	,, 20	20 14 35·1	A.R.
5	33 B Tauri	6·3	D	Feb. 9	14 47 27·2	V.
6	129 H′ Tauri	5·7	D	,, 10	15 07 40·7	M.G.
7	82 Gemi	6·2	D	,, 13	18 58 27·0	M.G.
8	B.D.+9° 321	6·8	D	Mar. 7	13 40 32·5	M.G.
9	B.D.+9° 322	8·5	D	,, 7	13 42 25·5	M.G.
10	34 Librae	5·9	R	Apr. 18	17 41 42·4	A.R.
11	η Leonis	3·6	D	Oct. 19	22 41 54·6	V.
12	η Leonis	3·6	R	,, 19	23 24 41·7	V.
13	B.D.−25° 3291	7·4	D	,, 30	14 47 55·4	V.
14	κ Gemi	3·7	R	Nov. 13	17 24 52·7	V.

The last column shows the initials of the following observers:

V.: M. V. Vaidyanatha Sastry.
M.G.: Mahomed Ghouse.
A.R.: A. Ramanathan.

The instrument used throughout was the 15-inch visual refractor. The corrections to the standard clock were determined from observations with the transit instrument.

The reductions were carried out by M. V. V. Sastry, assisted by S. Aravamuthan. No correction was added to the observed time.

TABLE II

No.	$\sigma'-\sigma$	$\cos(\rho-\chi)$	$\sin(\rho-\chi)$	No.	$\sigma'-\sigma$	$\cos(\rho-\chi)$	$\sin(\rho-\chi)$
	″				′		
1	−1·0	+0·83	+0·56	8	+0·5	+0·98	−0·22
2	−0·8	+0·99	+0·10	9	[+3·7]	+0·98	−0·18
3	−0·5	+0·99	+0·14	10	+1·9	−0·78	+0·62
4	+1·2	−0·92	−0·38	11	−1·5	+0·60	−0·80
5	+0·7	+0·68	−0·73	12	+1·3	−0·73	−0·68
6	−1·3	+0·92	+0·40	13	−0·4	+0·56	+0·83
7	−0·3	+0·66	−0·75	14	−2·5	−0·23	−0·97

The mean place of star No. 9 for 1946·0 is given below. Proper motions have been applied to the coordinates given in the catalogue in computing the mean place for use in the reduction. For the remaining stars, positions were taken from the Nautical Almanac.

No.	R.A. (1946·0)	Dec. (1946·0)	Remarks
9	$2^h\ 23^m\ 54^s{\cdot}47$	$+10°\ 20'\ 26''{\cdot}7$	A.G. Leipzig II, No. 910 ; P.M. $\mu_\alpha+0^s{\cdot}0030$, $\mu_\delta-0''{\cdot}016$

Nizamiah Observatory,
Hyderabad, Deccan, India:
1947 *April* 12.

OBSERVATIONS OF NOVAE, 1946–1947

W. H. Steavenson

(Received 1947 May 5)

All the observations given below were made with the 30-inch Hindle reflector.

Nova Aquilae (1918)

The brightness of this nova has been sensibly constant for many years and the slight fluctuations recorded below are probably not real, but it is perhaps worth while to give the individual estimates in view of the fact that this is one of the few novae known to have been variable in light prior to the principal outburst.

Date	Mag.	Date	Mag.
1946 July 2	11·3	1946 Sept. 8	11·3
7	11·2	13	11·3
23	11·3	28	11·4
29	11·3	Nov. 25	11·3
Aug. 10	11·3		

Nova Aquilae (1925)

The field was examined on 1946 July 2, September 13, 25 and 28, but no trace of the nova could be detected. I conclude that it cannot have been so bright as $16^{m}\cdot0$ on the dates mentioned.

Nova Aquilae No. 5 (1936)

Seen with great difficulty under good conditions on 1946 September 28. The magnitude was estimated to be about 16·7. At the altitude of the Pole the limit of the 30-inch mirror, as tested on stars of the North Polar Sequence, is close to $17^{m}\cdot0$.

Nova Aquilae No. 6 (1936)

This nova has probably now reached a steady state, having faded by only half a magnitude since 1938 July, when I last observed it.

Date	Mag.	Date	Mag.
1946 July 7	15·6	1946 Sept. 25	15·8
Sept. 13	15·7	28	15·7

Nova Aquilae (1945)

The fading of this recent nova continues at a fairly steady rate. Its image is stellar but the spectrum, as seen with a small direct-vision prism, appears to be that of a planetary nebula. The colour, on the first date of observation, 1946 May 21, was noted as being greenish white,

Date	Mag.	Date	Mag.
1946 May 21	12·0	1946 Sept. 15	13·1
July 2	12·3	25	13·1
4	12·5	27	13·1
7	12·7	28	13·3
27	12·8	30	13·2
31	12·8	Oct. 3	13·2
Aug. 9	12·9	7	13·3
10	12·9	Nov. 18	13·5
17	12·8	25	13·4
25	12·9	30	13·6
29	13·0	Dec. 3	13·5
Sept. 2	13·1	7	13·6
5	13·1	10	13·6
8	13·2	12	13·7
12	13·1	17	13·7
13	13·1	20	13·8

Nova Aurigae (1891)

Observed on 1946 November 22 and 30, when the magnitude was estimated as 14·9. There has been no sensible change in light for a great many years.

Nova (*T*) *Coronae* (1866)

When observed on 1946 May 7 and 12 the nova was found to have sunk nearly to the level from which it had risen to a sudden fresh maximum three months before. On both occasions the magnitude was estimated as 9·81. The colour was sensibly white, whereas it had been markedly yellow in the years preceding the second outburst.

Nova Cygni (1876)

This is one of the definitely variable novae and the usual slight fluctuations were observed, the range in 1946 amounting to $0^{m}\cdot65$.

Date	Mag.	Date	Mag.
1946 July 2	14·65	1946 Sept. 12	15·00
23	14·71	13	15·00
27	14·76	15	14·96
31	14·91	25	14·60
Aug. 9	15·05	28	14·60
10	14·98	30	14·55
17	15·01	Oct. 3	14·66
25	15·11	7	14·71
29	15·11	28	14·71
Sept. 5	15·05	Nov. 18	14·71
6	15·20	Dec. 24	15·00
8	15·05		

Nova Cygni (1920)

The nova appears to have reached a steady state and there has been no fading or sensible variability for some years.

Date	Mag.
1946 May 4	15·6
21	15·7
July 2	15·6
27	15·7
Sept. 30	15·7

Nova Cygni (1942)

This nova is still fading, having dropped about a magnitude since 1945 October. It was observed on 1946 September 5, 8, 12, 13, 25 and 28, the magnitude being estimated at 15·5 on each occasion.

Nova Geminorum (1912)

Observed on 1946 November 24 and 30. Estimated magnitude 14·6. There has been no sensible change in brightness for many years.

Nova Herculis (1934)

There has been no general fading of this nova since 1945, though it is still more than a magnitude brighter than before its outburst in 1934. Under a high power it has the appearance of a planetary nebula about 3″ in diameter. It is greenish in colour and appears to have a stellar nucleus. The nebulous character of the image interferes with estimates of brightness, which are particularly affected by differences of transparency and illumination of the field. I therefore attach little weight to the apparent fluctuations suggested by the figures below.

Date	Mag.	Date	Mag.
1946 May 3	13·2	1946 July 2	13·0
4	13·2	23	13·3
12	13·2	27	13·2
21	13·2	31	13·3
28	13·2	Sept. 15	13·3

Nova Lacertae (1910)

There has been no significant change in the light of this nova for many years. It was observed on 1946 August 10 and September 28, the estimates being 14·4 and 14·5 respectively.

Nova Lacertae (1936)

General fading appears to have ceased and there is little if any real fluctuation in brightness.

Date	Mag.	Date	Mag.
1946 July 2	14·8	1946 Sept. 13	14·8
23	14·7	28	14·9
Aug. 10	14·8	Nov. 18	14·8
29	14·7		

Nova Lyrae (1919)

The nova appears to have reached a steady state and there has been no significant change in brightness for many years past.

Date	Mag.
1946 May 21	15·3
July 2	15·5
4	15·5
Sept. 28	15·5

Nova Ophiuchi (1848)

This nova has long been known to be slightly but definitely variable in light. Though stellar in appearance and comparatively bright, it has always been a

difficult object to observe photometrically by visual means, the estimates being more than usually affected by the presence of twilight or haze.

Date	Mag.	Date	Mag.
1946 May 21	12·1	1946 July 31	12·5
July 2	12·7	Aug. 17	12·6
4	12·5	25	12·7
7	12·6	Sept. 13	12·4
23	12·3	15	12·3
27	12·3	28	12·7

Nova Persei (1901)

This is the most markedly variable of all the old novae. A maximum range of $2^{m}\cdot2$ has been observed within the past twenty years, though the total range in any one year is generally a good deal smaller. In 1946 it amounted to a little less than one magnitude. The nebulosity that was formerly visible close to the nova on its south-preceding side was looked for on several of the best nights, but no trace of it could be detected. A few years ago it was an easy object in a much smaller telescope.

Date	Mag.	Date	Mag.
1946 July 2	12·64	1946 Nov. 17	12·84
23	12·69	18	13·10
27	12·69	22	13·05
31	12·89	24	12·74
Aug. 9	12·94	25	13·05
10	13·00	30	13·05
17	12·46	Dec. 2	13·05
29	12·80	3	13·15
Sept. 2	12·74	4	13·05
5	12·80	10	13·05
6	12·84	12	13·31
13	13·41	17	12·95
15	13·05	18	13·00
24	13·21	20	13·05
25	13·41	24	12·95
26	13·26	28	13·05
27	13·20	30	13·26
28	13·20	31	13·10
30	13·10	1947 Jan. 2	13·20
Oct. 3	13·26	5	13·05
7	13·25	9	13·41
18	13·10	13	12·84
28	13·00	16	13·05
29	13·26	17	12·95
Nov. 4	13·31	22	12·95

Nova Sagittae (1913)

The magnitude of this nova is said to have been steady at about 15 since it ceased to fade from the maximum of 1913. It underwent a second outburst in the summer of 1946 and reached $8^{m}\cdot1$ on June 29. By the time it was observed with the 30-inch telescope it had faded by about six magnitudes, and thereafter only a slight fall in brightness was noted, as shown by the figures below. The nova is preceded at a distance of a few seconds of arc by a star of nearly the same

brightness. The following estimates are based on the assumption that the magnitude of this star is 14·0.

Date	Mag.	Date	Mag.
1946 Aug. 17	13·8	1946 Nov. 25	14·1
25	13·8	30	14·15
Sept. 6	13·8	Dec. 3	14·2
26	13·8	12	14·2
30	13·95	20	14·25
Nov. 18	14·05		

Nova Vulpeculae (1670)

A few observations were made of the faint star found in 1934 close to the supposed site of this nova.* No certain variability was shown by the observations, and Humason has given reasons for doubting the identity of this star with the nova of 1670.†

Date	Mag.
1946 July 2	15·6
23	15·6
27	15·6
31	15·5
Sept. 28	15·5

Cambridge:
1947 *May* 3.

* *M.N.*, **95**, 78, 1934-1935.
† *Ap. J.*, **88**, 228-243, 1938.